BERICHTE
aus dem Fachbereich Geowissenschaften
der Universität Bremen

No. 262

Bohrmann, G., F. Abegg, A. Bahr, M. Bergenthal, M. Brüning, F. Brinkmann, S. Dentrecolas, P. Franke, A. Gassner, S. Hessler, H.-J. Hohnberg, D. Hüttich, T. Illhan, S. Klapp, E. Kopiske, J.-P. Meyer, A. Nikolovska, K. Olu -LeRoy, T. Pape, A. Pollmeyer, V. Ratmeyer, J. Renken, M. Reuter, E. Sick, I. Suck, Ö. Temel, T. Truscheid, C. Waldmann, T. Wilhelm, M. Zarrouk

IRAKLION - IRAKLION, 21 NOVEMBER - 8 DECEMBER 2006. COLD SEEPS OF THE ANAXIMANDER MOUNTAINS / EASTERN MEDITERRANEAN.

Berichte, Fachbereich Geowissenschaften, Universität Bremen, No. 262, 75 pages, Bremen 2008

ISSN 0931-0800

The "Berichte aus dem Fachbereich Geowissenschaften" are produced at irregular intervals by the Department of Geosciences, Bremen University.

They serve for the publication of experimental works, Ph.D.-theses and scientific contributions made by members of the department.

Reports can be ordered from:

Monika Bachur

Forschungszentrum Ozeanränder, RCOM

Universität Bremen

Postfach 330 440

D 28334 BREMEN

Phone: (49) 421 218-65516

Fax: (49) 421 218-65515

e-mail: MBachur@uni-bremen.de

http://elib3.suub.uni-bremen.de/publications/diss/html

Citation:
Bohrmann, G., and cruise participants
Report and preliminary results of R/V METEOR Cruise M70/3, Iraklion – Iraklion, 21 November – 8 December, 2006. Cold Seeps of the Anaximander Mountains / Eastern Mediterranean.
Berichte, Fachbereich Geowissenschaften, Universität Bremen, No. 262, 75 pages. Bremen, 2008.

ISSN 0931-0800

R/V METEOR
Cruise Report M70/3

Cold Seeps of the Anaximander Mountains / Eastern Mediterranean

M70
Leg 3
Iraklion – Iraklion,
21 November – 8 December, 2006

Cruise within the framework of
DFG-Forschungszentrum Ozeanränder
Research Center Ocean Margins

At University Bremen

Research Area E:
"Seepage of Fluid and Gas"

Edited by
Gerhard Bohrmann and Greta Ohling
with contributions of cruise participants

The cruise was performed by
MARUM Center for Marine Environmental Sciences

Universität Bremen

marum

R/V METEOR Cruise Report M70/3

Table of Contents

1 Preface

R/V METEOR Cruise M70/3 was an interdisciplinary cruise which brought together an international group of scientists from institutions within Germany (AWI, RCOM, University of Bremen) and other countries (IFREMER, France; NIOZ, The Netherlands; TPAO and DEU, Turkey). The cruise and research programme were planned, coordinated, and carried out by the Earth Sciences Department and MARUM Center for environmental sciences at University of Bremen. The cruise was financed by German Research Foundation within the DFG Research Center Ocean Margins. The shipping operator (Reederei F. Laeisz GmbH, Bremerhaven) provided technical support on the vessel in order to accommodate the large variety of technical challenges required for the complex sea-going operations. We would like to especially acknowledge the master of the vessel, Niels Jakobi and his crew for their continued contribution to a pleasant and professional atmosphere aboard R/V METEOR.

1.1 Personnel aboard R/V METEOR M70/3

Table 1: Scientific crew.

Name	Discipline	Affiliation
Friedrich Abegg	Autoclave	RCOM
André Bahr	Geology	NIOZ
Markus Bergenthal	MOVE	MARUM
Gerhard Bohrmann	Chief scientist	RCOM
Markus Brüning	Hydroacoustic	RCOM
Florian Brinkmann	Carbonate geology	RCOM
Stephane Dentrecolas	Biology	IFREMER
Phillip Franke	ROV	MARUM
André Gassner	Geochemistry	RCOM
Silvana Hessler	Geochemical	RCOM
Hans-Jürgen Hohnberg	Autoclave	RCOM
Daniel Hüttich	ROV	MARUM
Tarik Illhan	Hydroacustic	DEU
Stefan Klapp	Geology	RCOM
Eberhard Kopiske	ROV	MARUM
Jörn-Patrick Meyer	ROV	RCOM
Aneta Nikolovska	Hydroacoustic	RCOM
Karin Olu -LeRoy	Biology	IFREMER
Thomas Pape	Geochemistry	RCOM
Achim Pollmeyer	Documentation	Taglicht media
Volker Ratmeyer	ROV	MARUM
Jens Renken	MOVE	MARUM
Michael Reuter	ROV	MARUM
Erik Sick	Documentation	Taglicht media

Inken Suck	ROV	Fielax
Özgür Temel	Geology	TPAO
Torsten Truscheid	Meteorology	DWD
Christoph Waldmann	MOVE	MARUM
Thorsten Wilhelm	Geochemistry	AWI
Marcel Zarrouk	ROV	MARUM

AWI	Alfred-Wegener-Institut für Polar- und Meeresforschung, 27570 Bremerhaven, Germany
DEU	Dokuz Eylul University, Depart. of Geophysics and Institute of Marine Sciences and Technology, Baku Bulvari No. 32, 35340 Izmir, Turkey
DWD	Deutscher Wetterdienst, Geschäftsfeld Seeschifffahrt, Bernhard-Nocht-Straße 76, 20359 Hamburg, Germany
IFREMER	Centre Ifremer de Brest, departement geosciences marine, département environment profond, B.P.70, F-29280 Plouzané, France
NIOZ	Royal Netherlands Institute for Sea Research, P.O.Box 59, 1790 AB Den Burg, Texel, The Netherlands
Taglicht media	Film- & Fernsehproduktion GmbH, Klopstockstraße 1, 50968 Köln, Germany
TPAO	Turkish Petroleum Company, Exploration Group, Mustafa Kemal Mah. 2.cad. No: 86, 06520 Ankara, Turkey
RCOM/MARUM	DFG-Forschungszentrum Ozeanränder, University of Bremen, Postfach 30440, 28334 Bremen, Germany
FIELAX	Gesellschaft für wissenschaftliche Datenverarbeitung mbH, Schifferstrasse 10– 14, 27568 Bremerhaven, Germany

Fig. 1: Group of scientists and technicians sailed during M70 Leg 3 onboard R/V METEOR.

Table 2: Crew members onboard R/V METEOR.

Name	Work onboard	Name	Work onboard
Niels Jakobi	Master	Peter Neumann	Chief Engineer
Uwe-Klaus Klimeck	Officer	Uwe Schade	Engineer
Walter Baschek	Officer	Bjoern Brandt	Engineer
Tilo Birnbaum	Officer	Rudolf Freitag	Electrician
Heinz Wentzel	Chief Electronics	Werner Sosnowski	Fitter
Olaf Willms	Electronics	Enric Schaefer	Motorman
Katja Pfeiffer	System operator	Frank Sebastian	Motorman
Anke Walther	Surgeon	Heinrich Riedler	Motorman
Wolf-T. Ochsenhirt	Weather technician	Andreas Wege	Chief steward
Manfred Gudera	Boatswain	Rainer Götze	Steward
Horst Klingelhöfer	Seaman	Michael Both	Steward
Ralf Kaiser	Seaman	Peter Eller	Steward
Pjotr Bussmann	Seaman	Klaus Hermann	Chief cook
Björn Pauli	Seaman	Willy Braatz	Cook
Günther Stänger	Seaman	Seng-Choon Ong	Launderer
Günther Ventz	Seaman	Matthis Alte	Trainee
Peter Blenn	Trainee	Michael Janek	Trainee

1.2 Participating Companies

Reederei F. Laeisz GmbH,	"Haus der Schifffahrt", Lange Straße 1a, D-18055 Rostock, Germany
FIELAX	Gesellschaft für wissenschaftliche Datenverarbeitung mbH, Schifferstrasse 10 – 14, 27568 Bremerhaven, Germany

2 Introduction

2.1 Objectives, Background and Research Program
(G. Bohrmann)

The prime objective of the research in the investigation area of the "Anaximander Mountains" south of Turkey (Fig. 2) was to decipher key processes at cold seeps. The cruise was planned as an interdisciplinary work conducted in the project "Fluid and Gas Seepage" in the frame of the Research Center Ocean Margins (RCOM). Ocean margins host large systems of circulating aqueous fluids. In some areas these are associated with hydrocarbon migration and focused emission of fluids, gases and muds at the sea floor. Some estimates suggest that the magnitude of upward flow through continental margins could be similar to that at hydrothermal systems. Associated with fluid outflow at seeps are chemosynthetic communities that utilize the chemical energy of reduced components such as H_2, H_2S, CH_4, and other hydrocarbons. The biomass of these communities is often several orders of magnitude greater than in the non-seep vicinity. The primary energy flow to these highly specialized communities comes from microbial turnover of sulfide, methane and other hydrocarbons. Cold seep ecosystems are recognized by distinct morphological features (e.g. pockmarks, chimneys, and irregular build-ups), specific biological communities, highly reduced chemical environments, high sulfide fluxes, mineral precipitates (e.g. authigenic carbonates, barite, and gas hydrates), and diagnostic stable-isotope signals in inorganic and organic phases.

Emissions of reduced compounds such as methane, hydrogen sulfide and iron-II affect the cycling of elements around seep locations in unique ways. Cold-seep environments may also serve as model systems for past perturbations of the carbon cycle that were presumably triggered by release of methane from subsurface reservoirs. Previous studies of seep environments were often concerned with local geologic features and/or specific biogeochemical processes such as the anaerobic oxidation of methane (AOM), a main sink for methane in the sea floor. Systematic approaches to an investigation of different seep systems (i.e., asphalt-, petroleum-, methane-, CO_2-, brine-seepage; carbonate-paved or fluid muds; methane- or sulfide based chemosynthesis; focused versus diffuse fluid flow, etc.) and their element fluxes have not yet been undertaken and form a focus of the RCOM.

Similar to hot vent ecosystems, cold seeps support enormous biomasses of tube worms, vesicomyid, mytilid, and solemyid bivalves, as well as mats of giant sulfide-oxidizing bacteria. These chemosynthetic communities are nourished by the chemical energy, i.e. methane and sulfide, rising from subsurface sources and forming the basis of cold-seep ecosystems. High chemoautrotrophic production at these habitats supports additional seep-associated organisms. In areas of high hydrocarbon fluxes, the benthic biomass fueled by chemosynthetic processes can be 1,000 to 50,000 times greater than the biomass of detritus-based deep-water ecosystems. Some recently discovered microbial communities at seep systems represent important barriers for the release of greenhouse gases and toxic substances. Examples are methanotrophic archaea mediating AOM, and various bacterial groups oxidizing sulfide with oxygen or nitrate. The role of iron, manganese and other metals in anoxic hydrocarbon and sulfur turnover is not well known. Also, little is known on the

biogeography of seep-related microbial communities, the endosymbiotic chemosynthetic fauna and other seep fauna. Methane-seep deposits are typically dominated by authigenic carbonates, iron sulfides, barite, calcium sulfates, and gas hydrates. Mineral authigenesis is linked to biogeochemical cycling of carbon and sulfur. The anaerobic oxidation of methane leads to an increase in alkalinity, which results in the precipitation of carbonate minerals including aragonite, calcite, and dolomite with low $\delta^{13}C$ values (as low as -69‰). The product of AOM, sulfide, interacts with iron and other sedimentary compounds. Mineral fabrics, stable isotopes, and lipid biomarkers track microbial processes in the formation of modern and ancient seep precipitates.

In order to achieve this goal within the Anaximander Mountains the ROV QUEST was used as the main tool in order to map the sea floor and take samples on the spot (Fig. 3). ROV served as platform for the deployment and recovery of autonomous tool measuring, e.g. the flow of bubbles at the sea floor.

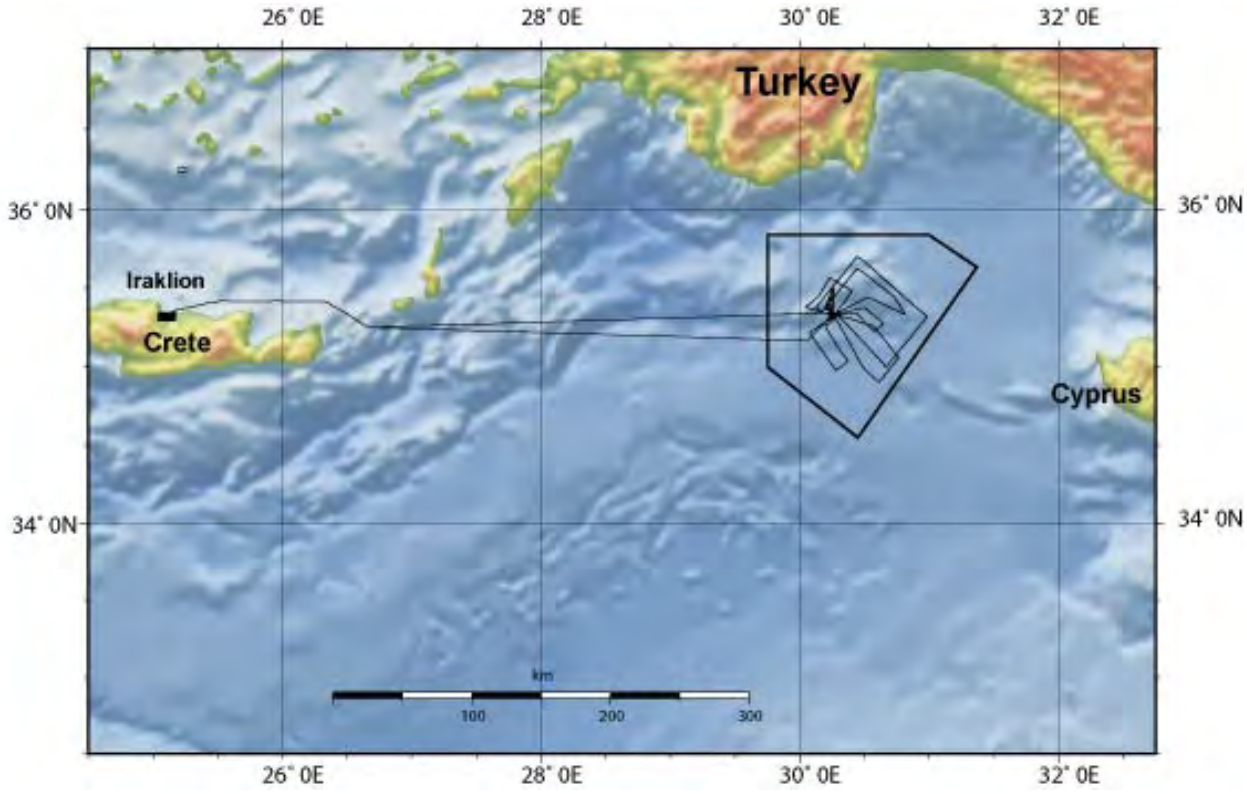

Fig. 2: Cruise track of R/V METEOR Cruise M70/3 within the research area of the Anaximander Mountains. The pentagonal box represents the limits of research permission.

Investigations in the Anaximander area before the cruise have documented methane seeps at several mud volcanoes in about 2000 m water depth. Gas hydrates exist in the sediments of the mud volcanoes and there was strong evidence that at some of the structures methane escapes as gas from the sea floor. The main objective during leg M 70/3 was to sample the gas and determine how much methane is escaping from the sea floor as bubbles. Tools that were specially designed for the acoustic and optical detection of bubbles are presently under development at the RCOM. It was planned to deploy these as well as the entire suite of other sampling tools at the seeps south of Turkey. A main goal in this area was to quantify the amount of gas and gas hydrate in the sediments using the dynamic autoclave piston corer

(DAPC; Fig. 3). DAPC can retrieve sediment cores of up to two meter in a pressure-tight housing at in-situ pressure. Degassing of this core under controlled pressure conditions allowed quantifying the amount of gas and gas hydrate in the sediments.

Fig. 3: Research vessel METEOR in the port of Iraklion (above left) ROV QUEST 4000 m on the working deck during a pre-dive check before deployment (above right); Moving lander MOVE (below left) and the autoclave piston corer (DAPC) deployed from R/V METEOR.

The following scientific questions were addressed during the cruise:

- Which processes control the different types of cold seeps at the sea floor?
- Which conditions control the escape of fluids (liquid, gas) and mud and how does this shape the appearance of the seeps?
- What is the origin of the different mineral phases that precipitate at seeps and what controls their composition?
- How much methane is escaping as gas bubbles from the sea floor to the water column?
- What is the advective fluid flow and what is the source of the fluids?
- How much gas and gas hydrates exist in the sediments?
- Which organisms live at the seeps?

2.2 Geological Setting of the Anaximander Mountains
(Ö. Temel)

The Anaximander mountains represent the offshore continuation of the geological units exposed onshore southwest of Turkey. According to lithological and geological correlation, Anaximander and Anaximanes mountains are located on the Beydag Unit. The Anaxagoras mountains are located in continuation of the Antalya nappe. The Beydag Unit was named by an area in Turkey west of Tauros. This unit is composed of upper Triassic to upper Cretaceous rocks. Triassic sediments are represented mostly by clastic and fine grained deposits. Upper Jurassic and lower Cretaceous sediment represent lagoonal environments and have excellent source rock potential. The Antalya nap complex comprises ophiolitic melange, ophiolitic sequences, and medium to high grade metamorphic rocks of the Mesozoic clastic deposits and carbonates.

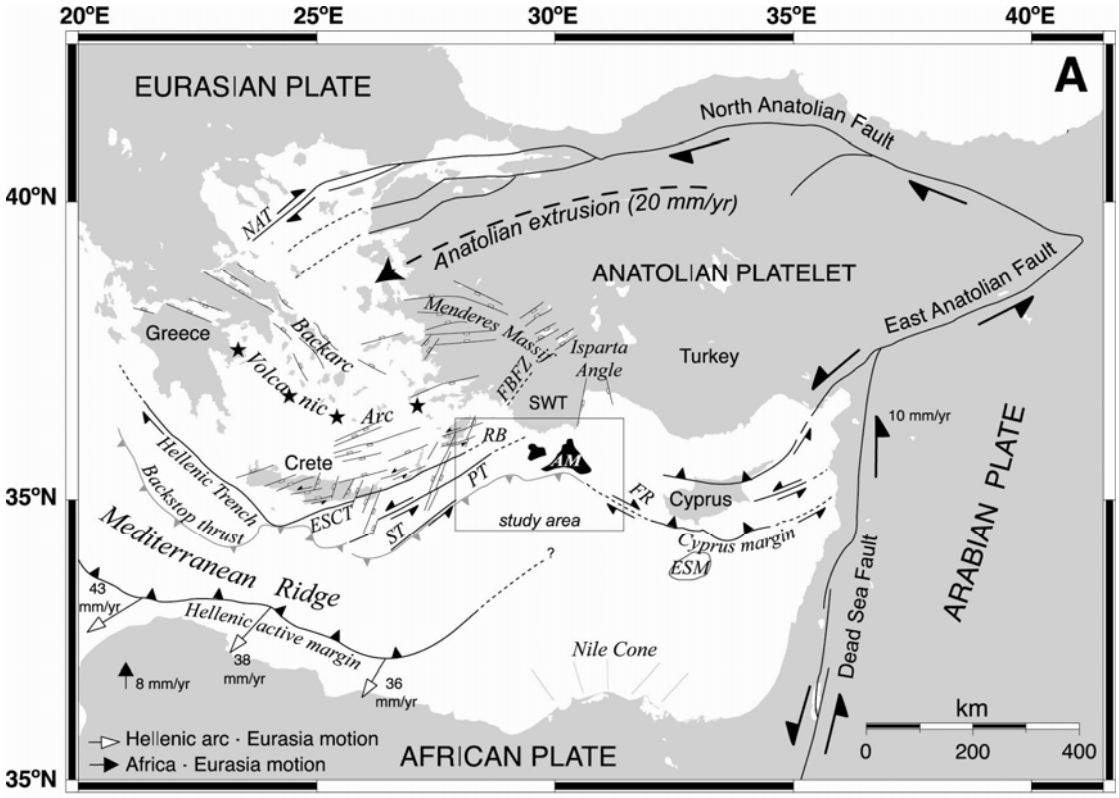

Fig. 4 (A): Geodynamic framework of the eastern Mediterranean from Zitter et al., 2005. The motion vector of Africa is from DeMets et al. (1994) and the southwestward motion of the Hellenic Arc relative to Eurasia is from McClusky et al. (2000). The Hellenic forearc from Crete to Rhodes shows a strain pattern with N70°E-striking strike-slip faults and N20°E-striking normal faults, resulting from transtensional deformation since the Pliocene. The dextral shearing shown along the Florence Rise was inferred by Woodside et al. (2002). New results require the sense of shear in this locality to be sinistral instead. Abbreviations: ESCT = East South Cretan Trough, ST = Strabo trench; PT = Pliny Trench; RB = Rhodes Basin; AM = Anaximander Mountains; FR = Florence Rise; ESM = Erasthothenes Seamount; FBFZ = the hypothetical Fethiye-Burdur Fault Zone; SWT = Southwest Turkey; NAT = North Aegean Trough. Stars indicate subduction-related Quaternary volcanism.

The Antalya Neogen basin is surrounded by the Antalya nap complex. This area which is located in the southern part of Turkey, is characterized by northeast dipped sedimentary units. The area is NW/SE oriented and has an elongated shape. The thickness of the Neogene

sedimentary units comprise more than 2000 m sediments. The thickness and dipping of the sedimentary units increases to the north and continues in the northern sector (Huguen, et al., 2005). After the Early-Middle Miocene eastern sector emplacement of the Lycian nappes, Servalian and Tortonian was characterized by the development of graben structures (Dewey and Sengor, 1970). In the eastern Mediterranean offshore of Turkey, turbiditic facies are dominated in late Langian to Serravalian stage and Tortonian deposits are represented by thick fluvial and deltaic facies. The Anaximander Mountains which are situated in the southern sector of Finike Basin (Fig. 4 B), are located at the junction of Hellenic and Cyprus arcs (Fig. 4 B). This sector is located south-east of the Finike basin, and is a western part of the Antalya basin (Fig. 4 B). A different tectonic style started in late Miocene and the seamounts in the Anaximander area started to become formed in this stage. The Messinian and early Quaternary units around the Anaximander mountains are characterized by right lateral strike slip faults by onset of an extension on NE oriented normal faults and a depression (Huguen et al., 2005).

Ophiolitic rocks were observed in the southeast of the Finike basin, and have extension to the north. It is known that in the northeast part of the Anaxagoras mountains a melange is present (Woodside and Dumont, 1997). All these elements represent a southward continuation of the Antalya nappes.

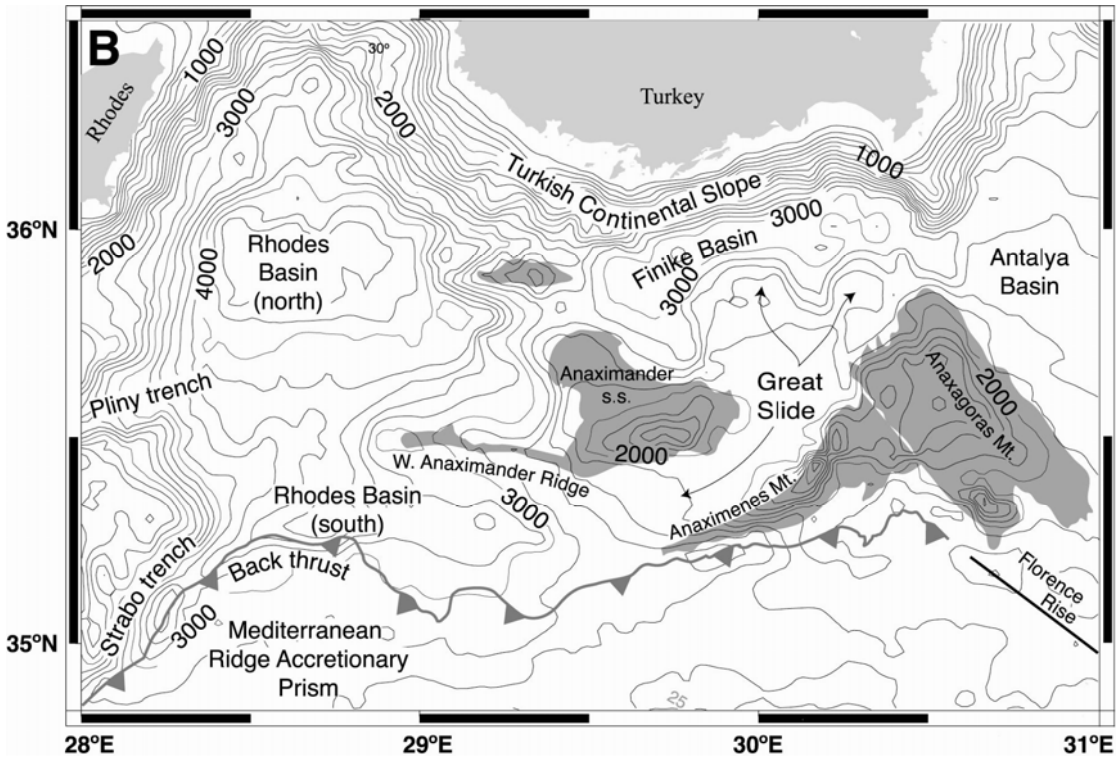

Fig. 4 (B): Detail of the Anaximander Mountains study area with bathymetry from etopo5, made available through the National Geophysical Data Center (NDGC), with 200-m contour interval.

Messinian evaporites reach 1000 m in the eastern Mediterranean offshore of Turkey. Rollover structures associated with growth faults within the large scale turtle structures above the Messinian unconformity are a result of salt mobilization. Messinian evaporites are close to the apex of the western Mediterranean ridge and have been deposited at the backstop contact.

The deeper backstop area is interpreted as the result of salt tectonics within a pre-existing fore arc basin (Chaumillon, 1995). The lower-middle Miocene deposits show a typical deep marine and flysch facies in southwest of Turkey. Plio-Quaternary sediments which were deposited in a deep marine environment, are mostly composed of siltstones, claystones, thin bedded and laminated sandstones and mudstone and there is an unconformity between the Plio-Quaternary and lower to middle Miocene flysch deposits. The thickness of the Plio-Quaternary unit is about 1500 m in Antalya offshore basin which is situated eastern of the Anaxagoras mountains and appears as a fold belt. This fold belt is represented by east-west oriented strike slip faults. Messinian-Quaternary deformation of the western part of Anaximander seamounts is characterized by right lateral strike slip faults. The eastern mountains are represented by left lateral strike slip faults and oblique faults. The mud volcanoes were discovered in the Anaximander area associated with strike slip faults (Huguen, et al., 2005). There was a change in the plate motions from north to south in the middle to Late Miocene (Dewey and Sengor, 1970). As a result of this change East Anatolian and North Anatolian transform faults developed.. The extensional tectonic regime in the western Turkey increased. At the same time eastern sector of the Hellenic and Cyprus zones became more transpressive and the subduction area developed into two separate arcs resulted in the tearing of the African plate (Dewey and Sengor, 1970).

3 Cruise Narrative

(G. Bohrmann)

The R/V METEOR sailed from Iraklion harbour, Crete at 10:00 am on Sunday, November 28 within the Mediterranean to the Anaximander Mountain area (Fig. 2). The submarine Anaximander Mountains are located about 75 nautical miles south of Antalya at the Turkish coast. The area (Fig. 5) is situated at the intersection between the Cyprus Arc in the East and the Hellenic Arc in the West. Both arcs represent elements within the zone of African convergence in the South against Europe /Anatolian Plate in the North (Fig. 4A).

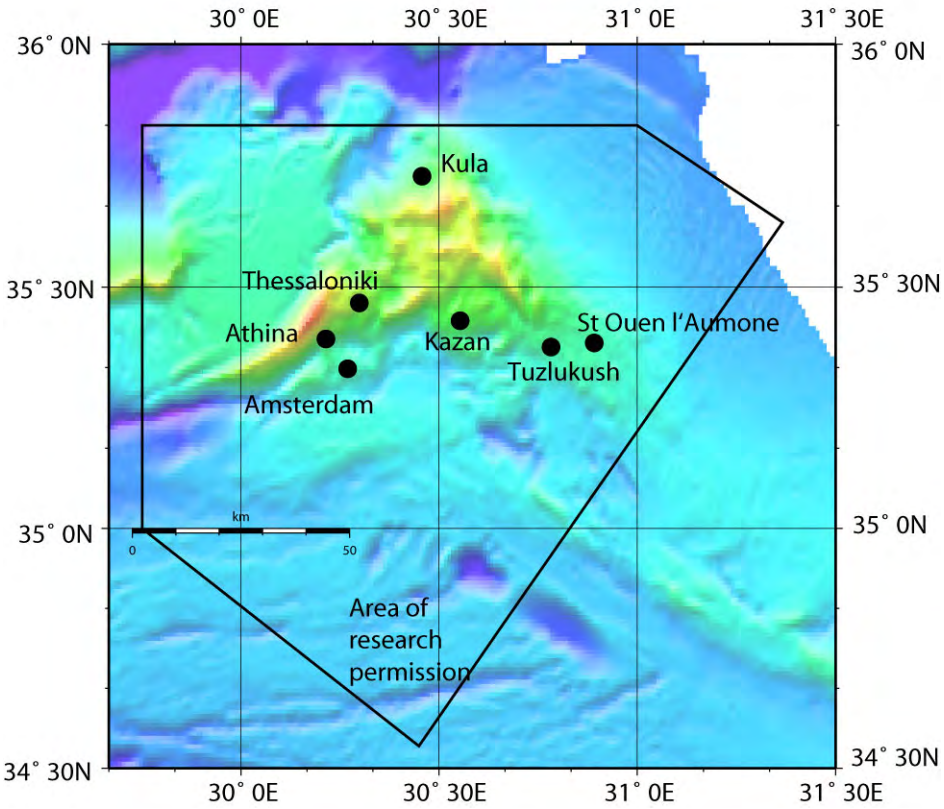

Fig. 5: Mud volcanoes known from the submarine Anaximander Mountains.

From the tectonic point of view the Anaximander Mountains represent rather a complicated structure dominated by sinistral strike-slip faults (Zitter et al., 2005). Within the frame of this compressive tectonic style several mud vulcanoes have been developed, where not only mud but also fluids and gas emanation from the sea floor are found. Those active emissions from the sea floor are a global phenomenon and are interdisciplinarily analysed by the DFG Research Center of Ocean Margins (RCOM) in the frame of several projects. Here the main interests are gas emission sites, where mainly methane bubbles ascent from the sea floor into the water column. It is known from other sites, that those bubbles emanating from the sea floor within the gas hydrate stability zone are protected by thin gas hydrate skins from being dissolved in the sea water. Those emissions of bubbles on the sea floor within the gas stability zone are always associated to near-sea floor gas hydrate deposits. Up to now, gas hydrates in the Eastern Mediterranean are only known from the Anaximander area, which was explained by the absence of Messinian evaporites because saline water or brines would

decrease the stability field of hydrates very much (Bohrmann and Torres, 2006). We used the gas hydrate presence in the Anaximander area to postulate that gas emissions should exist. Up to now such gas emissions could not yet be proved despite of several expeditions. The documentation of gas emissions was the main subject of our expedition, whereas besides the ROV QUEST also a certain number of further sea floor instruments and analysing techniques were planned to be deployed.

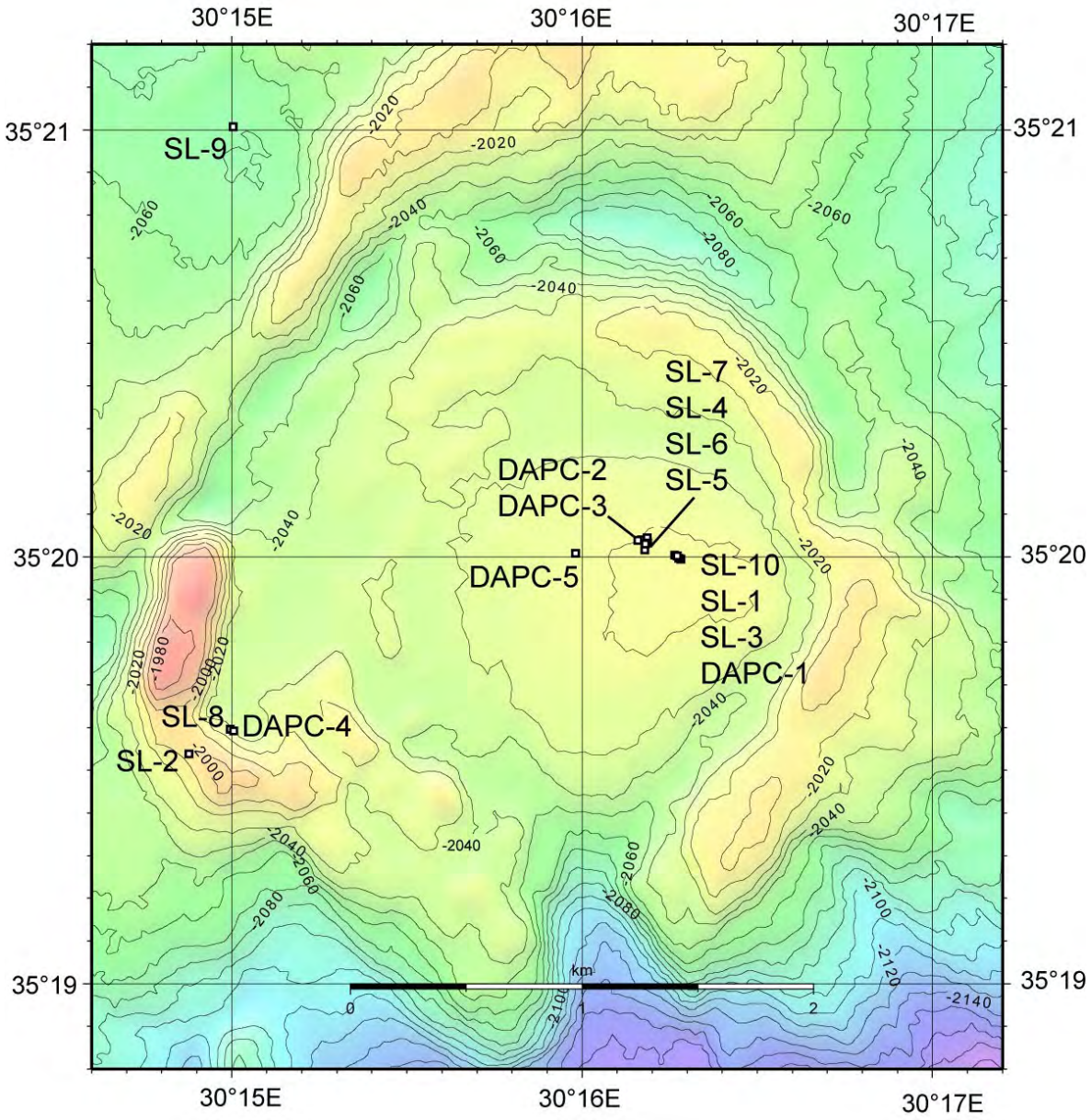

Fig. 6: Gravity corer, MUC and DAPC stations performed during M70/3 at Amsterdam Mud Volcano.

The R/V METEOR could sail after a three days port call in the port of Iraklion when the scientific crew and the main part of the scientific tools had been changed. The ROV QUEST was already on board since end of September and was the main tool on our cruise. The scientists from Germany, France, Turkey and Macedonia embarked on Saturday November 25. The port time was used to unload the scientific equipment, to install the labs as well as to have first scientific meetings on board. After a one days transit to the Turkish working area

we started with a detailed survey at the Amsterdam Mud Volcano on Monday November 27 followed by an overview survey covering three further mud volcanoes.

Our new survey showed much more detailed than earlier surveys the structure of the mud volcano which enabled us a better applications planning of the submarine ROV QUEST. During the first three dives on Tuesday, Wednesday and Thursday we collected data in the general spreading of the emission locations in the mud volcano. It was highly interesting and unusual that we could prove carbonate seeps inhabited by vestimentiferan tube worms along the outer wall. Vestimentiferan tube worms live in perfect symbiosis with endosymbiontic bacteria and are a safe indicator for active fluid emission. While one end of their tube is fixed in the sediment the other end grows into the water column. Besides the tube worms the cold seeps are also populated by chemoautotrophe bivalves - mytilid, thyrasid and licinid groups. During our ROV dives we found many dead shells of the chemosynthetic clams. At the eastern wall, where our French colleagues observed in the past more massive vestimentiferan tube worms, we only found single tube worms distributed in larger areas. Within the caldera of the Amsterdam Mud Volcano the detailed morphology of the sea floor varies. In the area of the "ring depression" plateau-like areas often alternate with depressions showing fresh edges of sediment fractures. In the centre of the mud volcano a morphologically chaotic sea floor was found, where we recovered several gas hydrate samples by gravity coring.

With the second dive we already could prove the postulated gas bubble emission at the sea floor. First of all the bubbles had been identified and localized as an acoustic anomaly in the water column, by means of the forward looking ROV-sonar. After moving the ROV to the anomaly, the ROV followed the bubbles down to the sea floor where the emission sites could be documented in detail with the new HDTV camera. The bubbles continuously leaked out at several points from the sea floor appearing in rather different speed and leaving the sea floor. This image reminded us very much to soap bubbles. The emission locations were limited to a small area < 1 square meter and the sea floor was definitely dark coloured by hydrogen sulfide, darker than outside this area. In the gas seep we found very small worms (pogonophora), bivalves, snails and crabs. Besides the dives we mostly applied successfully the gravity corer and the autoclave piston corer. Furthermore a new sea floor vehicle named MOVE had been applied the first time in the deep water, with only some initial problems which could be settled thanks to the ROV QUEST.

During the second week of our cruise we already had to think to finish our station work by Thursday around 06:00 a.m. Therefore, we discussed the results which we obtained up to now on Sunday during an extensive meeting and defined the priorities for the next days. A very important point in our Sunday program was the dive down to the central part of Amsterdam Mud Volcano. During the first week two gas seeps had been investigated by ROV QUEST on the sea floor. The colonisation of these cold seeps by pogonophora as well as by small clams initiated our French colleagues to deploy two colonisators at the seeps until next year. The idea is that the seep organisms will accept the substrate of the colonisators and will settle there. The French research vessel "Pourquoi pas" is planning to recover the colonisators next year so that the living chemosynthetic organisms can be transported in a safe way to the laboratory to do further experiments. Deployments of the heavy devices were successfully completed and the remaining dive time was used for exploration of some other gas seeps. A further gas seep which clearly provided large amounts of free gas was found. There we used

for the first time a recently developed pressure-tight gas sampler. Gas bubbles were collected in an upside-down funnel. Under the high pressure in the water depth of 2000 m and with 14°C gas bubbles turned immediately to porous gas hydrate. Thus the gas hydrate was drawn into the pressure-tight container which enabled us to sample the original gas stored in the gas hydrate and later into the sample container. This was successfully done and the gas analyses revealed that beside methane ethane occurs in small amounts. The gas hydrates sampled from sediments show a clearly increased ethane content.

On Monday December 4 we applied the submarine vehicle MOVE a second time. During the device autonomously made its measurements on the sea floor we performed ROV dive number 7 on Athina Mud Volcano (Fig. 5). Although it originally was planned to have a long profile above both peaks of the mud volcano we could only perfom the first half of the planned dive. Large areas covered by authigenic carbonates and dense populations of vestimentiferan tube worms where recovered which were unknown to occur in such densities in the Eastern Mediterranean up to now. During the night the vehicle MOVE could safely be recovered and the analysis of the registered data showed that the system worked successfully for the first time in 2000 m water depth. Prior to the next dive during which the autonomous French camera system was deployed for one year on the sea floor the autoclave piston corer was used to take a pressure core.

In the following night we applied special PARASOUND measurements for registration of acoustic plumes in the water column. The last dive was performed on Thessaloniki Mud Volcano (Fig. 5) and after a core program the station work of METEOR cruise M70/3 was finished on Thursday December 7 at 06:00 am. Although this cruise was very short it was very successful with its 9 ROV-dives, 10 gravity cores, 2 multi-cores, 5 autoclave samples, 2 MOVE deployments and additional EM 120 and PARASOUND profiling.

4. Hydroacoustic Work

4.1 Multibeam Swathmapping

(M. Brüning)

The SIMRAD EM120 multibeam echosounder installed on R/V METEOR was used to survey the working area. Especially the mud volcanoes of interest were surveyed to reveal small details (Fig. 7). The maps served as the basis for the planning of ROV dives and flare-imaging profiles. Nighttime breaks in the sampling and dive program were used to survey the main part of the work area over the Anaximander Mountains. The usual time available per night was six hours. Six profiles starting from Amsterdam Mud Volcano cover the central area of the permitted work area.

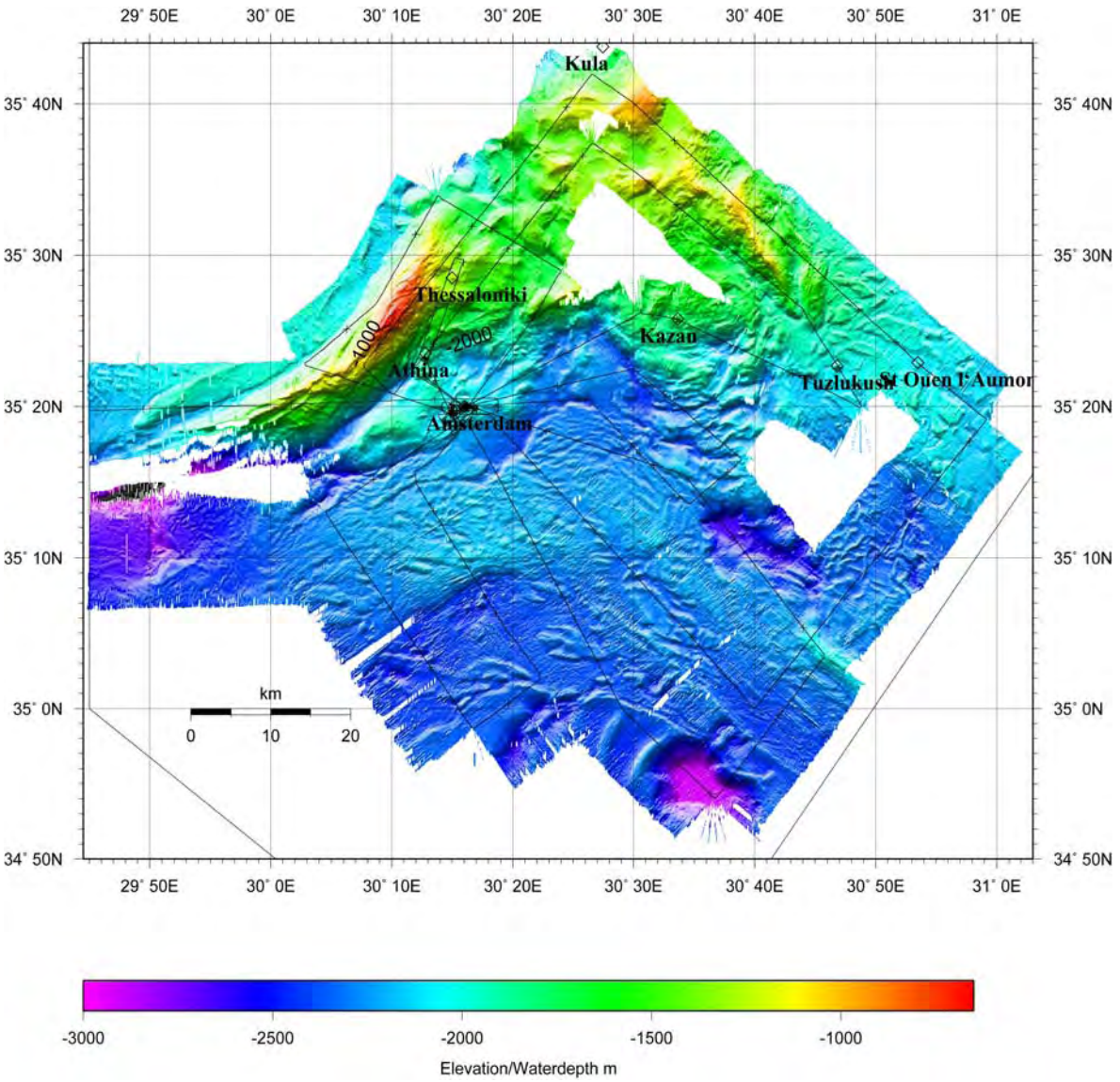

Fig. 7: Anaximander Mountain area covered by multibeam swathmapping during R/V METEOR Cruise M70/3.

The ship speed during the large scale surveys was 8 knots. The opening-angle of the multibeam sounder was 140°, for only one profile we selected an angle of 150°. The wider angle decreased the data quality and was not used again. The 191 beams available were distributed to yield an equidistant spacing on the sea floor. The coverage depends on the water depth. It is 5.5 km in 1000 m, 11 km in 2000 m, and 13.7 km in 2500 m water depth. SIMRAD provides a yaw correction, which directs the beams according to the mean heading. This decreases the actual beam number slightly for the optimization of full coverage along and across track.

For the detail-surveys of Amsterdam, Athina and Thessaloniki Mud Volcanoes the beam-angle was adjusted to cover about one nautical mile on the sea floor. The ship speed was reduced to 5 knots. During stations and ROV dives the multibeam was running, as long as it was not disturbing the flare-searching with the PARASOUND system. A sound velocity profile generated from the Levitus database was used to calculate the water depth. GPS served for the positioning of R/V METEOR. The IFREMER Caraibes software served as the processing tool for the SIMRAD data. The navigation data were manually edited and then interpolated. Bathymetric data were cut by depth-thresholds adjusted to the surveyed area. A very rough manual editing increased the success of the following filter. The filter used a grid calculated with relatively large grid-spacing to eliminate spikes in the soundings. Two runs of the filter were performed. The sensitivity in recognition of spikes was increased in the second run.

For detailed profiles the backscatter data were processed on the base of the bathymetry files. During the cruise the Levitus sound velocity profile was used in depth calculations. For the final maps of the cruise report a sound velocity profile from the MOVE's CTD survey was used. Depths data decreased around 3-5 m in a water depth of 2000 m with the change of the sound velocity profile. The map (Fig. 7) was generated with the Generic Mapping Tool (GMT) from Wessel, P. and Smith, W.H.F. (1998).

4.2 Sub-bottom Profiling and Flare Imaging

(A. Nikolovska)

In the research frames of METEOR Cruise 70/3 the hull-mounted ATLAS PARASOUND system was used for water column imaging and sub-bottom profiling. The area around Amsterdam Mud Volcano was operated at depths of up to 2500 m as well as in shallower areas around Thessaloniki and Athena Mud Volcanoes (water depths of about 1200 m).

The transmitted source signal (PHF) is a sequence of continuous sinusoidal wave pulses of 18 kHz frequency; the secondary low frequency (SLF) was set to 4 kHz. The pulse shape is rectangular with length of 0.500 ms, duration of 2 periods, and beam angle of 4°. The raw data from the acquired primary high frequency and the secondary low frequency were set to store the full water profile. The receiver amplification was set to 30 dB for the PHF and 12 dB for the SLF. While the ship was in station different PARASOUND parameters were tested in order to get a better understanding of the performance of the system for the purpose of the plume imaging surveys. It is noted that while using a beam shading of the PHF the detection of the sea bed is more distinct and the effect of the background noise was reduced; the

shading also affected weak scatters in the water column and disabled the possibility of detecting this features, thus during the plume surveys the shading of PHF was not used. Also, the use of beam stirring option did not result in improving the detection of scatters in the water column (while testing this feature the scattering intensity from the ROV was used as a reference).

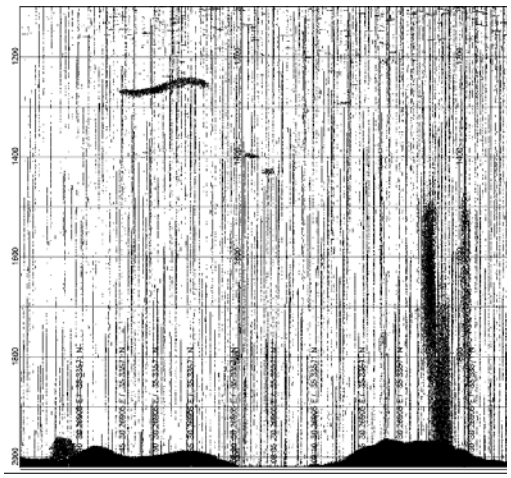

Fig. 8: Echogram of a bubble plume imaged with 18kHz in the South West part of Amsterdam MV at a water depth of 2025 m, the plume backscatter is visible up to 1500 m.

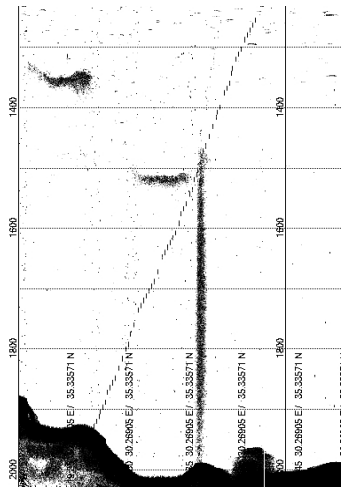

Fig. 9: Echogram of a bubble plume imaged with 18kHz in the North West part of Amsterdam MV at a water depth of 2025 m, the plume backscatter is visible up to 1500 m.

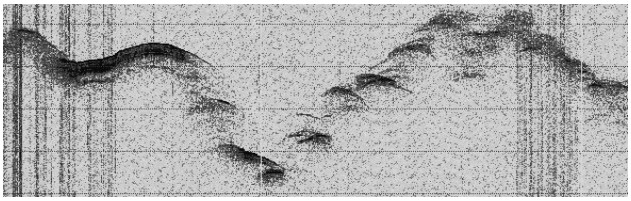

Fig. 10: Sub-bottom profile of the area in Fig. 8.

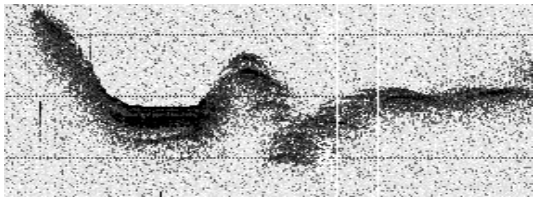

Fig. 11: Sub-bottom profile of the area in Fig. 9.

Figures 8 and 9 show some of the plume signatures detected at water depth of 2025 m in the area of the Amsterdam MV. In Fig. 8 the vertical lines are the noise induced by the SIMRAD swath sounder that operated at a frequency of 12 kHz, during the plume surveys the swath sounder was switched off enabling clear visualization of the plumes, as shown in Fig. 9. In the subsequent Figs. 10 and 11 the corresponding sub-bottom profiles are shown. These plots were generated through the SLF.

The maximum depth of the Sounder Environment in the Hydromap Control was varied from 1500 m (when surveying shallow areas between 1200 to 1400 m) and varied up to 2700 m (when surveying deeper areas below 1500 m). The minimum depth was set to values between 10 m to 100 m and remained constant disregarding the depth of the survey areas. When set to lower value the system was underestimating the real sea floor depth so it had to be reset to higher depth. After resetting the values for the depth were in the range of the ones measured by the SIMRAD multibeam system. The offset between the SIMRAD water depth estimation compared with the PHF evaluation was in the range of 40-20m. This is due to the

difference in the values of the sound speed used in both systems; SIMRAD is using a more accurate sound speed profile and in PARASOUND the water depth is calculated by a fixed sound speed value of 1500 m/s.

The echosounder profiles were registered at ship's speeds of ~5 and ~10 knots (when mapping the area), and at ~0.5 to ~1.5 knots (when surveying plume areas). At high ship speed it was almost not possible to detect any flare. The data quality was affected by extremely high noise from the ship’s thrusters; which made it impossible to visualize weak scattering produced by bubbles in the water column. The combination of low ship’s speed and the above mentioned echosounder settings allowed a very clear visualization of bubble plumes that were passed during the survey. This enabled getting relatively reliable information about the distribution and location of bubble plumes within the areas where there existence has not been detected before.

5 Remotely Operated Vehicle (ROV) QUEST

5.1 Technical Description and Performance

(V. Ratmeyer, P. Franke, D. Huettich, E. Kopiske, P. Meyer, M. Reuter, I. Suck, M. Zarrouk)

The deepwater ROV (remotely operated vehicle) QUEST 4000 m used during M70/1-3, is operated and installed at MARUM, Center for Marine Environmental Sciences at the University of Bremen, Germany. The QUEST is a commercially available, but specially adapted, 4000 m rated system designed and built by Schilling Robotics, Davis, USA. Aboard R/V METEOR for the 12th cruise since installation at MARUM in Mai 2003, the system is well adapted to the research vessel and could be handled during all stages of weather encountered during the cruise.

During M70/3, QUEST performed a total of 9 dives to depths around 2200 m. All dives with a total of 69 hours bottom time allowed successful scientific sampling and observation at different sites. The total QUEST system weighs about 45 tons (including the vehicle, control van, workshop van, electric winch, 5000 m umbilical, and transportation vans) and can be transported in four 20' vans. Using a MacArtney Cormac electric driven storage winch to manage the 5000 m of 17.6 mm NSW umbilical, no additional hydraulic connections are necessary to host the handling system.

The QUEST uses a Doppler velocity log (DVL, 1200 kHz) to perform Stationkeep, Displacement, and other auto control functions. Designed and operated as a free-flying vehicle, QUEST system exerts such precise control over the electric propulsion system that the vehicle maintained relative positioning accuracy within decimeters. Although these data were not used for absolute navigation, they are an essential tool for vehicle control during flight. The combination of 60 kW power with DVL based auto control functions provides exceptional positioning capabilities at depth. In addition, absolute GPS positions are obtained using the shipboard IXSEA POSIDONIA USBL positioning system. Due to the malfunction of a DGPS System, performance of the USBL system was limited to an absolute accuracy around 10-20 m.

The substantial empty space inside the QUEST 5 frame allowes installation of mission-specific marine science tools and sensors. The initial vehicle setup includes two manipulators (7-function and 5-function), five video cameras, a digital still camera (Insite SCORPIO, 3.3 Megapixel), a light suite (with various high-intensity discharge lights, HMI lights, lasers, and dimmable incandescent lights), a CTD, a tool skid with drawboxes, an acoustic beacon finder and a 675 kHz scanning sonar. Total lighting power is 5 kW, and additional auxiliary power capacity is 8 kW.

For detailed video closeup filming, a near-bottom mounted broadcast quality (1000 TVL) HDTV camera was used (Insite Zeus) during the entire cruise. It allowed very high resolution macroscopic video observation and filming. Video footage was recorded with the Zeus camera and two additional color zoom video camera (Insite PEGASUS or DSPL Seacam 6500). In order to gain a fast overview of the dive without the need of watching hours of

video, one PAL and the HD video feed is continuously frame-grabbed and digitized at 5 sec intervals.

Table 3: Overview about ROV dives performed during Cruise M70/3 including major meta data and dive characteristics (ISPS: in-situ pore water sampler; GBS: gas bubble sampler).

Dive number/ GeoB	**Dive 129 / 11301**	**Dive 130 / 11304**	**Dive 131 / 11308**	**Dive 132 / 11310**	**Dive 133 / 11311**
Area	Amst. MV	Amst. MV	Amst. MV	Amst. MV	Amst. MV
Scientist	Bohrmann	Olu-Le Roy	Brinkmann	Waldmann	Gaßner
Water depth (m)	1985-2070	2024-2034	2000-2023	1998-2011	2023-2025
Date	28 Nov 06	29 Nov 06	30 Nov 06	01. Dec. 06	02. Dec. 06
Start at bottom (UTC)	08:38	08:46	13:37	14:10	07:55
End at bottom (UTC)	16:57	17:58	20:31	18:41	17:03
Bottom time (h:m)	08:19	09:12	06:54	04:31	09:08
Push cores (no.)	2	2			4
Rotary sampler	1				
GBS					2
Net	1	1		.	
Marker		No 1, 2, 3	No 4, 5		
ISPS					1
Carbonate	2		1		1
others					

Dive number/ GeoB	**Dive 134/ 11315**	**Dive 135/ 11319**	**Dive 136/ 11322**	**Dive 137 11326**	**Total dives**
Area	Amst. MV	Athina MV	Amst. MV	Thessal. MV	**9**
Scientist	Olu-Le Roy	Brüning	Olu-Le Roy	Bahr	
Water depth (m)	2025-2028	1799-1815	2025-2023	1339-1345	
Date	03. Dec. 06	04. Dec. 06	05. Dec. 06	06. Dec. 06	
Start at bottom (UTC)	08:23	11:51	11:58	12:39	
End at bottom (UTC)	17:57	17:21	20:26	19:56	
Bottom time (h:m)	09:34	05:30	08:28	07:17	**68:53**
Push cores (no.)				1	**9**
Rotary sampler	2	2			**5**
GBS					**2**
Net				1	**4**
Marker					**5**
ISPS					**1**
Carbonate		1			**5**
others	Blade corer	Tube worm		Tube worm	

The QUEST control system provides transparent access to all RS-232 data and video channels. The scientific data system used at MARUM feeds all ROV- and ship-based science

and logging channels into a commercial, adapted real-time database system (DAVIS-ROV). During operation, data and video are distributed in realtime to minimize crowding in the control van. Using the existing ship's communications network, sensor data are distributed by the realtime database via TCP/IP from the control van into various client laboratories, regardless of the original raw data format and hardware interface. This allows topside processing equipment to perform data interpretation and sensor control from any location on the host ship.

Additionally, the pilot's eight channel video display is distributed to client stations in labs and on the bridge of the ship via CAT5 cable. This allows the simple setup of detailed, direct communication between the bridge and the ROV control van. Similarly, information from the pilot's display is distributed to a large number of scientists. During scientific dives where observed phenomena are often unpredictable, having scientists witness a "virtual dive" from a laboratory rather than from a crowded control van allows an efficient combination of scientific observation and vehicle control.

Post-cruise data archival will be hosted by the information system PANGAEA at the World Data Center for Marine Environmental Sciences (WDC-MARE), which is operated on a long-term base by MARUM and the Alfred-Wegener-Institute for Polar and Marine Research, Bremerhaven (AWI). During Cruise M70/3, additional scientific sampling equipment was installed:

1. rotary sampler with suction hose and capability of up to 8 discrete samples,
2. gas tight fluid samplers,
3. push cores,
4. various "hand" tools including nets, scoops, markers. In addition, the Kongsberg 625 kHz scanning sonar head provided acoustic information of bottom morphology and was used to detect and follow gas emissions at distances up to 50 m.

5.2 Dive 129 (GeoB 11301)

Area:	Amsterdam Mud Volcano, Anaximander Mountains Eastern part of the crater		
Responsible scientist:	Gerhard Bohrmann		
Date:	Tuesday 28 November 2006		
Start/end at Bottom (UTC)	08:38/16:57		
Total bottom time	8 h, 19 min		
Start at the bottom:	35°20.000'N	30°16.087'E	2070 m water depth
Start ascend:	35°19.850'N	30°14.860'E	1985 m water depth

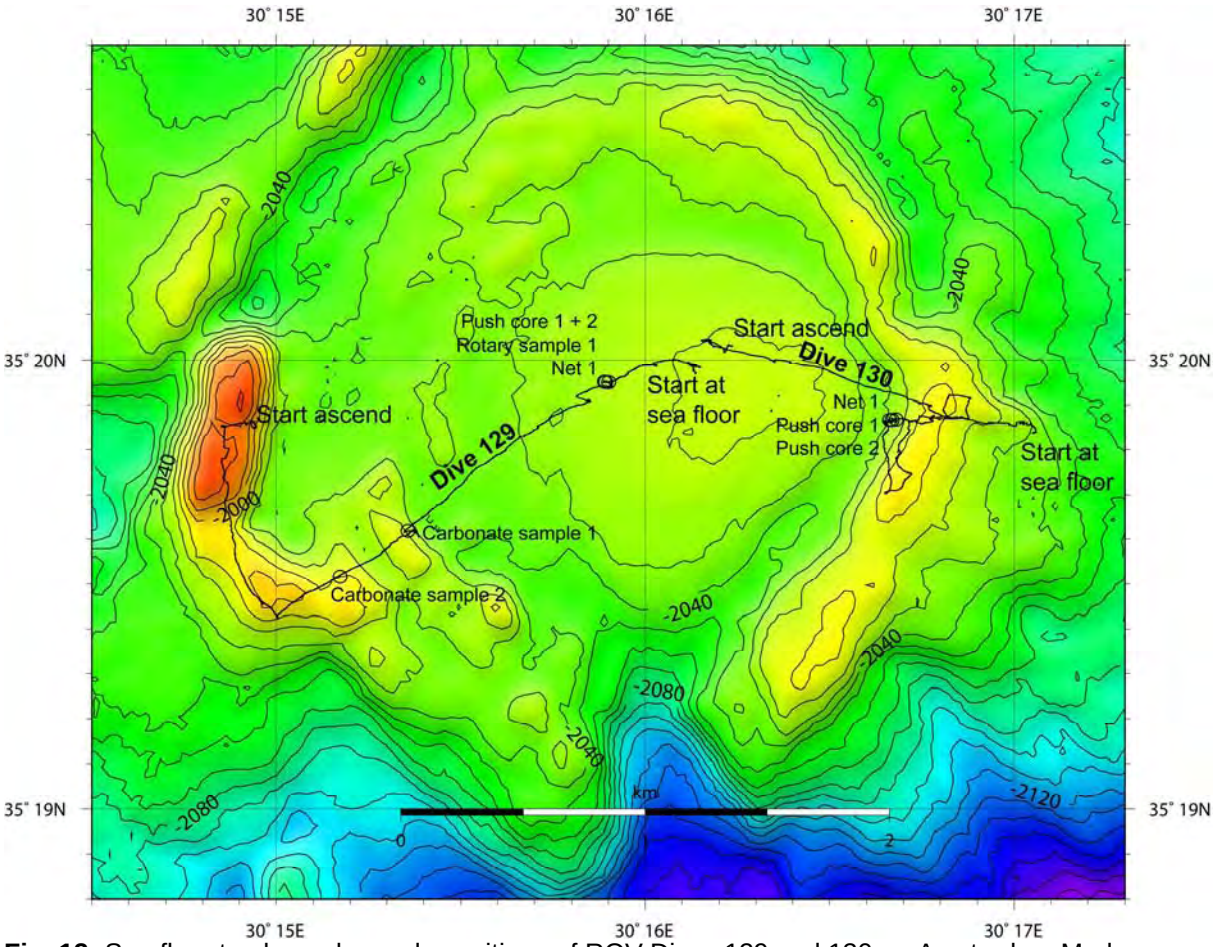

Fig. 12: Sea floor tracks and sample positions of ROV Dives 129 and 130 on Amsterdam Mud Volcano.

The first dive of the cruise (Dive 129) started on the sea floor in the centre of the mud volcano in the area which in general looked smooth at the bathymetric map (Fig. 12). A set of waypoints was used to guide the ROV QUEST to the southwestern rim of the Amsterdam mud volcano and then along the outer wall to the north from where the ROV ascended after more than 8 hours bottom sight (Fig. 12). Although the bathymetric map revealed a flat area in the centre the see floor looked rough, where hills and depressions on a scale of 1-5 m difference in height were present. In some areas accumulations of white shells have been observed as well as rock clasts of different sizes. Active seep sites were characterized by dark sediment colour, most probably caused by a sulphide-rich environment which contained also white patches from which we assumed that those areas represent accumulations of bacterial filaments. Two push cores have been taken, one within the seep area (GeoB 11301-1; push core 1; Fig. 13 left) and the other outside the dark seep environment (GeoB 11301-2; push core 2) representing non-seep background sediment. A rotary sample (GeoB 11301-3; Rotary sample 1; GeoB 11301-4; net 1) as well as a net collected animals and other constituents of the seep sediments.

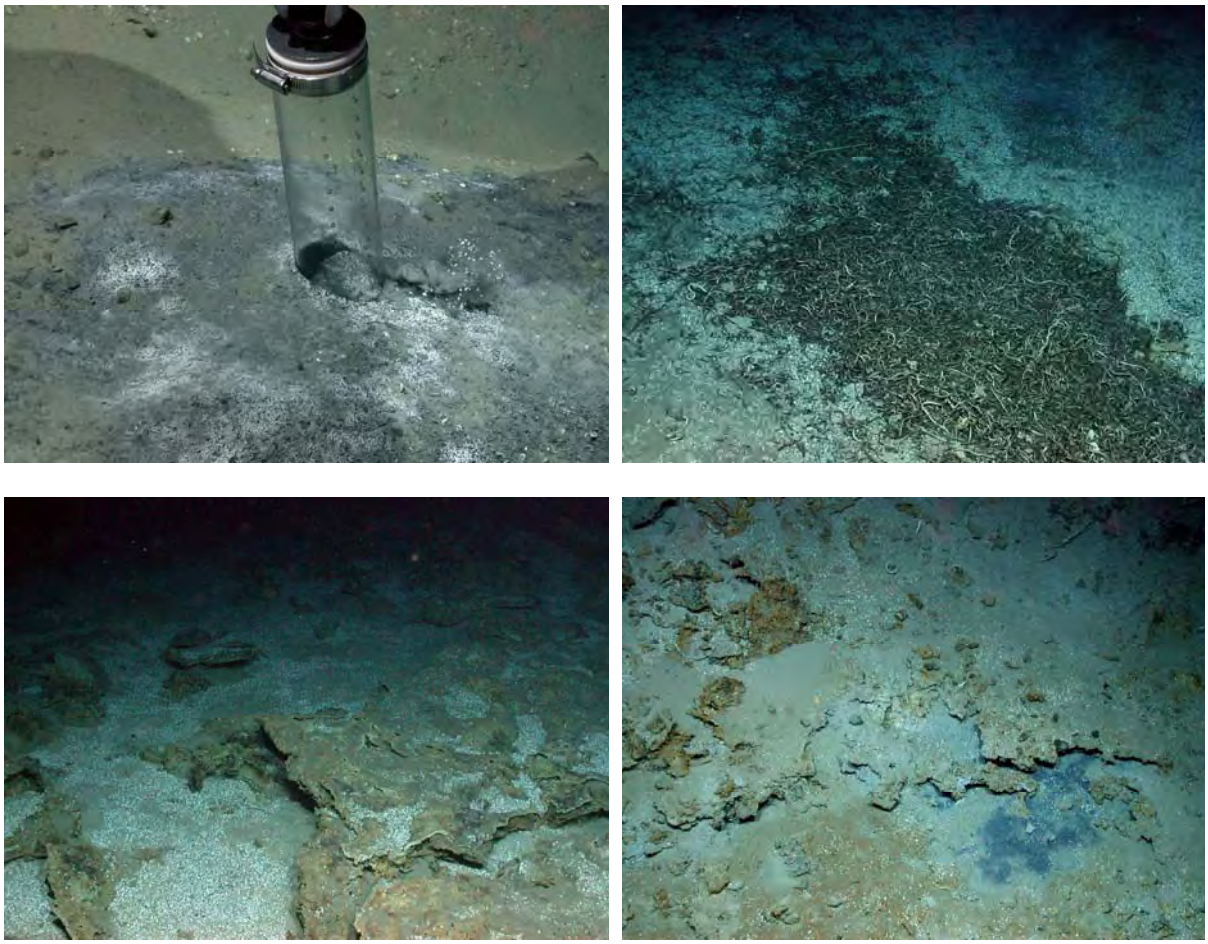

Fig. 13: Sea floor images taken during ROV Dive 129. Push core 1 was taken in an area where sea floor was coloured by sulfides and probably by bacterial mats (above left). Accumulation of dead tube worms in a depression (above right). Carbonate pavement on the sea floor filled by chemosynthetic shells in depressions (below left). Active seepage shown by a sulphide-rich patch within an environment dominated by authigenic carbonate crusts (below right).

On the way towards southwest the ROV QUEST crossed the inner ring depression and moved more than 20 m upwards following the sea floor to a first elevation (Fig. 12). This structure which followed in parts the curved wall structure showed steeper flanks covered by carbonate crust blocks and fractured plates. Tube worms in different densities are settling between the carbonate crusts, where they can root in sulphide-rich sediments. Two carbonates specimen have been sampled by the manipulator arm of ROV QUEST. One was taken on the northern flank (GeoB 11301-5; carbonate 1) of the first ridge and the second on the outer ridge (GeoB 11301-6; carbonate 2) which followed as a parallel to the first ridge in southwest direction (Fig. 12). Sea floor on the outer ridge appeared more densely covered by carbonate crusts and in one case we could observe a large accumulation of dead tube worms (Fig. 13) and a porcelain vase on the sea floor as a sign of human activities. ROV dive changed the direction when we reached the outer flank of the mud volcano and the vehicle moved along the outer ridge to the north. After a while we could observe a more flat sea floor area, which we selected for the upcoming deployment of the moving lander MOVE. We finished the dive at around 16:57 and started ascend from the bottom.

5.3 Dive 130 (GeoB 11304)

Area:	Amsterdam Mud Volcano, Anaximander Mountains Eastern part of the crater
Responsible scientist:	Karine Olu-Le Roy
Date:	Wednesday 29 November 2006
Start/end at Bottom (UTC)	08:46/17:58
Total bottom time	9 h, 12 min
Start at the bottom:	35°19.854'N 30°17.006'E 2034 m water depth
Start ascend:	35°20.041'N 30°16.168'E 2024 m water depth

The first task was to explore the eastern part of the Amsterdam mud volcano to find Siboglinidae tube worm bushes observed during the French MEDINAUT cruise in 1998. During the first part of the dive few carbonate and tube worm areas were observed in very rough seabed morphology with deep canyons or depressions, sea floor cracks and ridges, with fresh slide scars (Fig. 14). Some black spots likely related to fresh seeps were also observed going to the south (see dive track in Fig. 12).

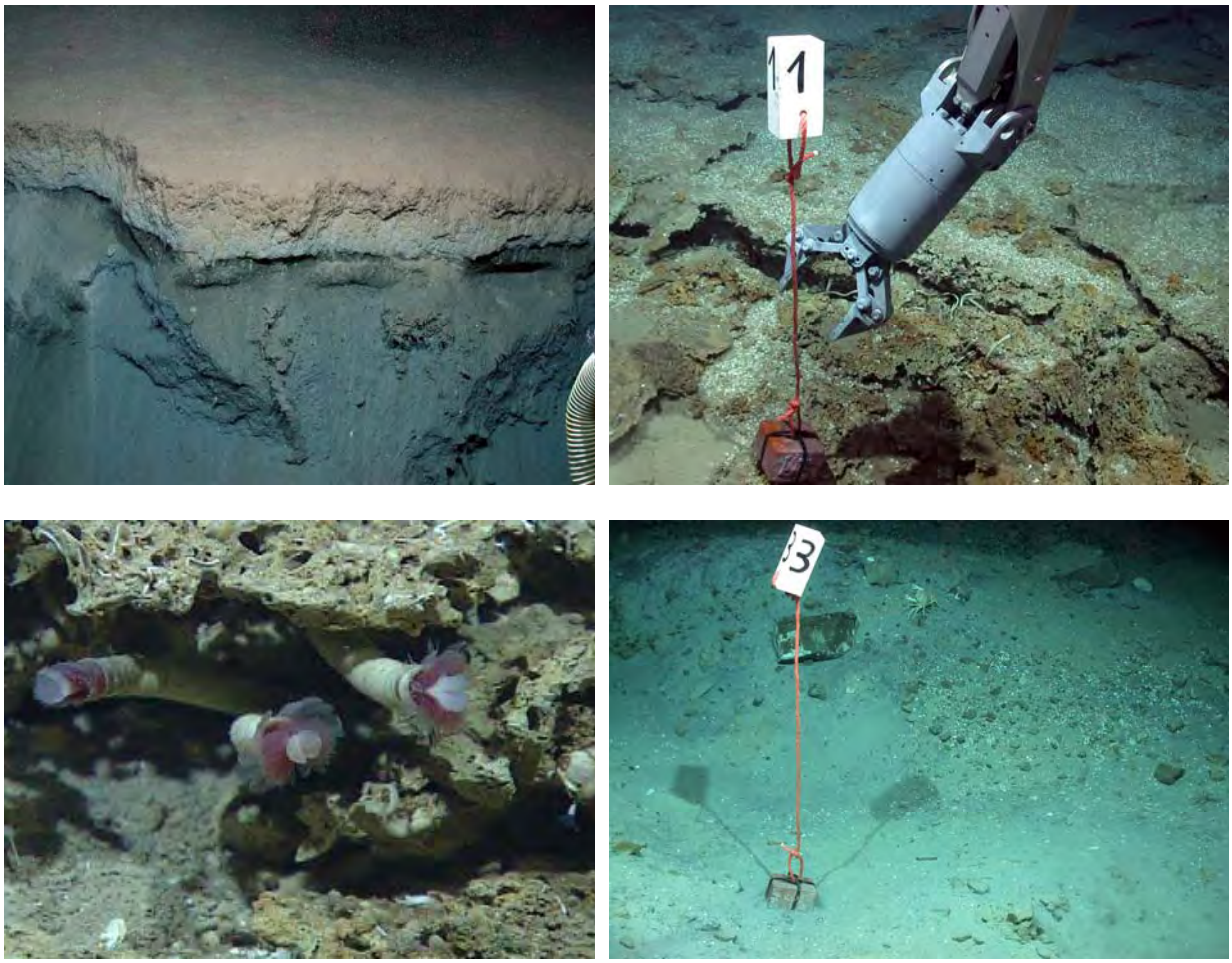

Fig. 14: Sea floor images taken during ROV Dive 130 at Amsterdam Mud Volcano. Outcrop of near-surface sediments shows fresh sediment colours (above left). Marker 1 deployed at the eastern rim of the mud volcano within a carbonate environment (above right). Tube worms are living (below left). Sea floor morphology and structure in the central part of the mud volcano at Marker 3. Bubble streams of free gas have been found (below right).

We went in the northern area again to find more areas where tube worms settled. A black spot with small tube worms, may be young siboglinid polychaetes was chosen for sampling of two push cores 1 and 2 (GeoB 11304-2; GeoB 11304-3) and a net (GeoB 11304-1). Siboglinidae tube worms (Marker 2: 35°19.864'N, 30°16.668'E) were observed in a carbonate area, HDTV images of high quality were recorded (Fig. 14) and Marker 1 was deployed at 35°19.901'N, 30°16.743'E.

The sonar was used in the second part of the dive to look for sites where bubbles escape at the sea floor in the central part of the volcano. A bubble site was found and Marker 3 was deployed at 35°20.043'N, 30°16.174'E. Backscatter data from the bubbles were recorded by the foreward-looking sonar up to 1550 m (~500 m above the sea floor).

5.4 Dive 131 (GeoB 11308)

Area:	Amsterdam Mud Volcano, Anaximander Mountains Northwestern part of the crater		
Responsible scientist:	Florian Brinkmann		
Date:	Thursday 30 November 2006		
Start/end at Bottom (UTC)	13:37/20:31		
Total bottom time	6 h, 54 min		
Start at the bottom:	35°19.900'N	30°14.958'E	2000 m water depth
Start ascend:	35°20.035'N	30°16.190'E	2023 m water depth

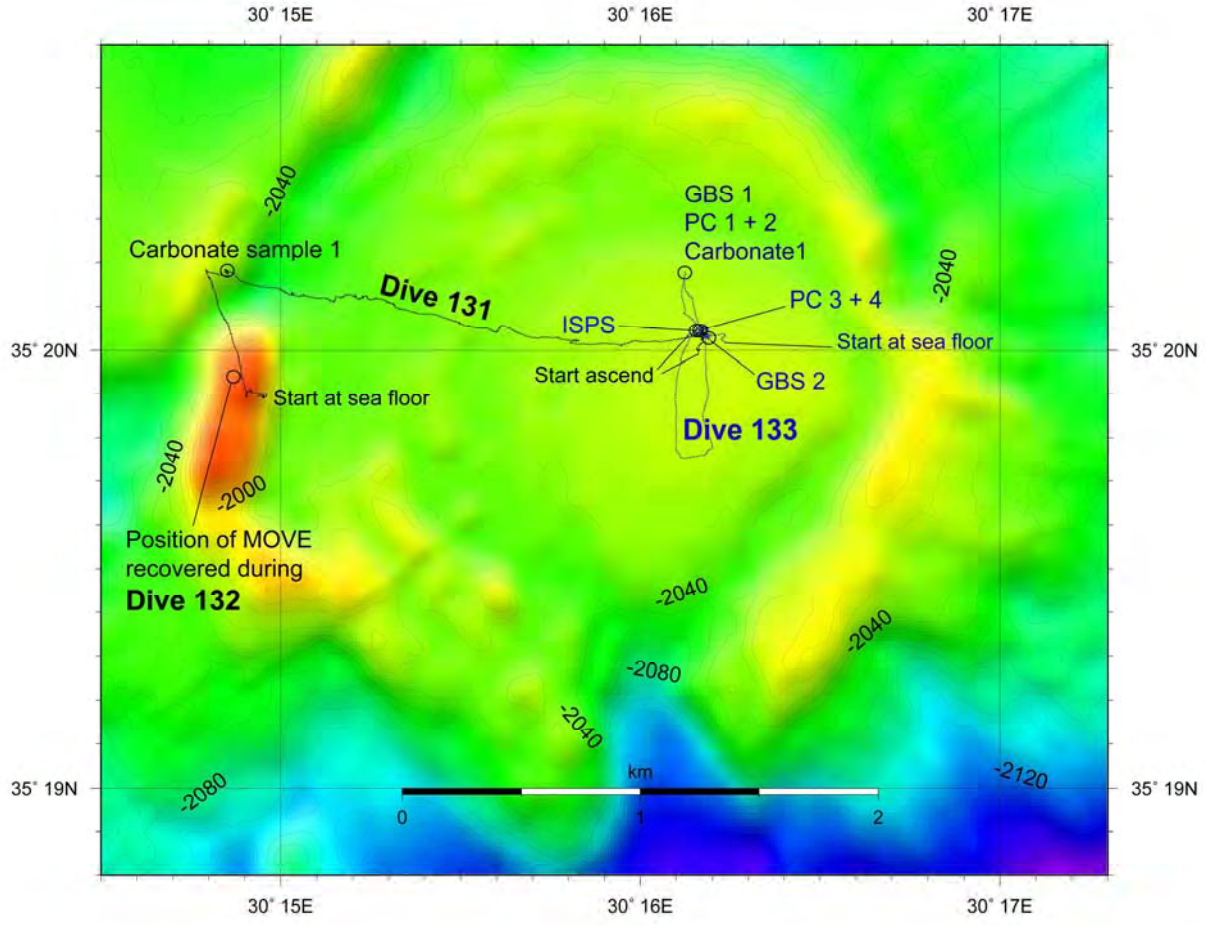

Fig. 15: Sea floor tracks and sample positions of ROV Dives 131 and 133 on Amsterdam Mud Volcano.

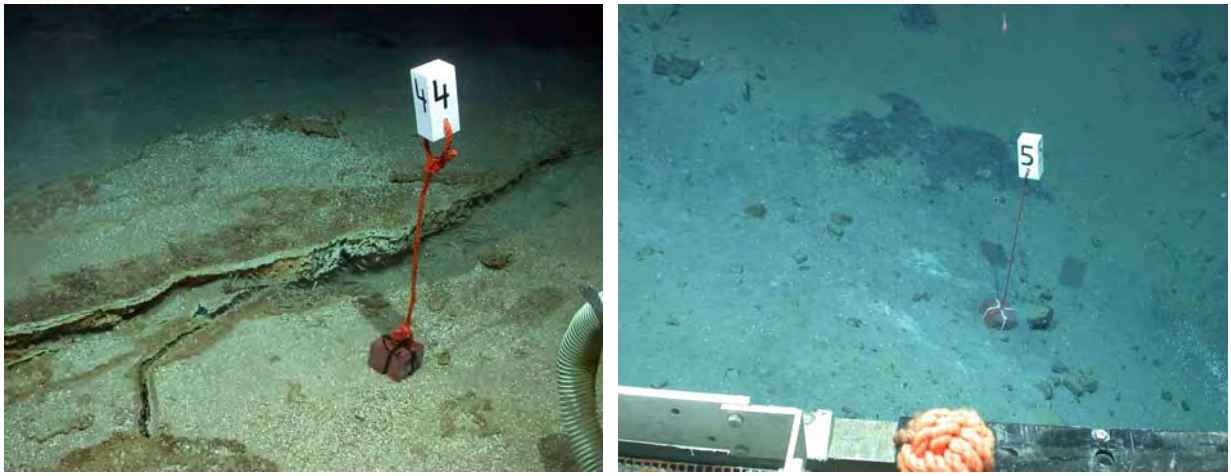

Fig. 16: ROV Dive 131 images: Carbonate pavement with settlement of tube worms in cracks at Marker 4 (left). Dark coloured seep site in the central part of the mud volcano at Marker 5 (right).

The main objective of Dive 131 was to explore and survey the western part of the Amsterdam mud volcano north of the Dive 129 track (Fig. 15). The dive started quite exactly at the same point where Dive 129 was finished. Seepage sites of visible active bubble expulsion should be found. This was done by flying about two metres above the ground. The survey followed a previously fixed track of seven waypoints, leading from the outer easter rim to the centre of Amsterdam mud volcano (Fig. 15). After a short time having a very rough topography that was very similar to the one we saw during Dive 129, the first part of the dive revealed a rather flat topography. The sea floor surface was covered with clams and shells. Shortly after the ROV turned eastwards (Fig. 15), the condition of the sea floor surface changed. Carbonate crusts occurred more and more (Fig. 16) and at fractures tube worms (sigoblinidae polychaetes) grew out of the very porous crust in a high density (Fig. 16). As a possible site for long time observation, e.g. by the imaging module (AIM) of tube worms Marker 4 was set at. 35°33.640'N, 30°24.740'E (Fig. 16).

A sample of the carbonate crust, that was covered by many shells and also built up by remains of other biota, was taken with the arm of the ROV QUEST (GeoB 11308-1). Shortly after leaving Marker 4, the sea floor surface turned to be flat surface. Occasionally it was covered with shells and at some site single tube worms have been observed. Coming closer to the centre of the mud volcano an alternating graben and canyon (about 5 metres deep) structures marked by fresh slide scraps were dominant. While most of these structures were linear in different scales (between 5 metres and a few centimetres in depth) others were more or less round. When we entered the inner part of the mud volcano the ROV ascended to about 25 metres altitude and we started to use the sonar to look for gas bubbles. After a few hours finally some bubbles were found and the origin was observed. The site where the bubbles were expelled was a similar seep site like the one we found during Dive 130 with some bacterial patches on a rough topography. There were no carbonate crusts. As we had to ascend and finish this dive we deployed Marker 5 at 35°20.049'N, 30°16.178'E (Fig. 16).

5.5 Dive 132 (GeoB 11310)

Area:	Amsterdam Mud Volcano, Anaximander Mountains Central area of the crater
Responsible scientist:	Christoph Waldmann
Date:	Friday 01 December 2006
Start/end at Bottom (UTC)	14:10/18:41
Total bottom time:	4 h, 31 min
Start at the bottom:	35°19.752'N 30°15.116'E 1998 m water depth
Start ascend:	35°19.303'N 30°14.131'E 2011 m water depth

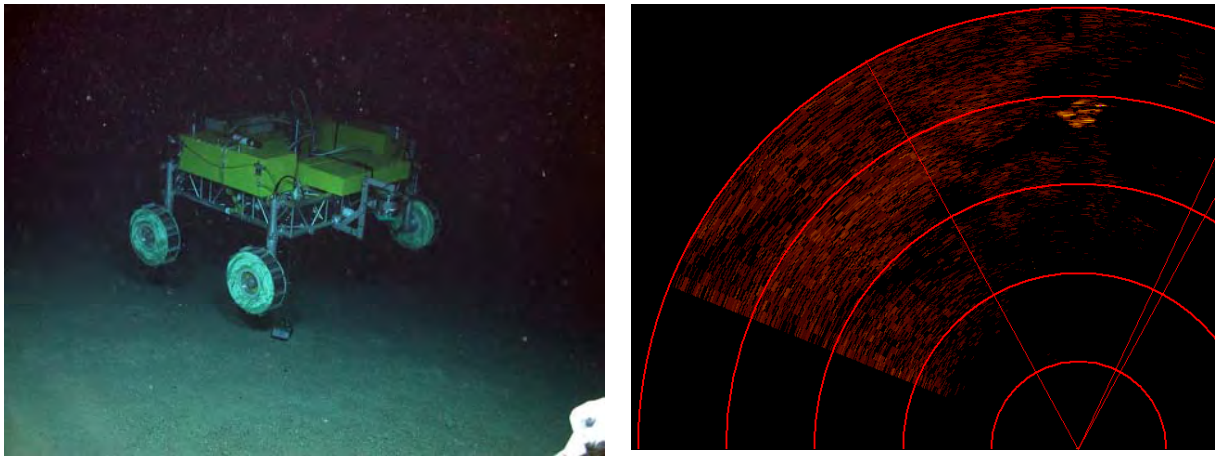

Fig. 17: Image from lander MOVE which floated some cms above the sea floor (left). Image from forward looking sonar detected lander MOVE 20-24 m ahead (right).

The first part of the dive was dedicated to find the moving lander on the sea floor and to explore the situation, why MOVE did not come up after it was released. MOVE was deployed the day before in a flat area of the southwestern part of the mud volcano (Fig. 15; see Chapter 6). The system was connected by a thin fibre optic cable, which should establish data transmission from the lander to the ship. This connection failed and it was then decided to release the moving lander from its weights in order to come up which failed also. ROV QUEST found the lander first by using the sonar (Fig. 17 right). After the ROV moved closer to the lander it became clear that the fibre optic cable got tangled in the drop weight which prevented the system to come up. After the fibre was cut through by a knife the vehicle moved upwards by its lifting bodies. After that part the dive was used to explore the southwestern part of the mud volcano without taking further samples. Rough topography with many fresh outcrops and carbonate crusts have been seen on the way to the centre of the mud volcano.

5.6 Dive 133 (GeoB 11311)

Area:	Amsterdam Mud Volcano, Anaximander Mountains Central area of the crater
Responsible scientist:	André Gaßner
Date:	Saturday 02 December 2006
Start/end at Bottom (UTC)	07:55/17:03
Total bottom time:	9 h, 8 min
Start at the bottom:	35°20.048'N 30°16.158'E 2025 m water depth
Start ascend:	35°20.051'N 30°16.144'E 2023 m water depth

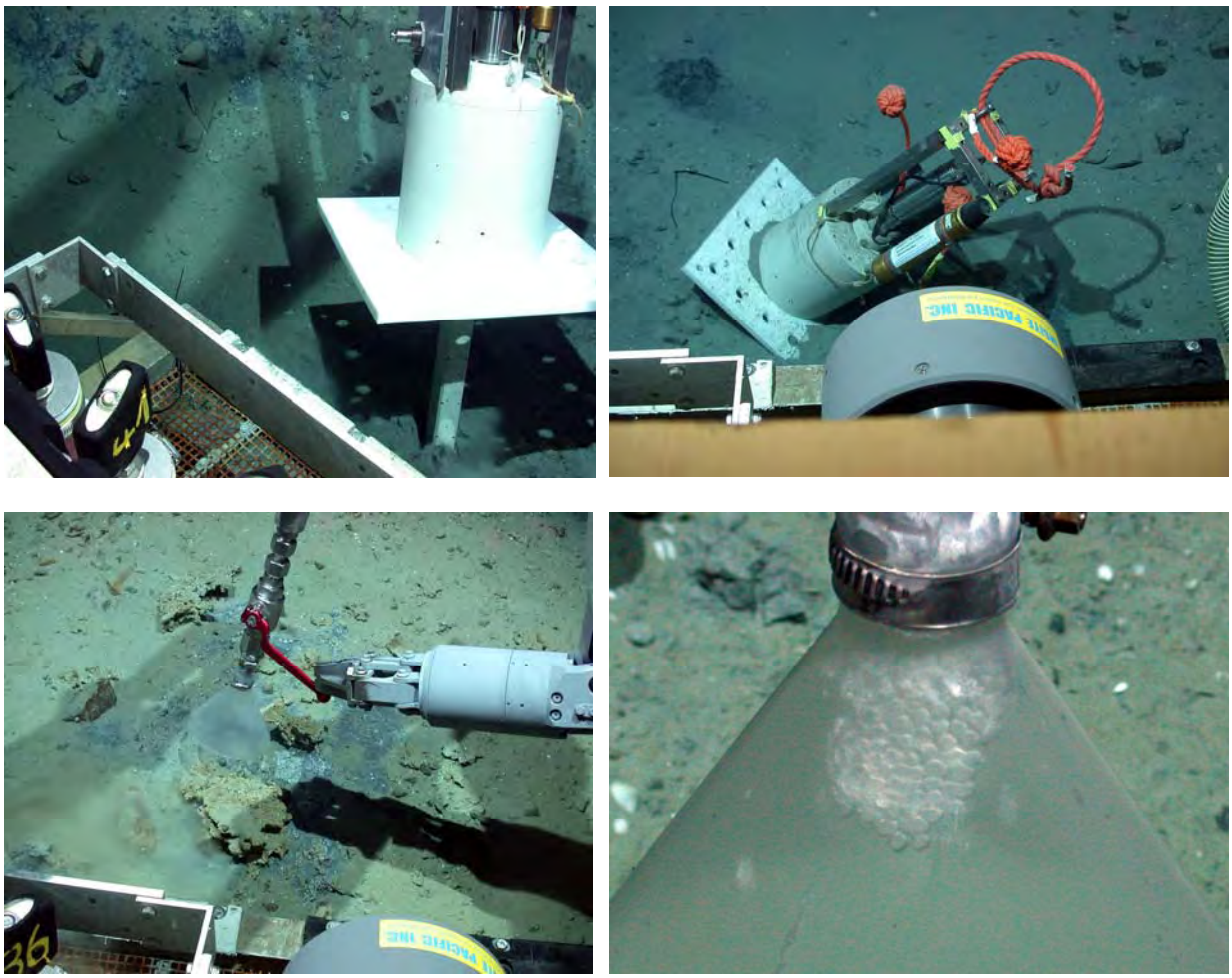

Fig. 18: In-situ Pore Water Sampler (ISPS) during Dive 133 deployment (above left) and during recovery at the end of the dive (above right). Gas bubble sampler (GBS) deployment above free gas bubbles emanating from the sea floor (below left). Gas bubbles collected in the funnel of GBS are coated by hydrate skins (below right).

The main objective of Dive 133 was to deploy the in-situ-pore water sampler (ISPS), and to sample gas with two pressure tight gas samplers and pore water profiles by 4 push cores. Additionally exploration and gas bubble survey with the forward-looking sonar of QUEST was performed. The dive started near the location of Marker 5 (35°20.037'N 30°16.185'E). The gas seepage site of visible active bubble expulsion should be found to deploy the tools. After approx. 30 minutes flight over a relatively rough seabed morphology with many clasts and dark patches, likely related to seeps, the bubble site was found. After having parked QUEST,

the ISPS (GeoB 11311-1) was successfully deployed directly into the bubble site (Fig. 18 left). Gas bubbles with the pressure tight fluid sampler (GeoB 11311-6; Fig. 18 right) and two push core samples (GeoB 11311-7, and GeoB 11311-8) should have been taken at this site as a reference for the ISPS, but due to a very bad visibility this task was shifted to the end of the dive. QUEST then flew northwards to deploy the fluid sampler over a dark seep patch. After approx. 500 m an appropriate site was found. Fluids seeping out of this dark patch were sampled with this device (GeoB 11311-2). Additionally 2 push cores (GeoB 11311-3, and GeoB 11311-4) were taken. The area was covered with many clasts and some smaller pieces of carbonate precipitates. One of these pieces was sampled with the ORION (GeoB 11311-5). QUEST then headed back to Marker 5 to deploy the fluid sampler over the bubble site and to take two push cores. After having sampled this site QUEST headed southwards again to unsuccessfully start searching for gas bubbles in the water column. The final task then was to recover the ISPS.

5.7 Dive 134 (GeoB 11315)

Area:	Amsterdam Mud Volcano, Anaximander Mountains eastern rim and central part		
Responsible scientist:	Karine Olu-Le Roy		
Date:	Sunday 3 December 2006		
Start/end at Bottom (UTC)	08:23/17:57		
Total bottom time:	9 h, 34 min		
Start at the bottom:	35°20.049'N	30°16.153'E	2028 m water depth
Start ascend:	35°20.100'N	30°15.325'E	2025 m water depth

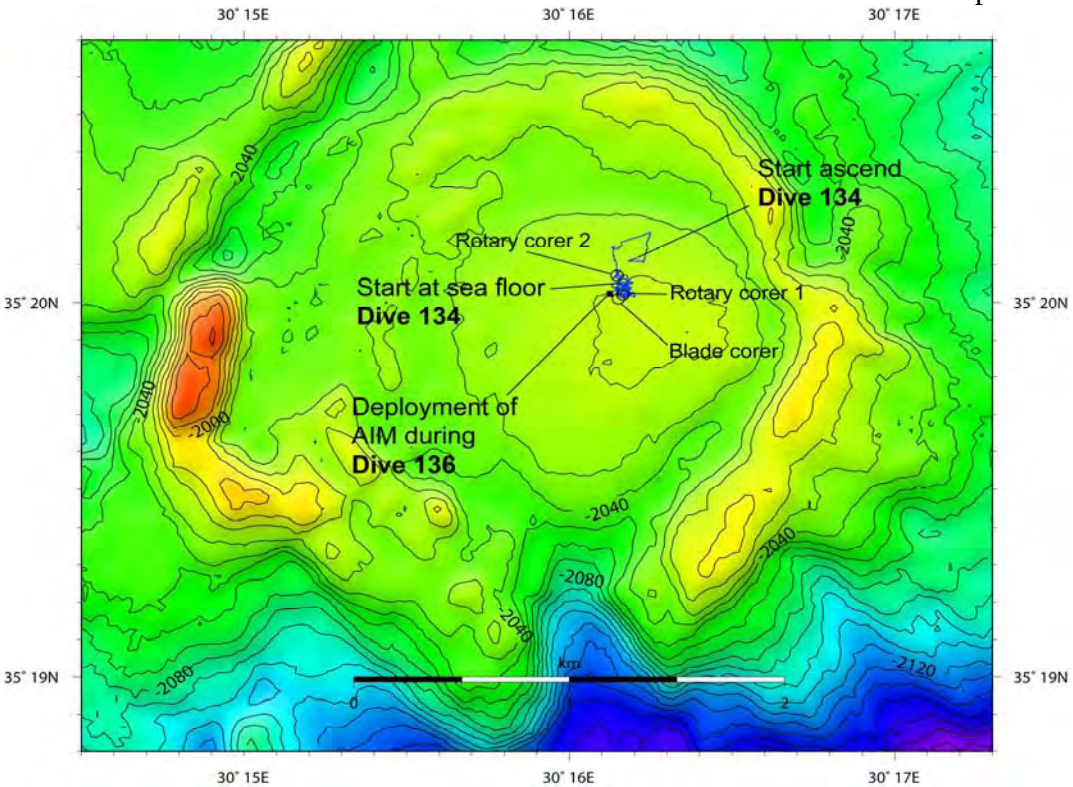

Fig. 19: Sea floor track of ROV Dive 134 in the central part of Amsterdam Mud Volcano. The position of the Autonomous Imaging Module (AIM) deployed during QUEST Dive 136 is also shown.

The main objective of this dive was to deploy two colonizator devices: the large one ("SMAC") is composed of 4 bowls filled with glass bowls enriched with organic matter at different concentrations and is dedicated to settlement experiments of species living in the soft substratum. The second one ("Rack") is made of twenty slates for settlement of hard substratum species. Both were deployed at a bubble site of Marker 5 deposed during Dive 131 and also sampled for gas during Dive 133 (Fig. 20 left). A blade corer to sample macrofauna was successfully used at the same site and in addition a rotary sample for gastropods (GeoB 11315-1).

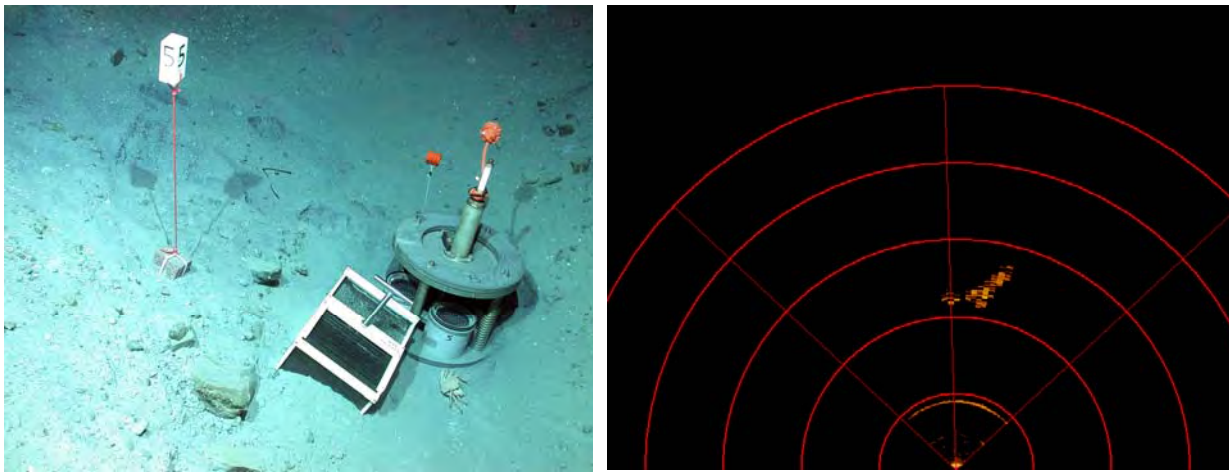

Fig. 20: Sea floor deployment of two colonizator devices at Marker 5 (left). Image from the forward looking sonar which detected a bubble stream approximately 4-8 m in front of ROV QUEST (right).

Marker 5 was found after two hours, because of positioning problems (up to 50 m shift). The second objective was the survey for additional gas bubble sites. A new site was detected on the sonar with a more active bubble stream (Fig. 20 right). Several holes where bubbles escape were observed on the sea floor. A rotary sample was done and revealed the occurrence of high density of vesicomyid bivalves (GeoB 11315-2). Finally two living and two dead *Lamellibrachia* sp. siboglinid tube worms were sampled on the ridge close to the bubble site (GeoB 11315-3).

5.8 Dive 135 (GeoB 11319)

Area:	Athina Mud Volcano		
Responsible scientist:	Markus Brüning		
Date:	Monday 04 December 2006		
Start/end at Bottom (UTC)	11:51/17:21		
Total bottom time:	5 h, 30 min		
Start at the bottom:	35°23.197'N	30°12.745'E	1799 m water depth
Start ascend:	35°23.447'N	30°12.659'E	1815 m water depth

Dive 135's target was the exploration of the Athina Mud Volcano, about 8 km northwest of Amsterdam Mud Volcano. The dive started on a southern high of the volcano (Fig. 21). The

track of the ROV formed a half-circle on the sea floor over the outer south-western elevated ring. The sea floor at the beginning of the dive was covered with carbonate-blocks of several decimetres to several metres in diameter.

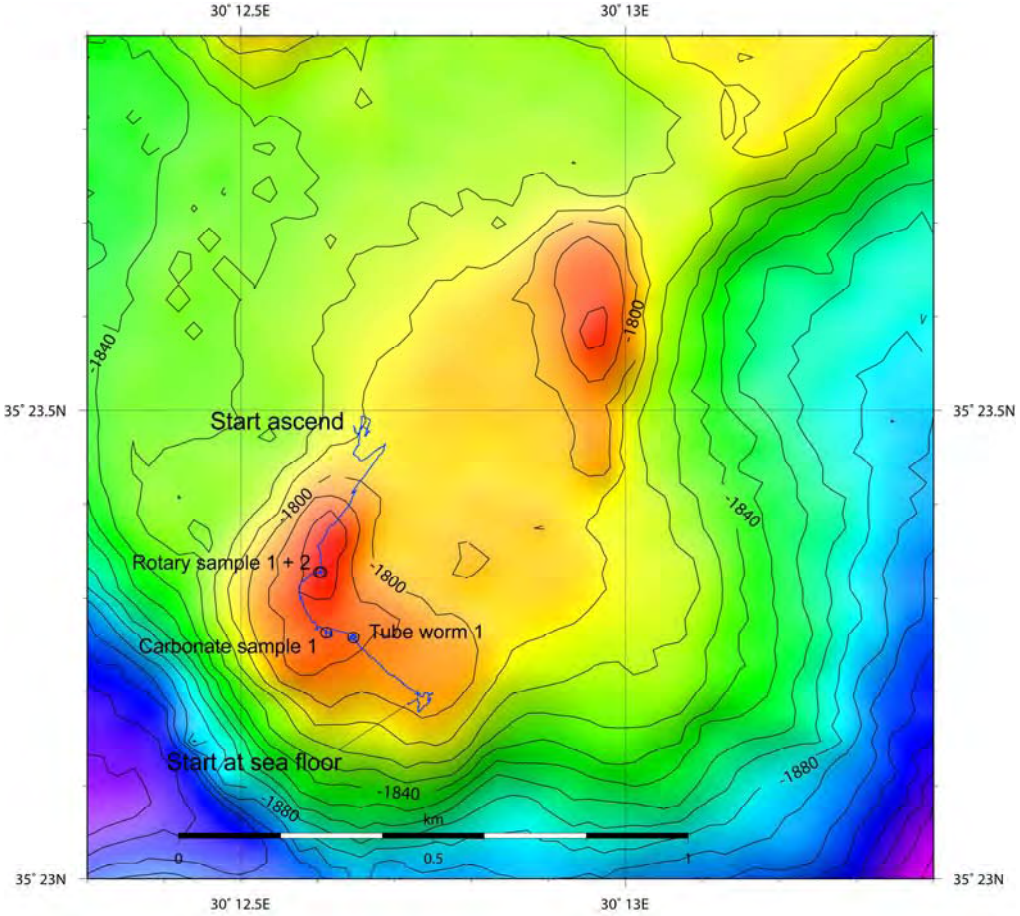

Fig. 21: Track and sampling positions of ROV Dive 135 on Athina Mud Volcano.

At 12:21 a colony of hundreds of tube worms was reached (Fig. 22). The colony might be 4-5 m x 2 m in area and is ca. 4 m high. Living tube worms of ca. 50 cm length are sitting on an unknown structure. No solid carbonate block or similar is visible as a basement of the elevated living population. In the background bacterial mats were visible. Between and over the tube worm colony several other animals could be seen: arthropods, crabs, fish and sea urchians. The scenery was extensively recorded with the Zeus-HD-camera. A few metres further west smaller colonies of only dozens of tube worms were based at the ground on the border between sediment and carbonate rocks. These tube worms are only 10 to maximum 20 cm long.

Again a few metres further on, embedded in a steep wall of the carbonate blocks, between the top and a second lower terrace a network of black tubes appeared (Fig. 22 right). The network was about 60 cm wide and 30 cm high. It probably existed of cemented dead tube worms. A first attempt to sample this with a net was unsuccessful. The material was not brittle enough. The ROV arm broke out a coin-sized piece, and latter a 30 cm long piece (GeoB 11319-1). After the sampling the dive to the summit of the western ridge was continued. Unfortunately the POSIDONIA positioning system was not working properly here. DVL navigation was used instead.

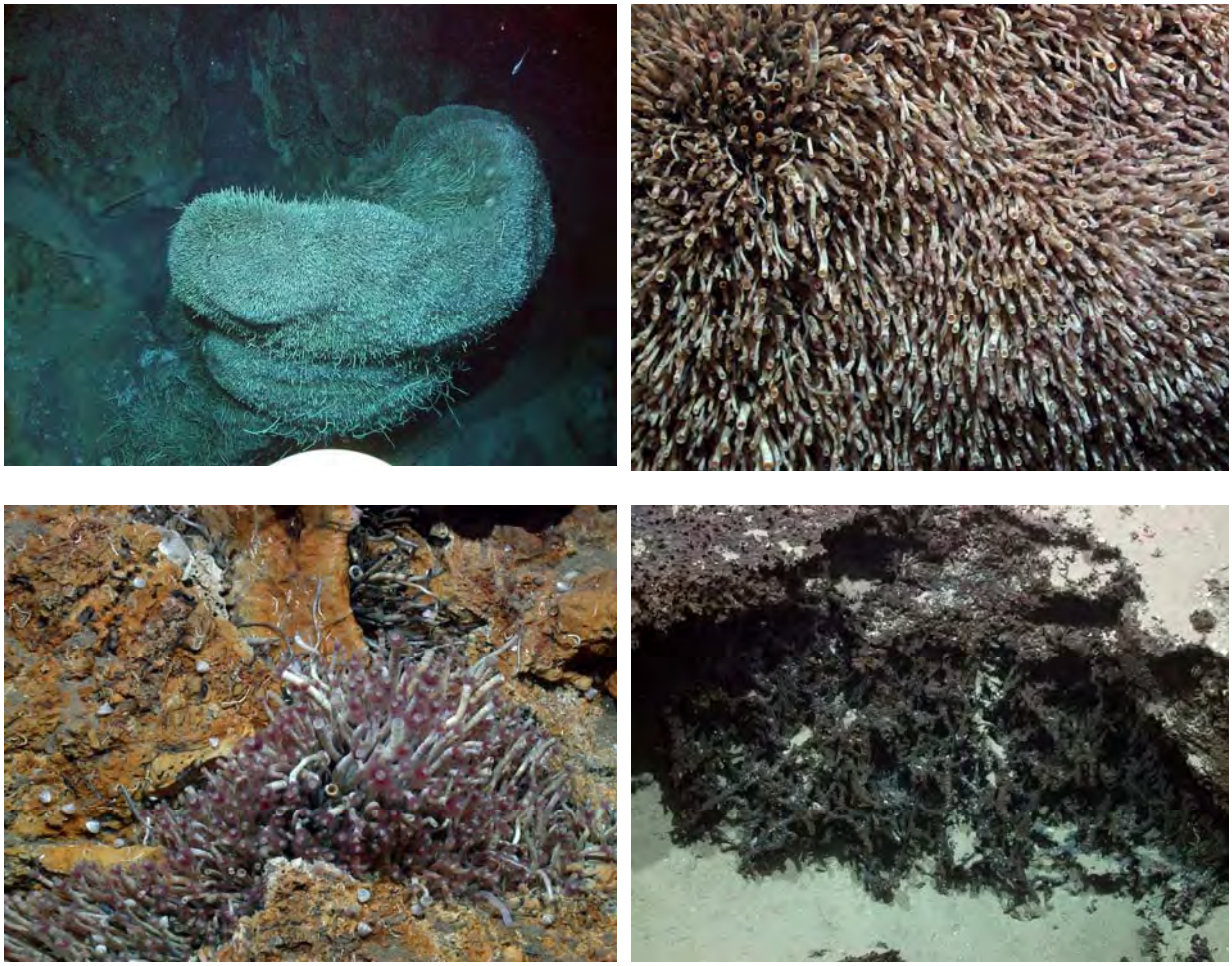

Fig. 22: Tube worm colonies found at the southwestern (above left) and during recovery at the end of the dive (above right). Carbonate and tube worm environment (below left) and fossile tube worms (below right) at the Athina Mud Volcano.

On an 80° inclined slope biological indications for venting occurred sporadically: some tube worms, dead and alive, bacterial mats, and shells. Several carbonate pieces covered the slope. A Zeus-HD sequence was recorded. Due to the steepness of the slope the ROV continued up without sampling, to prevent dangerous avalanches. Further up the slope chemoherm-carbonates were exposed. Many finger thick holes covered the carbonate. Tube worms were living in some of them. The robot-arm broke off a sample of 20 x 30 x 5 cm in size from the exposed carbonate (GeoB 11319-2). The track was continued northwards towards the summit. POSIDONIA started to work again. The ground was covered by carbonates. The ROV moved up to 15 to 30 m altitude above the sea floor to survey around for bubbles by using the sonar. Unfortunately there was no success On the summit a ring of rocks with pure sediment in the middle was passed. Further on the ROV, coming up to some kind of plateau, reached a spot of vent activity. Tube worms, bivalves, and maybe bacterial mats settled on the dark grey sea floor. Sampling by push core failed, the rotary sampler was used to sample the whitish particles which could not be identified by camera inspection (GeoB 11319-3 and 4). From the sampling on the summit the ROV moved northwestwards down along the crest. The sea floor consisted of much smaller carbonates and patches between plain sediment-covered

areas. The ROV again moved upwards to search for bubbles with the sonar. After a short view on mainly plain sea floor the dive was finished at 17:20 UTC.

5.9 Dive 136 (GeoB 11322)

Area:	Amsterdam Mud Volcano, Anaximander Mountains
Responsible scientist:	Karine Olu-Le Roy
Date:	Tuesday 05 December 2006
Start/end at Bottom (UTC)	11:58/20:26
Total bottom time:	8 h, 28 min
Start at the bottom:	35°16.164'N 30°16.164'E 2025 m water depth
Start ascend:	35°19.736'N 30°15.280'E 2023 m water depth

The main objective of this dive was to deploy the Autonomous Imaging Module (AIM) at a bubble site. The starting point was the active bubble site at Marker 6. The bubble stream was quickly detected on the sonar and after 1h 30 min the AIM was on the sea floor (Fig. 23). After testing and controlling the view angle, and zoom from the ROV container using the wireless connection, testing the lights without QUEST lights the activation of the periodic mode (one minute video every 12 hours) was done one hour after deployment. The view that will be recorded was checked. The camera focussed on the bubbling hole that we hope to see on the video, and gastropods. A crab was seen at this site, like at all the bubble sites visited. Marker 6 was put at the deployment site.

The second objective was to survey at the PARASOUND plume site at 35°19.5943'N 30°14.999'E. Bacterial mats, clam shells and very long tube worms were observed between the two targets. No bubbles were observed on the sonar backscatter.

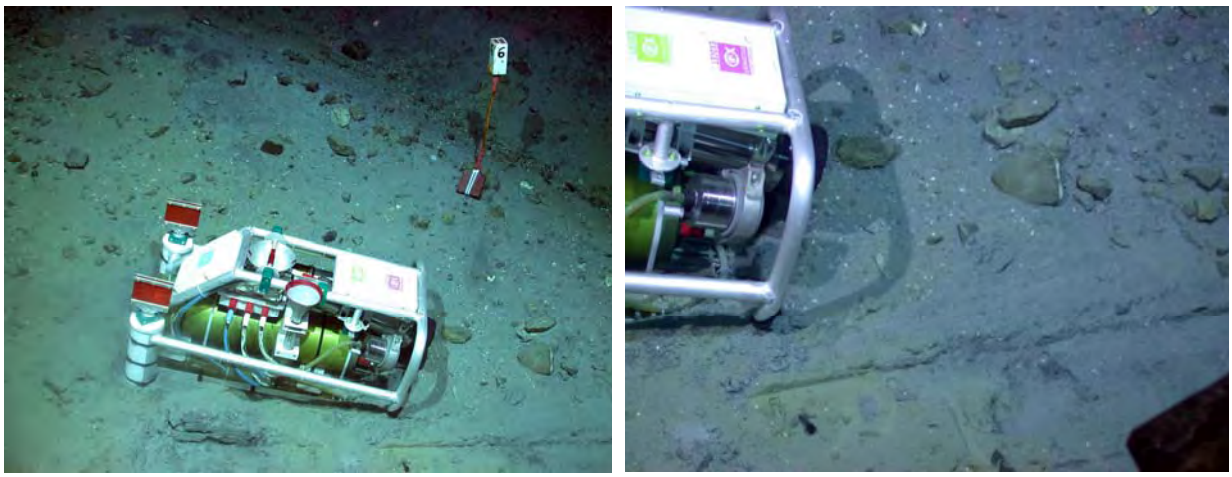

Fig. 23: Deployment of the Autonomous Imaging Module (AIM) at bubble site of Marker 6 (left). Detail of the frontal part of AIM showing the location on which the camera is focused (right).

5.10 Dive 137 (GeoB 11326)

Area:	Thessaloniki Mud Volcano, Anaximander Mountains		
Responsible scientist:	André Bahr		
Date:	Wednesday 06 December 2006		
Start/end at Bottom (UTC):	12:39/19:56		
Total bottom time:	7 h, 17 min		
Start at the bottom:	35°28.289'N	30°15.693'E	1345 m water depth
Start ascend:	35°28.509'N	30°15.403'E	1339 m water depth

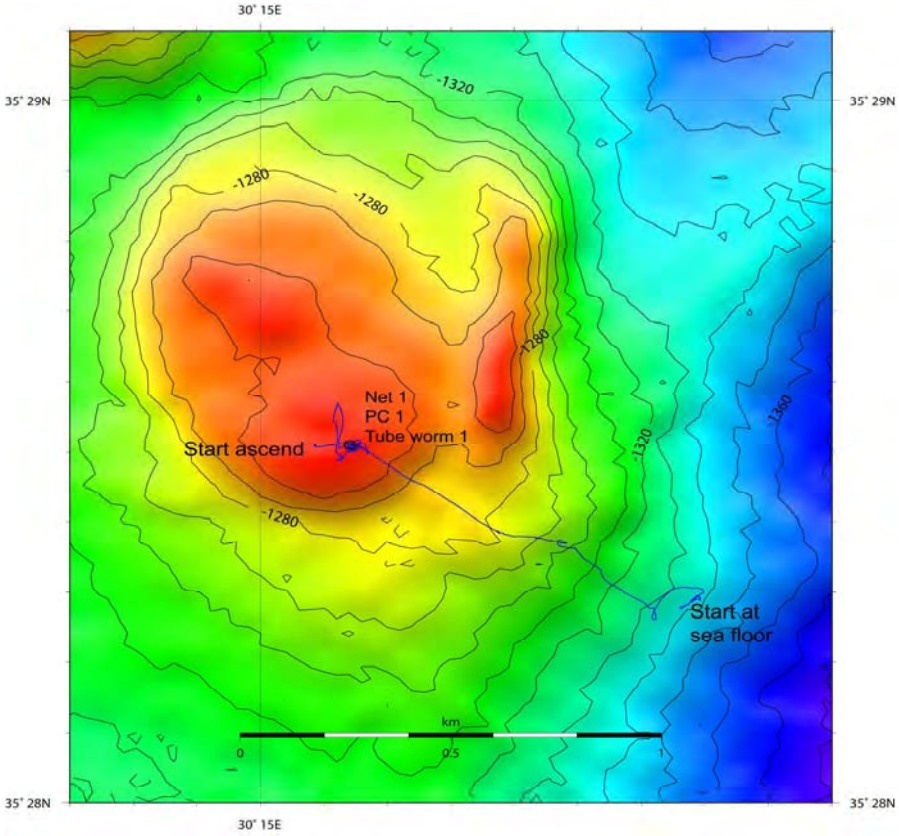

Fig. 24: Track of ROV Dive 137 on the Thessaloniki Mud Volcano.

Fig. 25: High-resolution images taken during ROV Dive 137. Sea floor area with parallel ridges and some patches with bivalves and pogonophora (left) zoom into zone with abundant bivalve shells, pogonophora (upper left corner) and brecciated rock fragments (right).

The task of Dive 137 was to find and document seeps at the Thessaloniki mud volcano. The route of the dive was constructed following observations of potential plume positions in the PARASOUND record. These plumes were supposed to be found with sonar flights and direct observations at the sea floor. After reaching the starting point on the southwestern flank of the mud volcano, the initially planned direction towards the summit was changed after a short while, because of the news of a plume observed in the PARASOUND record nearby the start position of the dive (Fig. 24). However, the sonar-survey from the ROV did not give any positive results, so the initially planned survey track along the presumed gas bubble sites was resumed, partly as a sonar flight, partly with sea floor observation. The sea floor topography on the first part of the survey along the outer part of the mud volcano was flat. With the ascent towards the summit of the mud volcano the topography got more and more irregular with several parallel ridges or terrace-like structures and authigenic carbonates covering the sea floor. Eel-shaped fishes were observed in several cases. Frequently dark patches with many bivalve shells (Fig. 25) and occasional pogonophora were found, but no evidence of seep activity could be detected. The original idea to survey the eastern or northeastern flank of the Thessaloniki mud volcano was abandoned and the search for bubble sites was fully concentrated on the central part of the mud volcano. Unfortunately the whole survey was hampered by frequent computer breakdowns and for the entire dive no bubble site could be found. Sampling of rock fragments (GeoB 11327-1), push corer (GeoB 11327-2) and tube worms (GeoB 11327-3) were concentrated on the areas with dark patches, bivalves and pogonophora at the centre part of the mud volcano. This has been the last ROV dive of Cruise M70/3.

6 MOVE: Moving Lander

(C. Waldmann, M. Bergenthal, J. Renken)

MOVE is an autonomous vehicle for exploring the sea floor in depths ranging from coastal waters to the deep sea. As part of the cooperative project MOVE between the NIOZ and MARUM, co-funded by the German BMBF and the Dutch NWO, the technological concept for constructing the wheel driven underwater vehicle has been developed and realised. The scientific application of this platform lies primarily in the field of biogeochemical measurements to investigate processes at the interface of the water column and the sea floor sediment. With its own energy supply and different communication options it allows either for completely autonomous operation or being interactively operated from board of a ship or through a relay station like a buoy.

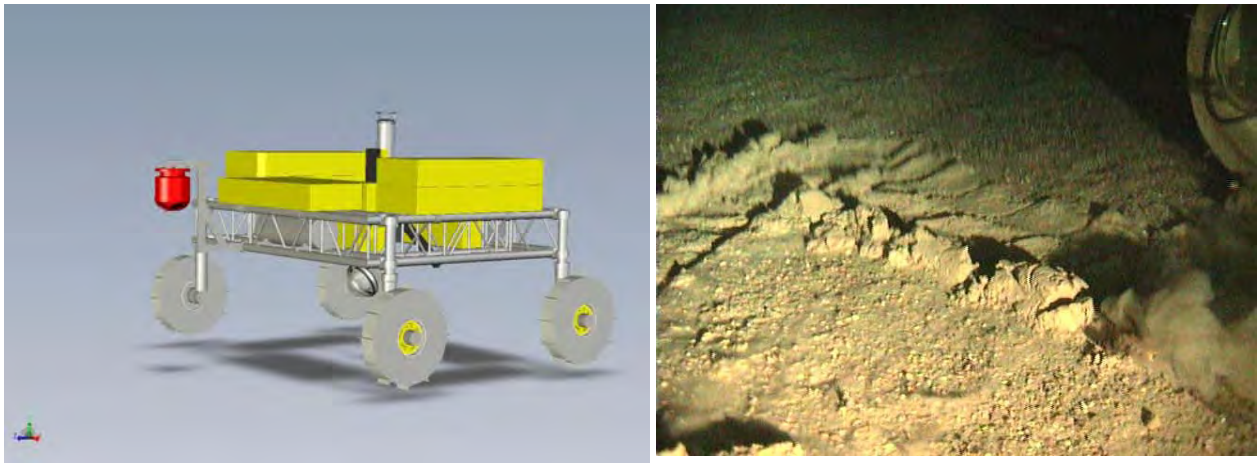

Fig. 26: Schematic drawing of the vehicle MOVE with the DVL localisation system in front (left). The tube in the middle is the acoustic releaser. Below the frame the on board camera in a glass sphere is attached. The flotation material is painted yellow. Picture taken from the onboard camera of MOVE while transecting (right). The structure of the tracks gives a clue to the performance of the wheels in relation to the properties of the sea floor sediments.

The main features of the vehicle are the easy extendable mechanical frame that allows for the flexible integration of vehicle related modules and the payload systems. By using commercially available, standard aluminum construction elements the frame can be tailored to different application scenarios. The weight of the vehicle is adjusted according to the individual application requirements. To be able to measure in almost undisturbed terrain the vehicle moves against the prevailing water current. The electronic architecture is designed to fully serve the demands of an autonomous system with according navigation, energy and communication management while allowing the easy electrical integration of additional scientific instruments. Payload systems can be interactively operated by employing manufacturer specific software tools that communicate through the MOVE platform. The basic sensor suite of the vehicle consists of:

- Navigation related sensors: Doppler Log System, Tiltmeter, POSIDONIA beacon
- Environmental - CTD, Current meter
- Observational - Video camera

Additional to that the power consumption and all propulsion related parameters are monitored and stored in the vehicle internal data archive. For this cruise the vehicle has been equipped with a scanning sonar system to localise methane bubbles in the water column. As part of a basic sensor suite a CTD collects data on its way down to the bottom.

Wich this innovative tool new opportunities for biogeochemical investigations have evolved that will either prove the vehicle's excellent applicability as a stand-alone system and its role in complementing ROV and AUV missions. It is the long term capability, its high payload capability and its flexibility which makes the MOVE unique under the multitude of existing mobile, underwater platforms.

During the short cruise the system has been deployed twice. The first dive (MOVE Dive 36; GeoB 11307) started at 30 Nov and ended at 1 Dec. Using the ROV QUEST a reasonable flat terrain had been identified first before the vehicle was deployed there (Position 35° 19,550'N, 30° 14,88'E). The topography allowed for an operating radius of about 100 m. For reaching the correct position and for tracking the vehicle a POSIDONIA transponder has been attached. With this system position accuracies of the order of ~20 m can be reached.

For the first time a dedicated fibre optic transmission system has been tested in a deep water deployment that should allow for direct communication with the vehicle. The transmission path goes from the vehicle through a thin (~ 1 mm) fibre optic cable ending in a fibre optic spool at a surface buoy. The spool contains a reservoir of 3 km fibre which by spooling off fibre allows for a maximum operating radius of ~ 2 km at the surface. From there a WLan transponder links the buoy with a ship based transceiver. This effort has been undertaken to establish a permanent contact to the vehicle controller so that malfunctions could be identified easily and live video pictures can be transmitted. In case of software problems the system could also be reprogrammed. All housekeeping and payload sensor data are stored internally and can through the fibre optic link as well be displayed and stored on the surface station.

As the handling of the fibre spool has been tested the first time malfunctions can be expected. In this case extended spin in the used recovery line of 20 m length caused excessive strain on the fibre which led to breakage. Therefore no contact to the vehicle could be established. Another problem arose due to the fact that the fibre got tangled in the drop weight which prevented the system to come up to the surface after releasing the ballast. That made the deployment of the QUEST ROV necessary. The system collected all data from the payload and housekeeping sensors internally.

Due to the problems that showed up with the fibre spool the second MOVE deployment has been dismissed (MOVE Dive 37; GeoB 11318). A fixed mission was pre-programmed into the vehicle which included a schedule for every installed instrument (two cameras, lighting, scanning sonar, CTD, current meter). To speed up the deployment and recovery process the drop weight was raised by 80 % which led to a lowering speed of 35 cm/s and a rising speed of 55 cm/s. The deployment position had been the same as during the first deployment (35° 19,528'N, 30° 14,874'E). During the lowering of the vehicle all sensors collected data that has been stored internally in a data bank. The first transecting cycle had been programmed for three hours after reaching the sea floor. The vehicle was programmed to drive in a circle consisting of 8 straight lines of about 5 m length and repeat this twice each

circle after two hours. After recovery the data and video footage had been analysed and it was detected that the vehicle went along a straight path and then got stuck. The reason for that has been identified as resulting from the usage of new wheels. These wheels are significantly less flexible as the older ones which have been done as to minimise proper motions of the vehicle in the resting phase. It appears that during the turning of the wheels sediment is accumulated in front of the wheels which apparently are easier to overcome with more flexible wheels.

Besides that all sensors worked excellent and delivered informative results. In Fig. 26 an example picture is presented which shows the vehicle crossing a former track. Due to the compactness of the sediment the wheels do not sink in significantly. On the other hand the sediment has a tendency to stick to the wheel which causes the traction to be diminished. With sediment accumulations in front of the wheel being generated during the turning process while the vehicle is at rest the risk of getting stuck is raised. Here a trade off between stability against proper motion and mobility of the vehicle has to be selected. One of the major aims of the cruise was to detect bubbles in the water column with the integrated scanning sonar. In the deployment region no free bubble outflow has been found.

7 Geological Sampling

7.1 Autoclave Sampling

(H.-J. Hohnberg, F. Abegg, T. Pape)

Two autoclave tools for sampling gas hydrate-containing sediments, free gas bubbles and water were used:

1. The Dynamic Autoclave Piston Corer (DAPC) was developed with the aim of recovering, preserving and analyzing sediment cores under in-situ conditions of the deep sea
2. The gas bubble sampler (GBS)

The DAPC, which was developed and built in the frame work of the OMEGA-Project, is a sediment pressure-core sampling device. The length of the DAPC is 7.2 m in total, its total weight is 500 kg. It was designed to cut sediment cores from the sea floor surface to a maximum length of 2.5 m and preserve them under in situ pressure corresponding to water depths of up to 1400 m. The DAPC is equipped with a pressure control valve allowing deployment to up to 5000 m water depth. The *in situ* pressure of up to 200 bar (2000 m water depth) can be preserved, higher pressures up to 500 bar then will be released down to 200 bar. The core cutting barrel, which is relatively short (2.7 m), hits the sea floor with a very strong impact. Therefore, it is especially suitable for sampling layered, gas hydrate-bearing sediments. The device allows various analytical approaches. Due to the novel construction of the pressure barrel, this is the first system that allows CT scanning of such cores (80 mm in diameter) in their pressurized state. The pressure chamber consists of glass fiber reinforced plastic (GRP), aluminum alloys, seawater resistant steel and aluminum bronze. The pressure chamber is 2.6 m long and weighs about 180 kg. All parts of the pressure chamber exposed to sea water are suitable for long-term storage of cores under pressure for several weeks. A new developed pressure-preserving-system has been added to the accumulator. The DAPC is to be deployed from a research vessel on the deep sea cable. It can be released from variable heights (1-5 m) and enters the sea floor in free fall. The pressure chamber was checked and approved by the Berlin TÜV (Technischer Überwachungsverein, technical inspection authority in Germany).

The GBS is an *in situ* pressure-sampling-device for sampling gas-bubbles escaping from the sea floor. In dual use it can sample seawater. In principle it consists of a steel tube with valves on each end. The valve at one end is connected to a funnel and can be operated by the manipulator. The other valve is used to subsample the GBS upon recovery. Before deployment, both valves are closed preserving the atmospheric pressure. While at the sea floor the pressure difference sucks in water, gas or gas hydrate when the valve is opened.

DAPC Dynamic Autoclave Piston Corer

The deployment of DAPC during R/V METEOR Cruise was similar to that of common piston corers. It penetrates the sea floor in a free-fall mode using the release mechanism developed by Kullenberg (1947). Five DAPC-deployments were made during Cruise M70/3.

Table 4: DAPC deployments during R/V METEOR Cruise M70/3.

Deployment No.	Station. Nr. GeoB	Date	Time (UTC)	Position at sea floor contact (N°; E°)	Water depth (m)
DAPC 01	11303	29.11.06	05:15	35:19.9965; 30:16.2785	2024
DAPC 02	11309	01.12.06	05:06	35:20.0412; 30:16.1771	2023
DAPC 03	11314	13.12.06	05:19	35:20.0393; 30:16.1726	2023
DAPC 04	11320	05.12.06	05:25	35:19.5941; 30:15.0072	2026
DAPC 05	11325	06.12.06	09:10	35:20.0071; 30:15.9810	2023

Station 11303: The first deployment of the DAPC on this Leg was successfully recovered with the retrieval-pressure of 185 bar in the pressure-chamber and a core of 950 mm length. The accumulator pressure had been adjusted to 160 bar, the water depth was 2024 m. The deployment speed was 0.3 m/sec. The core has been degassed and was used for sedimentological descriptions and pore water chemical analyses (see chapter 8). The gas volume was 87.5 litre. Gas sampling and analyses are described in chapter 8.1.

Station 11309: The second deployment of the DAPC on this Leg was like the first successfully recovered with the retrieval-pressure of 185 bar in the pressure-chamber and a core of 2500 mm length. The accumulator pressure had been adjusted to 160 bar, the water depth was 2023 m. The deployment speed was 0.2 m/sec. The core has been degassed and was used for further analyses (see above). The gas volume was 116.8 litre.

Station 11314: The third deployment of the DAPC on this Leg was also successfully recovered with the retrieval-pressure of 185 bar in the pressure-chamber and a core of 2480 mm length. The accumulator pressure had been adjusted to 160 bar, the water depth was 2023 m. The deployment-speed was 0.1 m/sec. The core has been degassed and was used for further analyses (see above). The gas volume was 138.4 litre.

Station 11320: The fourth deployment of the DAPC was also successfully recovered, but in the pressure-chamber we had no pressure because the procedure of retrieval failed. We recovered a core of 2500 mm length. The accumulator pressure had been adjusted to 160 bar, the water depth was 2026 m. The deployment-speed was 0.2 m/sec. The core has not been degassed but was used for further analyses.

Station 11325: The fifth deployment of the DAPC was also successfully recovered with the retrieval-pressure of 185 bar in the pressure chamber and a core of 1450 mm. The accumulator pressure had been adjusted to 160 bar, the water depth was 2023 m. The deployment-speed was 0.2 m/sec. The core has been degassed and was used for further analyses. The gas volume was 14.2 litre.

Gas Bubble Sampler

The Gas Bubble Sampler (GBS) was applied by means of the ROV's manipulator just above the sea floor. During Station 11311 two GBS were used for sampling of near sea floor water and of rising gas bubbles.

Table 5: GBS deployments during ROV dives.

Deployment No.	Station. Nr. GeoB	Date	Position at sea floor contact (N°; E°)	Water depth (m)
GBS 01	11311-2	02.12.06	35:20.1809; 30:16.1231	~ 2025
GBS 02	11311-6	02.12.06	35:20.0412; 30:16.1771	~ 2025

Station 11311-2: The first deployment of GBS was successful. We sampled seawater very close to a benthic microbial mat. The water probe was used for analyses of gases dissolved in near-bottom water.

Station 11311-6: The second deployment of GBS was successful. We sampled gas bubbles. The pressure upon recovery was 149 bar. Controlled degassing released 22 litres of gas. The sub-samples obtained during the degassing were used for gas chemical analyses and stored.

7.2 Sampling Equipment and Performance

(F. Abegg, A. Bahr, F. Brinkmann, A. Gassner, H.-J. Hohnberg, S.A. Klapp, T. Pape, T. Wilhelm)

Sea floor sampling in general was conducted with a variety of different tools covering sophisticated devices as the dynamic autoclave piston corer down to short push cores obtained with the ROV QUEST. Here we describe application and performance of the gravity corer (SL) and the TV-guided multiple corer (TV-MUC). The SL- and TV-MUC deployments during M70/3 are listed in Tables 6 and 7.

The SL with a weight of 1.5 tons was used with core barrels of 6 m and 3 m length. The outer diameter of the barrel was 14 cm, the inner diameter was 13.2 cm. The 6 m barrels used for the first two deployments proved to be too long. Either carbonates or massive gas hydrate layers led to bending of the core barrel. All other deployments were conducted with a 3 m barrel without any bending. Onboard R/V METEOR the deep sea winch No. 11 is used for SL deployments. The winch speed has been set to 0.8 m/s for the first deployment and 1.0 m/s for all other stations. As liner we used grey PVC pipes and plastic hoses. Plastic hoses allowed rapid access to the recovered material which is very important if the core is dedicated to sub sampling of gas hydrates or other geochemical specimen which decompose or change their structures rapidly during extended exposition to the atmosphere. Cores recovered inside the PVC liner were also used for geochemical analyses, and pre-cut PVC line have been used for rapid freezing of core sections in liquid nitrogen for shore-based analyses of gas hydrate contents using computerised X-Ray Tomography (CT). In order to assure a rapid transfer of the whole gas hydrate containing cores into the liquid nitrogen immediate upon recovery the liners were pre-cut. in five segments of 55 cm and one segment of 25 cm length. The segments were taped together with broad Scotch tape prior to deployment of the SL. In most cases the gravity corer was equipped with a POSIDONIA transponder (underwater navigation system) for precise deployment of the tool. Operation of the gravity corer was done by the scientific team and the deck team whose professional and friendly support is kindly acknowledged.

The TV-MUC is a large individual sampling tool with 'spider-like' legs. It was equipped with a head for the deployment of 8 liners with a diameter of 10 cm and 4 liner with a diameter of 6 cm. The TV system consisted of a black and white camera and two lamps. For the deployment R/V METEOR's winch 12 with the coaxial cable was used. The cable provided power for the camera and both lights and served also for the video signal uplink. The lowering speed was set to 0.8 m/s, lifting speed was set to 1.0 m/s.

Table 6: List of gravity corer stations.

GeoB No.	Device No.	Lat. N°	Long. E°	Water depth (m)	Core barrel	Type of liner	Core recovery
11302	SL-1	35:19.999	30:16.275	2023	6 m	Hose	205 cm
11305	SL-2	35:19.536	30:14.877	2020	6 m	Hose	25 cm
11306	SL-3	35:19.997	30:16.275	2024	3 m	Pre-cut PVC	200 cm
11312	SL-4	35:20.035	30:16.189	2024	3 m	PVC	130 cm
11313	SL-5	35:20.017	30:16.179	2023	3 m	Pre-cut PVC	230 cm
11316	SL-6	35:20.030	30:16.181	2022	3 m	Hose	243 cm
11317	SL-7	35:20.043	30:16.185	2020	3 m	Hose	250 cm
11321	SL-8	35:19.596	30:14.997	2020	3 m	PVC	45 cm
11327	SL-9	35:21.006	30:15.004	2083	3 m	Hose	458 cm
11328	SL-10	35:20.003	30:16.266	2023	3 m	Hose	290 cm

Table 7: List of TV-MUC stations.

GeoB No.	Device No.	Lat. N°	Long. E°	Water depth (m)	Core numbers
11323	TV-MUC-1	35:19.578	30:14.990	2025	8
11324	TV-MUC-2	35:20.064	30:16.189	2015	8

7.3 Sedimentological Description

(A. Bahr, F. Abegg, S. Klapp)

Sediments from the center of the Amsterdam Mud Volcano

In an area with active mud volcanisms and fluid seepage, the sedimentation should be influenced by these processes. This is in fact very evident for the cores GeoB 11302, 11303, 11309, 11314, 11316, 11317 taken at the center of the Amsterdam MV (Fig. 6): they entirely consist of mud breccia deposits, a typical mud volcano sediment with angular to subangular rock clasts embedded in a grey clay matrix. The lack of pelagic sediments can be explained by the position of the cores in the centre of an active mud volcano, where the expulsion of mud is the dominant process and detrital sediments will be eroded during mud eruptions. The upward rising mud carries pieces of bedrock that are later found in the mud breccia deposits. In the sampled cores, the rocks represent a variety of lithologies, including limestones, sandstones, tuffits and pieces of bituminous shales that might represent the Miocene source rock for the thermogenic hydrocarbon generation.

Differences between the gravity cores from the center part of the Amsterdam MV are only minor and are mostly defined over the presence or absence of mollusc shells (mainly bivalves) and carbonate precipitates. Cores that are located on the same position (Fig. 6) show naturally the greatest similarity: GeoB 11302 and 03 have both abundant authigenic carbonate pieces throughout the entire core, which is not the case at the other positions. These carbonates differ in size from gravel to rock size fragments and often contain tube worm tubes

and mollusc shells. Bivalve or gastropod shells are mostly found in the uppermost few centimeters, only in GeoB 11302 in the upper decimeters of the cores, but they are also absent in some cases (GeoB 11309, 11316, 11328). This absence might be explained by core loss, however, the ROV dives have shown that at the Amsterdam MV the morphology and property of the sea floor is changing rapidly on a small scale and cores located a few meters apart might therefore record different environments (e.g. patches of shell-covered sea floor) and different evolutionary stages of the chemosynthetic community.

An important factor for the texture of the sediments is the presence of gas hydrates. Gas hydrate decomposition forms typical "moussy" and "soupy" sediment textures, which both have been found in all opened gravity cores or DAPCs from the central Amsterdam MV. Beside these indirect indications, gas hydrates have been sampled in cores that were opened and examined directly after their recovery on deck. The clathrates are generally finely dispersed over a certain section of the cores; massive clathrates have not been found.

Core sites on the outer rim of the Amsterdam Mud Volcano

The situation is different in the cores taken on the outer margin of the Amsterdam MV (Fig. 6), GeoB 11320 (DAPC) and GeoB 11321 (gravity core). Here no evidence of gas hydrates has been found. In the (longer) core GeoB 11320 small degassing voids have been observed below 1.85 mbsf, however, both cores show an undisturbed sequence of terrigeneous mud, without moussy or soupy textures. In the case of the shorter gravity core GeoB 11321 carbonate slabs with a typical cold seep fauna (pogonophora, bivalves, gastropods) are covering the upper 5 cm, below this depth the sediment consists of terrigeneous mud similar to that in GeoB 11320. Interesting to note are two observations: first the difference in the sediment cover (absence or presence of authigenic carbonates) from cores only a few meters apart and second the successive increase in shells size and abundance of the bivalves found in GeoB 11320. This trend in shell size seems to reflect the colonization history at this location, following the gradual emplacement and improvement of the environmental conditions favorable for the chemosynthetic biota at this site. It seems that for the recent time interval covered by GeoB 11320 and 11321, mud flows from the center of the mud volcano are not affecting this marginal location, sandy layers that might hint at turbidites have also not been found.

Background sedimentation

The station GeoB 11327 was chosen as representative for the typical hemipelagic sedimentation in the area of the Amsterdam MV. The gravity core consists entirely of homogeneous clayey mud, with little lithological variations and no macroscopically visible bigger components such as shells or rock fragments. The color variations observed are the result of changing postdepositional processes signal, although the dark brown interval between 0.41 and 0.65 mbsf might be the Mediterranean sapropel S1, from the time interval of ca. 6.5 to 9.5 kyrs BP. However, a confirmation of this assumption is difficult, since the core was not fully accessible, due to sampling for geochemical probes with a closed liner, but the depth of the supposed sapropel S1 is similar to that found in a core north of Crete by (Sperling et al., 2003).

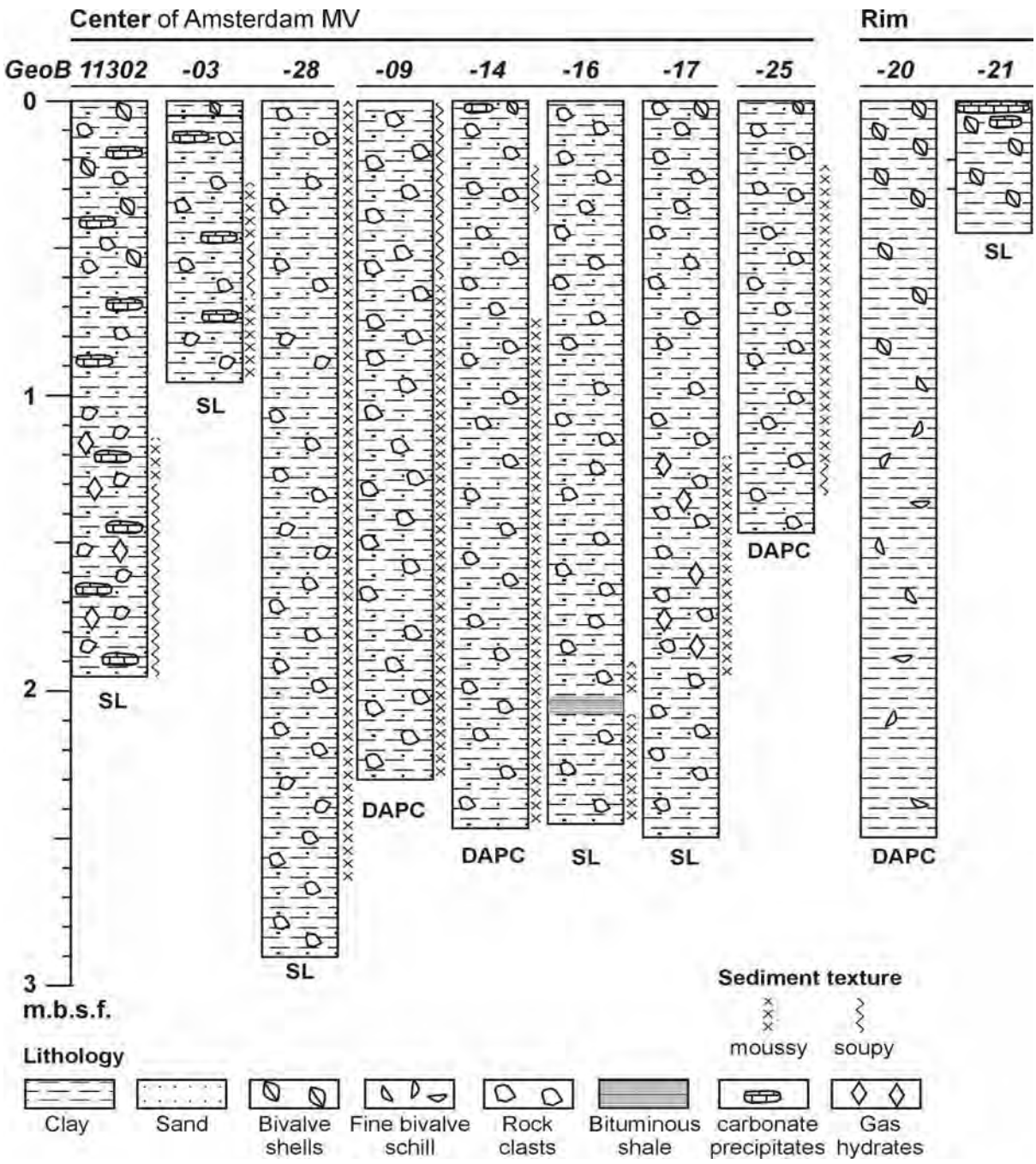

Fig. 27: Lithological logs of sampled gravity cores (SL) and DAPCs from the Amsterdam MV. The lines beneath the core numbers indicate parallel cores.

7.4 Carbonates

(F. Brinkmann)

Introduction

At cold seep sites gaseous hydrocarbons, often particularly methane, H_2S and other trace gases bubble out of the sea floor. The expelling fluids support life in specially adapted ecosystems. Many communities based on chemosynthetic carbon fixation were discovered through time after first occurrence in the late 70´s (Campbell, 2006). Different populations of metazoans and microbes were found in different stratigraphical and tectonic settings. Venting

occurs either directly through soft sediments but the fluids can also be expelled through authigenic carbonate crusts, which are created as a direct (cementation) or indirect (sedimentation and compaction of carbonated shells of seep depending organisms) influence of seepage. These seep carbonates are often strongly porous, depleted in ^{13}C, and commonly occur as cemented shelly biota, forming at or near the sea floor (Campbell, 2006). The associated organisms, which are used as biological indicators for seepage, gain energy either directly by consumption of methane (anaerobic oxidation of methane, AOM) by symbiontic, methanotrophic bacteria during the sulphate reduction (1) or indirectly by consuming the generated hydrogen sulphide (like pogonophora and their endosymbiotic bacteria).

$$(1)\ CH_4 + SO_4^{2-} \rightarrow HCO_3^- + HS^- + H_2O$$

Detailed site analyses at seeps and gas hydrate localities have verified the importance of sulfate-dependent, anaerobic oxidation of methane (AOM) in authigenic carbonate formation, and have revealed the microorganisms that are responsible for major biogeochemical processes. The resultant carbonate species (mainly calcite, aragonite, or dolomite) is incorporated in the carbonate mineral lattice (Peckmann et al., 2002). Consequently the isotopic signal of the source methane can be found in these Methane-Derived Authigenic Carbonates (MDACs) as well, either in authigenic cements or in cemented shells of common vent taxa. Using the isotopic composition of carbon, oxygen, and hydrogen the influence of seepage or even source type of methane (thermogenic or bacterial methane) can be determined. Isotopic values in bacterially derived methane can show $\delta^{13}C$ values as low as -110‰ PDB (Whiticar, 1999). Consequently, very low $\delta^{13}C$ values found in carbonates indicate a seepage influence and microbial oxidation of isotopically light hydrocarbons (Aloisi et al., 2000).

Besides using depleted ^{13}C signatures for determining seepage sources, venting sites can also be characterized by characteristic chemical compounds that are included in the carbonates. These so called biomarkers can be for example isoprene-based archaeal lipids, acetate-based lipids carrying non-isoprenoid carbon chains, hopanoids (Campbell, 2006). These compounds preserve a robust record of microbial methane utilization and can be used for recent sediments but also for samples generated far back in earth's history. The objective of carbonate sampling in this expedition should be the usage of palaeontology and petrography to characterize seep influence on the one hand, but on the other hand isotopic composition and especially biomarkers should be analysed to confirm the seep influence, and also the involved organisms, on precipitating the carbonate crusts.

Sampling

Carbonate crusts were mainly recovered using the ROV QUEST, which could be used to directly sample areas of massive carbonate crust formation. Six locations were sampled at the sites of Amsterdam and two locations at the Athina Mud Volcano.

Table 8: List of carbonate samples taken at Amsterdam and Athina Mud Volcanoes.

GeoB number	Comment
11301-5	Carbonate crust taken by the ROV, many tube worms from cracks (Fig. 28)
11301-6	Carbonate crust taken by the ROV, carbonate crusts cracked by sea floor movement
11304-1	Some small carbonate specimen taken by the ROV with a net at a bacterial patch
11308-1	Carbonate crust taken by the ROV at a tube worm site
11311-5	Very small piece of carbonate taken at an active venting site where bubbles were visibly
11317	Carbonate clasts taken from the first 10 centimetres of a gravity core.
11319-1	Dead black cemented tube worm structure taken by the ROV. Interesting intermediate stage between recent tube worm structures and fossil records. The extensive network structure is covered with carbonate crusts (Fig. 28)
11319-2	Carbonate crust. Very light carbonate specimen containing lots of cemented shells. In the pores and burrows many clams are included (Fig. 28)

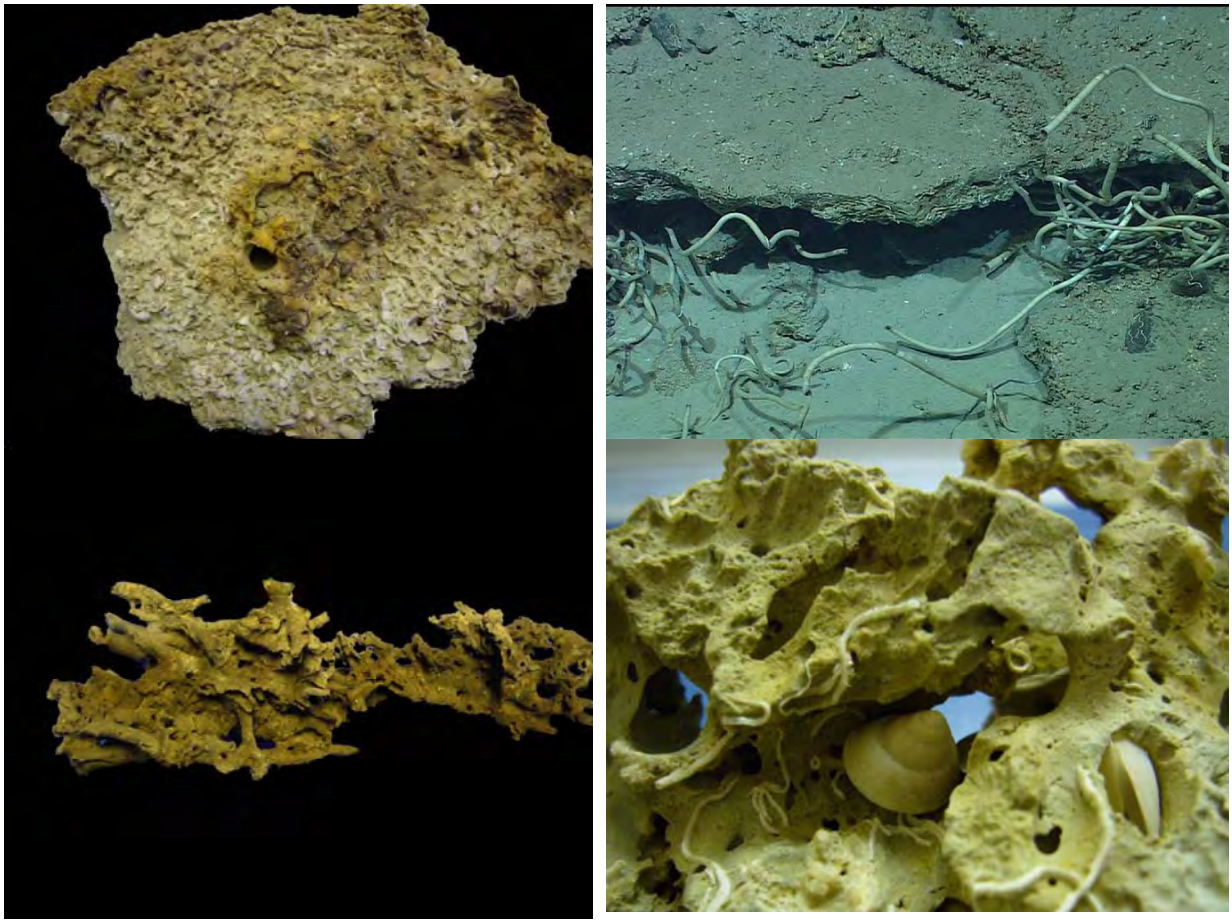

Fig. 28: Examples for authigenic carbonates sampled during Cruise M70/3: Sample GeoB 11301-5. The carbonate matrix includes shell fragments, creating a porous rock. The hole in the centre of the specimen might have been a former discharge channel (above left). Sea floor image of sample site GeoB 11301-5 (above right). Fossilized pogonophora of GeoB 11319-1 sample (below left). The tubes are completely filled with carbonate and cemented to a solid structure. Pores and burrows in whitish carbonate rock (Sample GeoB 11319-2) with clams living in this harboured environment (below right).

A first result is that extensive carbonate crusts do not appear directly linked to the active sites if visible seepage. But they are found in areas of high shell concentrations. The cemented shells seem to build the main part of carbonate crusts at Amsterdam Mud Volcano. Carbonate matrix material cements shell fragments creating a porous rock. Extensive burrows seem to be a result of former hydrocarbon discharge. Massive crusts are often associated with dense pogonophora populations. At locations of sea floor expansion or other cracks and breaks, the crusts are most densely populated by tube worms. Sometimes a distinct stratification can be found.

A comprehensive approach using palaeontology, petrography, stable isotope geochemistry and biomarker analyses will be applied to the study of these seep carbonates. The combination of these techniques will be used to confirm seep influence. Studies on recent seep carbonates on Anaximander Mud Volcano shall be compared to different ancient samples from different periods throughout earth`s history. There will be two different main foci:

- Analysis of the cemented pogonophora sample (GeoB 11319-1)
- Comparison of living and cemented shells and analyse indicators for sulphur-oxidising and possibly methylotrophic symbionts. Mytilids (*Idas modiolaeformis*) might play a key role in the seep ecosystems.

8 Gas and Pore Water Analysis

8.1 Gas Analysis

(T. Pape, H.-J. Hohnberg, F. Abegg and S. Klapp)

Introduction

Previous cruises into the Mediterranean southwest off Turkey revealed comparably high methane concentrations in sediments and near-bottom waters as well as the presence of hydrocarbon gas seeps and shallow-buried gas hydrates at specific sites (Woodside et al., 1998; Charlou et al., 2003). Based on these observations the working area of Leg M70/3 provides great opportunity for studies of key processes affecting submarine fluid circulations at gas and fluid seeps and, in particular, those of low-molecular-weight hydrocarbons (LMWHCs). In this context, a characterization of the amount and fate of the potent green-house gas methane discharged at these sites is of major concern.

The major goal of the onboard gas analytical work was to quantify *in situ* abundances of LMWHCs (C_1 through C_6) contained in gas- and hydrate-rich sediments. Since sample recovery using conventional tools does not prevent degassing of the samples, autoclave technology was applied instead, which preserves the deep sea samples under ambient pressure (Chapter 7.1; Abegg et al., subm.). In the course of incremental degassing of autoclave cores, gas sub-samples were taken for a detailed onboard characterization of their composition and for storage for further analyses onshore. For comparison, the distribution patterns of volatile hydrocarbons were likewise determined for bubbles caught with the newly designed Gas Bubble Sampler (GBS, Chapter 7.1), for gas hydrates, and for selected sediment samples recovered by conventional coring techniques. Primary subjects of the study were selected sites at the Amsterdam Mud Volcano in the Anaximander Mountains Region.

Samples

In order to determine the *in situ* amounts of volatile hydrocarbons contained in gas-laden sediments and to elucidate molecular stripping effects during upward migration and gas hydrate generation, focus was laid on the quantitative degassing and subsampling of sediment cores retrieved with the Dynamic Autoclave Piston Corer (DAPC). For this purpose 5 stations were covered by DAPC and a total of 131 gas samples were obtained by incremental degassing. The sample set was completed by I) bubble-forming gas retrieved with the GBS, II) by gas released by controlled dissociation of a gas hydrate piece recovered with gravity core, III) by gases obtained from sediments sampled with conventional push cores, and IV) by gas extracted from a near-bottom water sample recovered with the GBS. Thus, a comprehensive sample set was secured for measurements of the gas compositions onboard and for onshore analyses of stable isotope contributions ($^{1}H/D$, $^{12}C/^{13}C$) of LMWHCs. Table 9 summarizes the samples taken during M70/3.

Table 9: List of samples taken for measurements of the gas compositions. DAPC: **D**ynamic **A**utoclave **P**iston **C**orer, PC: **P**ush **C**orer (ROV-based), GBS: **G**as **B**ubble **S**ampler (ROV-based), GC: **G**ravity **C**orer. A detailed sample list is given in the Appendix.

GeoB No.	Device	Lat. N°	Long. E°	Water Depth (m)	Type of sample	No. of (sub-) samples
11303	DAPC	35:19.9965	30:16.2785	2024	Released gas	28
11309	DAPC	35:20.0412	30:16.1771	2023	Released gas	47
11314	DAPC	35:20.0393	30:16.1726	2023	Released gas	42
11320	DAPC	35:19.5941	30:15.0072	2026		0
11325	DAPC	35:20.0071	30:16.0000	2023	Released gas	14
11301-1	PC	35:19.9510	30:15.8890	~ 2070	Sediment	6
11301-2	PC	35:19.9521	30:15.8929	~ 2070	Sediment	6
11304-2	PC	35:19.8621	30:16.6555	~ 2034	Sediment	6
11304-3	PC	35:19.8619	30:16.6610	~ 2034	Sediment	6
11311-3	PC	35:20.1809	30:16.1231	~ 2025	Sediment	3
11311-4	PC	35:20.1809	30:16.1231	~ 2025	Sediment	2
11311-7	PC	35:20.0521	30:16.1560	~ 2025	Sediment	9
11311-8	PC	35:20.0500	30:16.1550	~ 2025	Sediment	9
11311-2	GBS	35:20.1809	30:16.1231	~ 2025	Near-bottom water	1
11311-6	GBS	35:20.0500	30:16.1751	~ 2025	Gas bubbles	5
11302	GC	35:19.9993	30:16.2755	2023	Gas hydrate	1
					Total	**190**

Total gas volumes preserved in the DAPC cores were specified by quantitative degassing (Heeschen et al., 2007). During the procedure the pressure preserved inside the DAPC was monitored and sub-samples were taken at selected time points with a gastight syringe and transferred into 20 mL glass vials pre-filled with concentrated NaCl solution a) for immediate analyses of the gas composition on deck and b) for storage and further measurements on shore.

Sediments taken with push corers deployed by the ROV QUEST 4000 m were analyzed for their LMWHC distribution patterns. From selected horizons of the push cores, which were simultaneously prepared for pore water analyses (Chapter 8.2), 25 mL of sediment were taken in syringes with the needle-ends cut off and transferred into 50 mL glass ampoules, pre-filled with 20 mL of NaCl-saturated water. Subsequently, the ampoules were capped and the solutions were shaken exhaustively in order to ensure overall flushing of the sediment and pore space.

Gas bubbles were caught at a distinct gas seep with the newly designed GBS (Chapter 7.1) during ROV dive GeoB11311. The GBS was degassed quantitatively right upon recovery using the same technique as for DAPC cores. Gas sub-samples were injected into glass vials pre-filled with concentrated NaCl solution.

Gases dissolved in near-bottom waters sampled above a benthic microbial mat with the GBS (Chapter 7; GeoB11311-2) were extracted using a high grade vacuum combined with ultrasonification and heating until boiling (Lammers and Suess, 1994).

A gas hydrate piece retrieved with a gravity corer (GeoB11302) was filled into a gas tight syringe and stored at room temperature for dissolution. The escaping gas was transferred into a glass vial and a sub-sample was taken from the headspace for compositional analyses.

Gas Analyses

For onboard measurements of their chemical compositions the gas samples were analyzed with a two-channel HP6890N (AGILENT TECHNOLOGIES) gas chromatograph (GC). Volatile hydrocarbons (C_1 to C_6) were separated, detected and quantified with a capillary column (OPTIMA-5; 5 µM film thickness; 0.32 mm ID, 50 m length, carrier gas: N_2), which is connected to a Flame Ionisation Detector (FID), while permanent gases (O_2, N_2, CO, CO_2) were determined using a packed (Molecular sieve, carrier gas: He) stainless steel column connected to a Thermal Conductivity Detector (TCD). The GC oven temperature program was: initial 45°C held for 4 min; heating with a rate of 15°C min^{-1} up to 155°C (constant for 2 min), 25°C min^{-1} up to 240°C (7 min). A PC-operated integration system (GC Chemstation, Agilent Technologies) was used for recording and calculation of the data. Calibrations and performance checks of the analytical system were conducted using commercial pure gas standards and gas mixtures (AIR LIQUIDE). The coefficient of variation determined for the analytical procedure was lower than 2 %.

For onshore determination of stable isotope ratios ($^1H/D$, $^{12}C/^{13}C$) of volatile hydrocarbons by GC-Isotope-Ratio-Mass-Spectrometry (GC-IRMS) gas samples were stored in sealed glass vials filled with NaCl-saturated water.

Preliminary Results

A total of 80 gas samples recovered with the DAPC and the GBS, as well as sample of hydrate-bound gas, were analyzed onboard for their molecular composition. By GC-FID analyses 11 hydrocarbons were detected in the C_1 to C_6 range. All samples measured so far were strongly dominated by methane (between 98.68 and 89.38 mol-% of C_1 to *i*-C_4 hydrocarbons) followed by ethane and smaller amounts of propane, iso-butane and two compounds tentatively assigned as C_5 components (Fig. 29). Structural identifications of unidentified hydrocarbons will be made on the basis of retention indices and co-elution experiments in the home lab. Concentrations of N_2 and O_2 in the gases will be determined in the home lab, though some estimation on-board yielded less than 5 mol-% as a maximum for all gas samples retrieved from the DAPC. Detailed results of the hydrocarbon compositions are given in the appendix (Appendix 3).

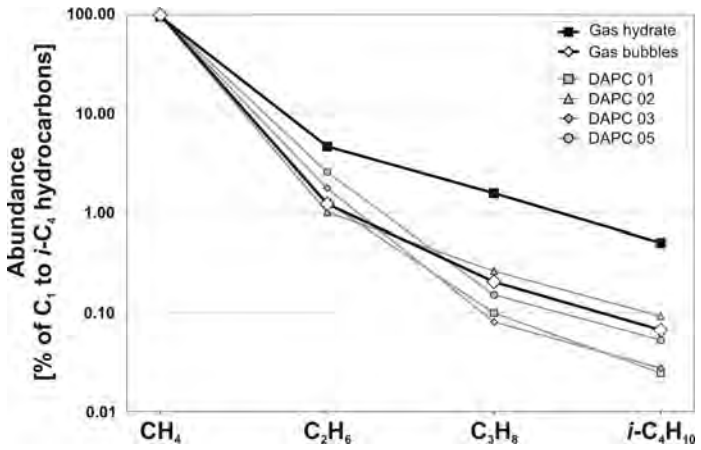

Fig. 29:
Distribution of C_1- to *i*-C_4 hydrocarbons in hydrate-bound gas, bubble-forming gas, and in gases obtained at the onset of gas-release from the DAPC cores. Note that a logarithmic scale is used for relative amounts of hydrocarbons.

DAPC 01 and DAPC 02 (GeoB11303 and GeoB11309)
Volatile hydrocarbon analysis of whole sub-sample sets was performed onboard for DAPC cores 01 and 02. Core recoveries were 95 cm and 244 cm corresponding to about 4,775 and 12,266 mL core volume, respectively. At the beginning of the gas-release, 51 and 78 bar were preserved in the autoclave and overall volumes of the gases liberated from the cores were measured to be 87.530 and 116.840 mL.

Methane contributed 98.60 and 98.62 mol-% of the volatile hydrocarbons and molar ratios between methane and higher homologues (commonly expressed as $R = C_1 / (C_2 + C_3)$; Bernard et al., 1976) were 71.9 and 76.9 (Figs. 29. and 30) in the gases initially released from the autoclave cores, i.e. the first samples obtained by degassing. These values point to a predominantly thermogenic origin of the gases. During the degassing procedure a considerable change in the hydrocarbon composition was observed for both cores. In the early stages, when comparatively high pressures still persisted in the autoclave, a general decrease in the $C_1 / (C_2 + C_3)$ ratio down to 15.6 and 9.5, indicating a significant decline in the portion of methane with increasing volume of gas released, was observed. However, in the later course of the experiment, when huge amounts of gas (about 69 and 74 L) have been released from the cores and pressures declined down to <8 bar (DAPC 01) and < 20 bar (DAPC 02), the relative portion of methane slightly increased again.

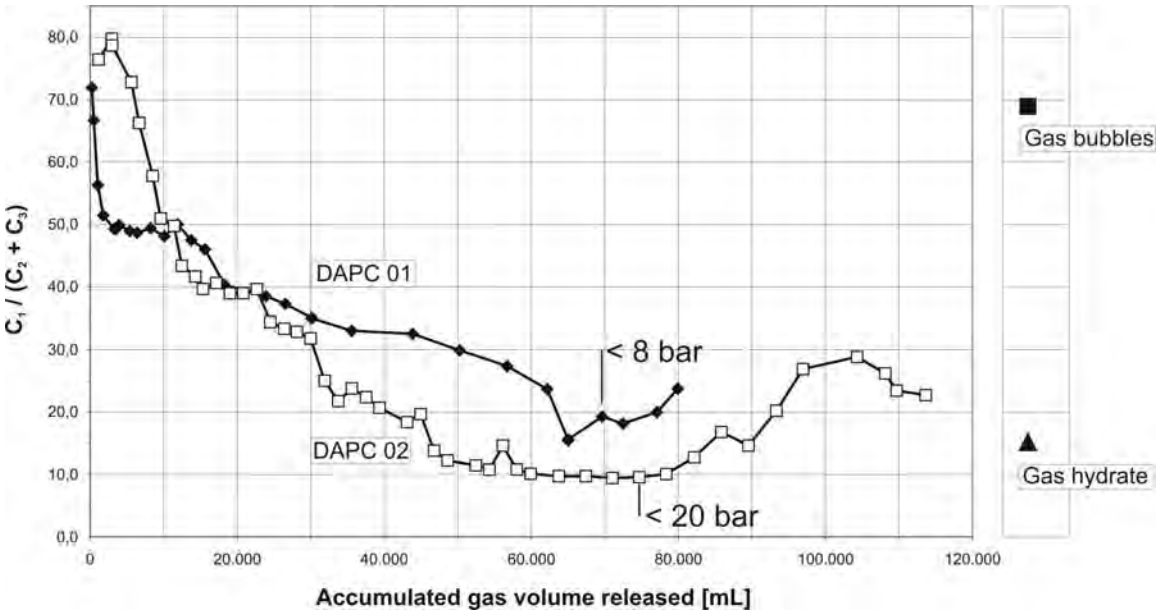

Fig. 30: Cross plot of ratios $C_1 / (C_2 + C_3)$ and gas volumes during gas release from DAPC cores 01 and 02. For comparison ratios for gas bubbles sampled with the GBS and for a gas hydrate piece are illustrated in the right row.

DAPC 03 and DAPC 05 (GeoB11314 and GeoB11325)
At stations DAPC 03 and 05 cores of 248 cm and 148 cm length were recovered and the released gases summed up for 138.40 and 14.20 mL. Sub-samples of the gases were stored for analyses of compound specific concentrations and stable isotope measurements onshore. For an overview, only the first sub-samples obtained at the beginning of the degassing were analyzed for hydrocarbon distributions. $C_1 / (C_2 + C_3)$ ratios of 52.9 and 35.7, respectively,

were remarkably small in comparison to those of the initial sub-samples of cores DAPC 01 and 02.

DAPC 04 (GeoB11320)
Due to pressure loss during recovery gas samples were not retrieved from the core.

Gas bubbles (GeoB11311-6)
Methane was also the predominant volatile hydrocarbon (98.50 mol-%) in gas bubbles sampled in close vicinity to the sea floor. The compound distribution pattern resembled those of gases released in early stages of the degassing experiments of DAPC cores 01 and 02, with the C_1 / (C_2 + C_3) ratio being 68.9 (Fig. 30). So far, only the first sub-sample out of five obtained during degassing of the GBS was analysed.

Gas hydrate (GeoB11302)
Hydrate-bound volatile hydrocarbons were strongly enriched in ethane and propane (C_1 / (C_2 + C_3) = 15.2) compared to those escaping the sea floor (Fig. 30). Their hydrocarbon distribution is very similar to that determined for sub-samples obtained at intermediate stages of degassing of DAPC cores 01 and 02.

Push cores (GeoB11301; 11304; 11311)
The gas samples from selected sediment layers in push cores were secured for analyses of volatile hydrocarbon distribution patterns and stable isotope ratios (^{1}H/D; ^{12}C/^{13}C) of hydrocarbons onshore.

Conclusion
During M70/3 a diverse set of gaseous samples was retrieved from sediments and waters of a close area in the Eastern Mediterranean Sea by use of conventional and novel deep-sea sampling tools. Onboard measurements of selected samples showed a strong predominance of LMWHCs in the gases.

Considerable variations in the hydrocarbon distribution patterns were observed for the sample set. These variations point to molecular differentiation processes during gas hydrate crystallization and preferential gas release from specific hydrocarbon reservoirs during incremental degassing of autoclave cores.

Future onshore work using combinatory methodological approaches (computer tomography scanning, cryo-scanning electron microscopy, isotope-ratio-monitoring mass spectrometry, X-ray diffractometry) will help to specify the type(s) of the source gas(es), as well as the internal dynamics during accumulation in and discharge from gas- and gas hydrate bearing sediments. Gas hydrate structure will be determined in order to characterize the source gas – hydrate interrelationships prevailing at the Amsterdam Mud Volcano.

8.2 Pore Water Chemistry

(A. Gaßner, T. Wilhelm and S. Hessler)

Introduction and Methods

The focus of geochemical investigations carried out during this cruise in the frame of RCOM projects E1 and E3 was a detailed examination of the influence of methane seepage and mud volcanism on geochemical processes in and at the sea floor as well as the quantification of gas/ fluid fluxes across the sediment/water interface. The Anaximander Seamount area in the Eastern Mediterranean south of Turkey is characterized by overall oligotrophic surface water conditions. However, the focused and diffuse seepage/upward migration of methane (hydrocarbons) stimulates high turnover rates of geochemical and biogeochemical processes close to the sea floor - in particular involving the cycling of carbon, sulfur and iron - as also known from other cold seep environments. One of the research objectives therefore is to investigate and quantify processes of mineral formation and dissolution in these hydrocarbon-seepage influenced sites. A second major task will be the quantification of fluid/gas fluxes across the sediment/water interface and in this way to identify the significance of these unique hydrocarbon seeps and mud volcanoes for the carbon cycle and budget in the Eastern Mediterranean area.

Methods of Pore Water Sampling and Analysis

To prevent a warming of the sediments on board the sediment cores were transferred into the cooling room immediately after recovery and maintained at a temperature of about 4°C. Only the gravity cores (GeoB 11312, plastic liner; GeoB 11316 and 11327, plastic foil) and the DAPC cores (GeoB 11303, GeoB 11309, GeoB 11314, GeoB 11320, GeoB 11325, all plastic liners) were sampled on deck or in the Geo-lab at ambient temperature. The TV-MUC cores and the ROV push cores were processed within a few hours by means of rhizons (pore size 0.1 µm). One sample of the supernatant bottom water was taken by means of rhizons for subsequent analyses. The remaining bottom water was carefully removed from the multi corer tube by means of a siphon to avoid destruction of the sediment surface. During subsequent cutting of the core into slices for solid- phase analyses, pH and Eh measurements were performed with a minimum depth resolution of 1 cm.

Gravity core GeoB 11312 was taken with a plastic liner and holes were drilled into the liner to perform Eh, ph and conductivity measurements. Additionally rhizons were pushed into the sediment to obtain the pore water. Syringe samples of wet sediment were taken for methane (5 ml) and solid- phase analysis (10 -20 ml). Gravity cores GeoB 11316 and GeoB 11327 were taken in a plastic foil. For the extraction of pore water, rhizon samplers were used. Methane (every 25 cm) and solid- phase sampling was performed by cutting the plastic foil. PH, Eh and conductivity (every 10 cm) were determined directly on deck. Depending on the porosity and compressibility of the sediments, the amount of pore water recovered ranged between 5 and 20 ml (upper samples). Solid phase samples for total digestions, sequential extractions and mineralogical analyses were taken at 10 cm intervals, kept in gas-tight glass bottles under argon atmosphere and stored at 4°C.

Pore water analyses of the following parameters were carried out during this cruise: Eh, pH, ammonium, alkalinity, phosphate, iron (Fe^{2+}) and hydrocarbons - including methane. Eh

and pH were determined with punch-in electrodes before the sediment structure was disturbed by sampling for the solid- phase and methane. Ammonium was measured using a conductivity method. Alkalinity was calculated from a volumetric analysis by tritration of 1 ml of the pore water samples with 0.01 or 0.05 M HCl, respectively. For the analyses of dissolved iron (Fe^{2+}) sub-samples of 1 ml were taken directly from pore water extracted by rhizons, immediately complexed with 50 µl of "Ferrospectral" and determined photometrically. The analysis of phosphate was also performed photometrically.

Table 10: Coordinates of sites investigated geochemically.

Station	Device	Location	Latitude (°N)	Longitude (°E)	Water depth
GeoB 11301-1	PC 36	Amsterdam MV	35:19.9510	30:15.8890	2070 m
GeoB 11301-2	PC 41	Amsterdam MV	35:19.9521	30:15.8929	2070 m
GeoB 11303	DAPC	Amsterdam MV	35:19.9965	30:16.2785	2023 m
GeoB 11304-2	PC 9	Amsterdam MV	35:19.8621	30:16.6555	2034 m
GeoB 11304-3	PC 68	Amsterdam MV	35:19.8619	30:16.6610	2034 m
GeoB 11309	DAPC	Amsterdam MV	35:20.0412	30:16.1771	2023 m
GeoB 11311-1	ISPS	Amsterdam MV	35:20.0320	30:16.1890	2025 m
GeoB 11311-3	PC 36	Amsterdam MV	35:20.1809	30:16.1231	2025 m
GeoB 11311-4	PC 41	Amsterdam MV	35:20.1809	30:16.1231	2025 m
GeoB 11311-7	PC 14	Amsterdam MV	35:20.0521	30:16.1560	2025 m
GeoB 11311-8	PC 16	Amsterdam MV	35:20.0500	30:16.1550	2025 m
GeoB 11312	GC	Amsterdam MV	35:20.0346	30:16.1890	2024 m
GeoB 11314	DAPC	Amsterdam MV	35:20.0393	30:16.1726	2023 m
GeoB 11316	GC	Amsterdam MV	35:20.0301	30:16.1811	2022 m
GeoB 11320	GC (DAPC)	Amsterdam MV	35:19.5941	30:15.0072	2026 m
GeoB 11323	TV- MUC	Amsterdam MV	35:19.5783	30:14.9902	2025 m
GeoB 11324	TV- MUC	Amsterdam MV	35:20.0642	30:16.1890	2015 m
GeoB 11325	DAPC	Amsterdam MV	35:20.0071	30:15.9810	2023 m
GeoB 11326-2	PC 41	Thessaloniki MV	35:28.5110	30:15.1461	1345 m
GeoB 11327	GC	Background	35:21.0063	30:15.0039	2083 m

Abbreviations:		
	PC	**P**ush **C**ore
	DAPC	**D**ynamic **A**utoclave **P**iston **C**orer
	ISPS	**I**n **S**itu **P**ore water **S**ampler
	GC	**G**ravity **C**orer
	MUC	**M**ulti **C**orer

For further analyses at the University of Bremen and the Alfred Wegener Institute for Polar and Marine Research (AWI) in Bremerhaven, aliquots of the remaining pore water samples were diluted 1:10 and acidified with $HNO_{3\ (suprapure)}$ for determination of cations (Ca, Mg, Sr, K, Ba, S, Mn, Si, B, Li) by ICP-AES and AAS. Additionally, 1.5 ml subsamples of the pore water were added to a ZnAc solution (600 µl) to fix all hydrogen sulfide present as ZnS for later analysis – including stable sulfur isotopes. Subsamples for sulfate and chloride determinations were diluted 1:100 and stored frozen for ion chromatography (IC) analyses at the University of Bremen and the AWI Bremerhaven. Further aliquots of the pore water were taken to determine the concentration of sulfate and sulfide and their $\delta^{34}S$ values as well as concentrations and $\delta^{13}C$ of DIC and acetate.

A complete overview of sampling procedures and analytical techniques used on board and in the laboratories at the University of Bremen is available on http://www.uni-bremen.geochemie.de.

Shipboard Results - Pore Water Chemistry

During this cruise TV-MUC cores from 2 locations, 9 ROV push cores, 3 gravity cores, 1 DAPC cor (Dynamic Autoclave Piston Corer) and 1 In Situ Pore Water Sampler (ISPS) were sampled and investigated in detail for pore water chemistry. For all sediment cores pore water extraction was performed by the rhizon technique. All sites sampled geochemically, including parameters analysed on board as well as aliquots of pore-water and solid-phase samples taken and stored for further analyses at the University of Bremen and at the Alfred Wegener Institute (AWI) in Bremerhaven are listed in Tables 10 and 11.

The cores listed above were taken at five locations in- and outside the Amsterdam Mud Volcano. Main focus lays in the central area of the volcano, where fluids seeped out of the sea floor and gas bubbles rose through the water column. From this area the cores GeoB 11311-1 (In Situ Pore Water Sampler, ISPS), GeoB 11311-7/8 (PC 14 and 16), GeoB 11312, GeoB 11316 (both GC) and GeoB 11324 (TV MUC) were taken.

North of the central area at the point where the cores GeoB 11311-3 and 4 and gas sample GeoB 11311-2 were taken, the sea floor was covered with dark patches containing white parts which have been interpreted as bacterial mats. Cores GeoB 11311-3 and 4 were taken at this location. In the south-western area, the mud volcano's margin rises up to approx. 40 meters, representing the highest elevation of the volcanoes ring structure. In the south-eastern area similar structures can be observed. Both margin sites were often covered with thick carbonate crusts. Areas not influenced by carbonate precipitation were often covered with clasts of up to decimetre size.

One of the most important reasons for choosing the sample sites mentioned above is the left oriented strike-slip fault on which the volcano is situated. This fault passes the volcano in its centre in east-west direction. Close to this fault active gas seepage, detected as gas flares bubbling out of the sea floor was found. North and south of this fault the area is more or less flat with some smaller elevations. Further cores were taken at the south-western (GeoB 11320 and 11323) and at the south-eastern flank (GeoB 11304-2 and -3) of the mud volcano. Gravity core GeoB 11327 was taken as reference core outside the active area of the mud volcano. In the following, we present a small choice of cores showing some special characteristics of the mud volcano.

Table 11: Sites investigated geochemically during Cruise M70/3, including parameters analysed on board and aliquots of samples taken and stored for further analyses

Station	Device	Sampling	Alkal.	NH_4	PO_4	Fe	DIC* (conc.)	DIC* δ ¹³C	H_2S* (fixation)	$\delta^{34}S$* (HS)	CH_4* (headspace)	SO_4, Cl^* (1:100 dilution)	Cations* (1:10 dilution)	Wet Sediment* (cooled)
Geo B 11301-1	PC	X (Rhizon)	X	X	X	X	---	---	X	---	X	X	X	X
Geo B 11301-2	PC	X (Rhizon)	X	X	X	X	---	---	---	---	X	X	X	X
Geo B 11303	DAPC	X (Rhizon)	---	---	---	---	---	---	---	---	---	X	---	---
Geo B 11304-2	PC	X (Rhizon)	X	X	X	X	---	---	X	---	X	X	X	X
Geo B 11304-3	PC	X (Rhizon)	X	X	X	X	---	---	X	X	X	X	X	X
Geo B 11309	DAPC	X (Rhizon)	---	---	---	---	---	---	---	---	---	X	---	---
Geo B 11311-1	ISP	---	X	X	X	X	---	---	---	---	---	X	X	---
Geo B 11311-3	PC	X (Rhizon)	X	X	X	X	---	---	---	---	X	X	X	X
Geo B 11311-4	PC	X (Rhizon)	X	X	X	X	---	---	---	---	X	X	X	X
Geo B 11311-7	PC	X (Rhizon)	X	X	X	X	X	X	X	X	X	X	X	X
Geo B 11311-8	PC	X (Rhizon)	X	X	X	X	X	X	X	X	X	X	X	X
Geo B 11312	GC	X (Rhizon)	X	X	X	X	---	---	X	---	X	X	X	X
Geo B 11314	DAPC	X (Rhizon)	---	---	---	---	---	---	---	---	---	X	---	---
Geo B 11316	GC	X (Rhizon)	X	X	X	X	X	X	X	X	X	X	X	X
Geo B 11320	GC (DAPC)	X (Rhizon)	X	X	X	X	X	X	X	X	X	X	X	X
Geo B 11323	TV- MUC	X (Rhizon)	X	X	X	X	---	---	---	---	---	X	X	X
Geo B 11324 -A	TV- MUC	X (Rhizon)	X	X	X	X	X	---	---	---	---	X	X	X
Geo B 11324 -B	TV- MUC	X (Rhizon)	X	X	X	X	---	X	---	---	---	X	X	X
Geo B 11325	DAPC	X (Rhizon)	---	---	---	---	---	---	---	---	---	X	---	---

*** for analyses or further processings in the home lab**

Abreviations:

PC **P**ush **C**ore
DAPC Dynamic Autoclave Piston Corer
ISP **I**n **S**itu **P**rofiler
GC **G**ravity **C**orer
MUC **Mu**lti **C**orer

Gravity Core GeoB 11327 - background core

Gravity Core GeoB 11327 was retrieved north-west of the Amsterdam Mud Volcano. This sediment core, which was sampled in a plastic foil, did not contain any gas hydrates and can thus be regarded as a reference or background site for the study area which is not affected by hydrocarbon/gas seepage. At this site alkalinity is on a relatively low level with maximum values of 4 to 5 mmol(eq)/l. Nutrients in pore water reach concentrations of 150 µmol/l NH_4 and 1.6 µmol/l PO_4. In the upper part of this core dissolved iron concentrations increase with depth to a maximum of 55 µmol/l in 130 cm. At this site hydrogen sulfide could be detected by smell below a depth of 330 cm.

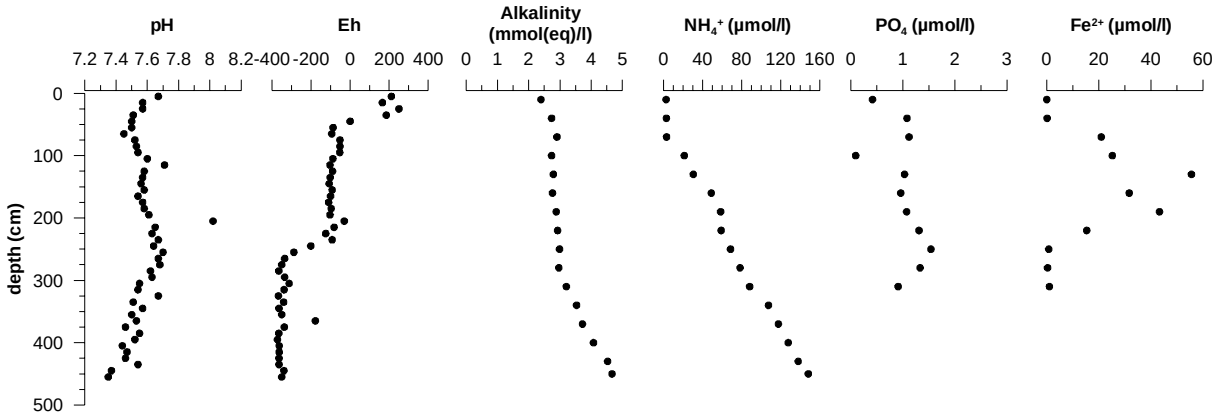

Fig. 31: Pore water concentration profiles of gravity core GeoB 11327 from the Anaximander Mountain area.

GeoB 11304-2 (PC 9) and GeoB 11304-3 (PC 68)

These two push cores were taken at the inner flank of the south-eastern rim of the Amsterdam MV. The sea floor in this area was rough and covered with some bigger clasts. Both cores contained shells in the upper centimetres and core GeoB 11304-2 was characterized by an intensive hydrogen sulfide smell and also had a very dark colour. With a value of 8 the pH is similar for both PCs. Eh values are oscillating between +200 and -200 at GeoB 11304-3 and around -200 at GeoB 11304-2.

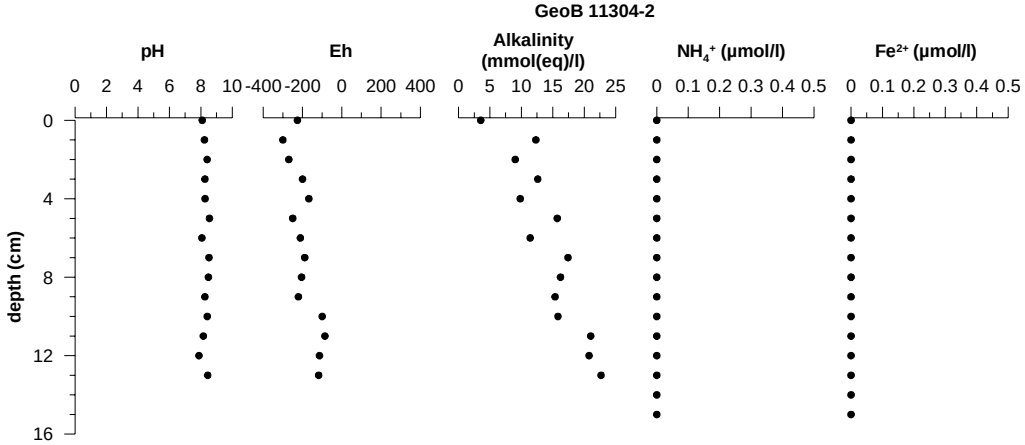

Fig. 32: Pore water concentration profiles of core GeoB 11304-2 (Push core 9).

Phosphate and iron were measured only in core GeoB 11304-3 because of the strong smell of hydrogen sulfide in core GeoB 11304-2. Alkalinity shows a constant value of 2.5 mmol(eq)/l for core GeoB 11304-3, while it increases with depth up to 22 mmol(eq)/l in core GeoB 11304-2.

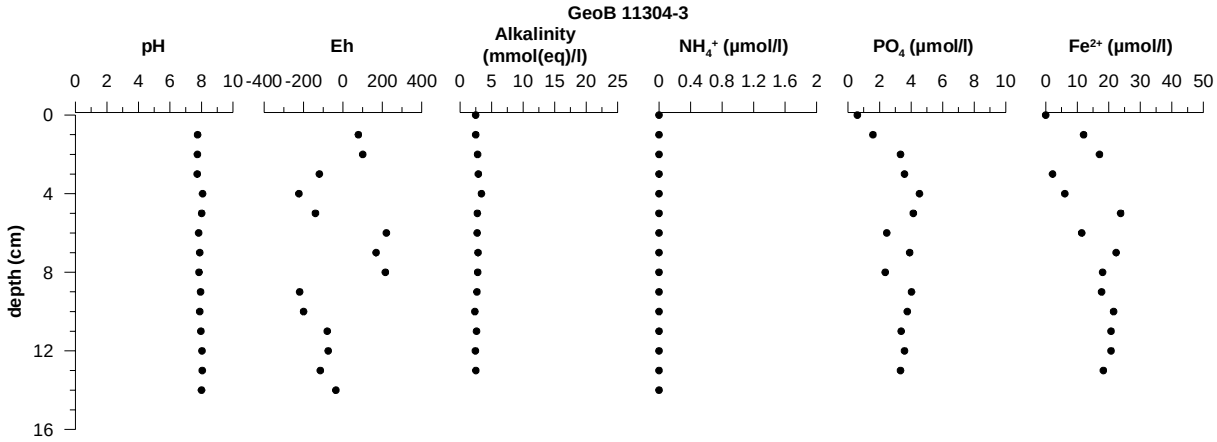

Fig. 33: Pore water concentration profiles of core GeoB 11304-3 (Push core 68).

GeoB 11311-3 (PC 36) and GeoB 11311-4 (PC 41)

These two cores were characterised by a strong smell of hydrogen sulfide. We expect that below 4 cm sulfide will be detected in pore water. Phosphate was not measured. In both cores the dissolved iron concentrations are decreasing from approx. 2µmol/l at the top to 0 µmol/l at 4 cmbsf.

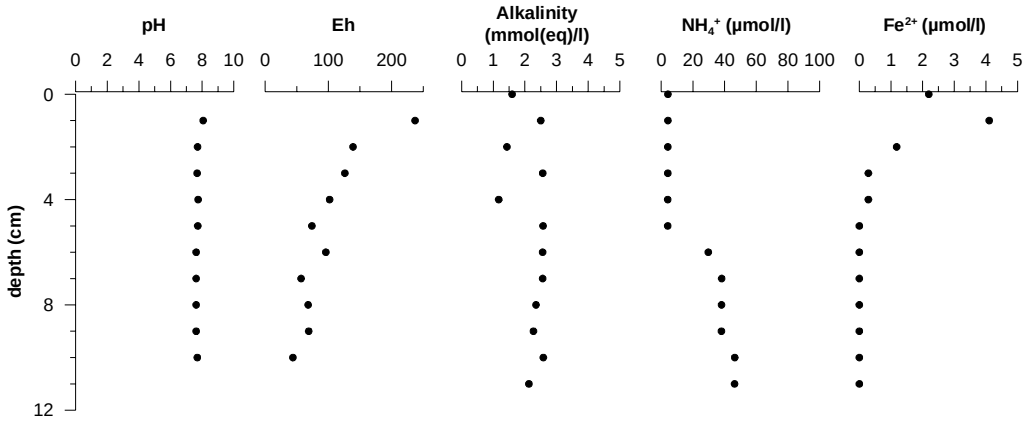

Fig. 34: Pore water concentration profiles of core GeoB 11311-3 (Push core 36).

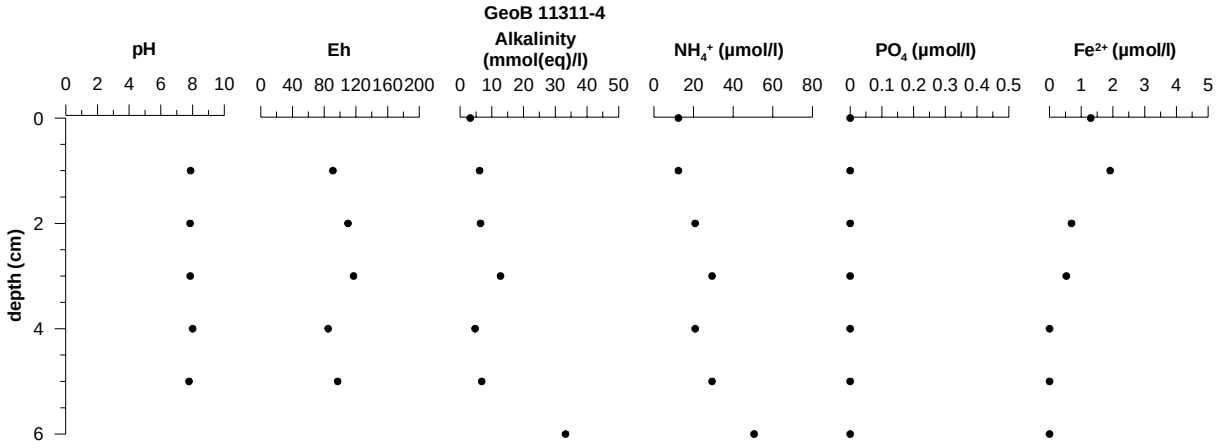

Fig. 35: Pore water concentration profiles of core GeoB 11311-4 (Push core 41).

Gravity Core GeoB 11320 (DAPC core)

This core was taken with the Dynamic Autoclave Piston Corer (DAPC) and was recovered from the inner part of the south-western flank of the MV. This core was sampled in a plastic liner and reached a length of 245 cm. The core did not show any indication of gas hydrate presence. The pH value of 8 is similar to the other cores taken in the mud volcano's area. In the upper 50 cm of the core a strong shift to negative Eh values is observed.

In the upper 80 cm alkalinity stays at very low values of 2 mmol(eq)/l increasing to values of 20 mmol(eq)/l at a depth below 130 cm. The prominent spike in alkalinity with values of 40 to 60 mmol(eq)/l at a depth between 110 and 130 cm might be sampling or analytical artefacts. Anyhow, the profile suggests that the sulphate-methane transition zone (SMTZ) is located at a depth of around 120 cm. Ammonium increases continuously below a depth of 50 cm to a value of 60 µmol/l in the lowest part of the core. Phosphate oscillates around values of 0.5 µmol/l from the surface to approx. 130 cm and then increases to values between 2 and 3 µmol/l at the bottom of the core. Iron was only detected at a depth of 30 cm. Below a depth of approx. 150 cm the core had a discernable smell of hydrogen sulfide.

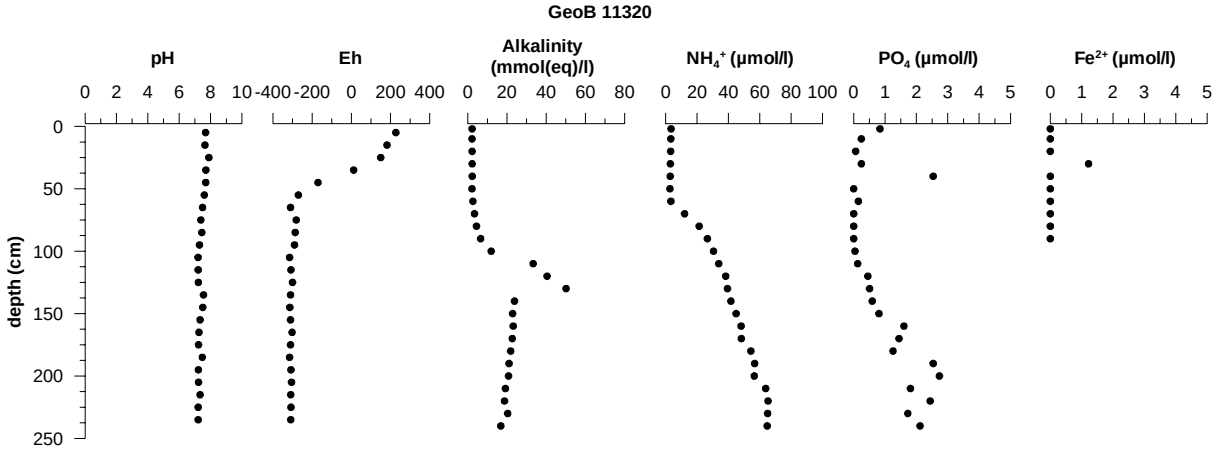

Fig. 36: Pore water concentration profiles of gravity Core GeoB 11320 (DAPC).

TV MUC GeoB 11324-B

Core GeoB 11324 gives additional information about the conditions in the central area of the Amsterdam MV. The core had a length of 18 cm, it was dark blue grey in colour and had a strong smell of hydrogen sulfide. The dissolved iron concentrations were fluctuating around 1 µmol/l. Phosphate starts with a concentration of 3 µmol/l at 1 cm depth increasing to 4.5 µmol/l at a depth of 10 cm. In the top part of the core ammonium is present in very low concentrations with values oscillating around 1 µmol/l. Below 9 cm it increases to a maximum value of 35 µmol/l at a depth of 17 cm. Alkalinity stays on a constant value around 2 mmol(eq)/l. Below a depth of 12 cm it increases to values around 6 mmol(eq)/l.

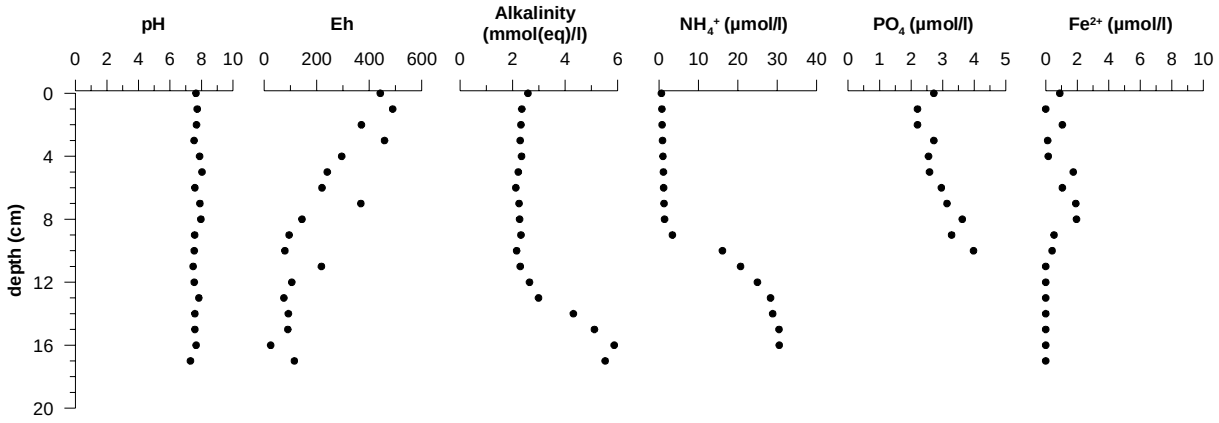

Fig. 37: Pore water concentration profiles of TV-MUC GeoB 11324-B.

Subsumption/Conclusions

The investigated area of the Amsterdam Mud Volcano is generally influenced by an active mud volcanism connected with several hydrocarbon seep sites. The mud volcano is a nearly circular volcano structure with an outer rim, build of massive carbonate crusts and an inner part covered with mud breccia. Mud volcanism combined with patches of active fluid and gas seepage is closely connected with a prominent, east - west oriented strike-slip fault system. Inside the mud volcano, large spatial heterogeneities in chemical and sedimentary properties often occur on a centimetre to decimetre scale. Pore water profiles of fluid seep spots, connected with sharp geochemical gradients on a narrow vertical range may reflect areas with high turnover rates. These seep patches are mainly situated close to and inside the MV´s active centre. Geochemical parameters of push core GeoB 11304-2 deployed in a black seep patch (in contrast to push core GeoB 11304-3 deployed in a significantly different environment as seen on the ROV pictures) clearly show an area of high turnover rates. A prominent increase in alkalinity values from 10 to 25 mmol(eq)/l at site GeoB 11304-2 may point to a shallow SMTZ located close to the lower part of the core. Due to a free gas discharge spot in the centre, sulfate reduction by anaerobic oxidation of methane is probably the dominant geochemical process. Sample sites not influenced by fluid seepage (e.g. push core GeoB 11311-3) reveal distinctly lower turnover rates. Massive authigenic carbonate precipitates are found at and close to the outer rim. Due to elevated alkalinity values measured there (e.g. GeoB 11304-2, GeoB 11320) it can be assumed that carbonate precipitation is concentrated at the inner flank of the outer rim.

9 Chemosynthetic Communities Associated with Cold Seeps on Amsterdam Mud Volcano

(K. Olu-Le Roy, S. Dentrecolas)

9.1 Introduction

Three main fluid flow systems have been explored so far in the Eastern Mediterranean Sea: the Olimpi Mud Volcano field along the Mediterranean Ridge south of Crete, the Anaximander Mountains south of Turkey and the Nile deep-sea fan. Two cruises with the French submersible NAUTILE were conducted, the dutch-french MEDINAUT cruise in 1998 (Woodside et al. 2000) and the French cruise NAUTINIL in 2003. The study of 4 dives on the Amsterdam mud volcano allowed to define different facies from the centre to the external zones of this 3 km wide mud volcano (Zitter et al. 2005) and the distribution of the visible chemosynthetic fauna (siboglinid tube worms or "pogonophorans") and bivalve shells have been decried from video analysis (Olu-le Roy et al. 2004). Several symbiotic species have been sampled, including 5 species of bivalves belonging to 4 families (Lucinidae, Vesicomyidae, Thyasiridae and Mytilidae) and two Siboglinidae polychaetes (a large *Lamellibrachia sp*. and smaller *Sclerolinum sp.*). These species have also be found in the Nile Delta and some of them in the Olimpi Mud Volcano field.

All have associated symbionts, either sulfide-oxidizing bacteria, either both sulfide-oxidizers and methanotrops for the small mytilid Idas modiolaeformis. The centre of Amsterdam MV was described as a very rough area with young mud flows and sparse chemosynthetic fauna, and the highest Lamellibrachia sp. density were observed in external areas associated with carbonate concretions. Dense bivalve fields were observed in these areas but also dispersed bivalves were observed in the whole summit of the volcano.

The general objective of this cruise was to get more data to document the cold-seep community structure and distribution on Amsterdam Mud Volcano and take the opportunity to have a cruise planned at one year interval to monitor in the faunal community.

Detailed objectives were to:

- Map habitats and community from video survey to compare their distribution with those documented in 1998.
- Characterize the composition of the epi- and endofauna at an active seep site, ideally close to carbonates and with a large Lamellibrachia bush.
- Deploy devices for colonisation experiments on hard and soft substratum.
- Monitor the community by the deployment of an autonomous imaging module.
- (AIM) to be recovered next year (MEDECO Cruise Oct 2007).

9.2 Preliminary Results

The three first dives were dedicated to surveys of the eastern, central and western parts of the volcano. On both eastern and western ridges we observed carbonate crusts and small Siboglinid groups generally under the carbonate pavements (Fig. 38 left).

Fig. 38: Siboglinidae among carbonate crusts (left). Chaceon crab among gas bubbles at Marker 3.

A large accumulation field of empty tubes was also seen in the eastern ridge. The western part where was observed and the higher density of tube worms in 1998 was cut by deep crevasses and fractures that seem to have broken carbonate pavements. Very fresh slide scars were seen. In the eastern part, a black spot was observed and sampled, showing small tubes at the sediment interface, maybe young Siboglinids. A net sample was done at these sites as well as two cores and bubbles were seen escaping during the sampling. In the central part several sites with bubbles were detected owing to the QUEST sonar. Gastropods were observed at these sites, probably grazing microbial mats on the sediment. Crabs, likely Chaceon mediterraneus (Fig. 38) were also frequent at these sites, moving the sediment very close to the bubbles. Small tubes in the sediment were also observed during the dives.

Table 12: Samples taken during METEOR Cruise M70/3.

Dive No	Site	Sample tool	GeoB No	Preliminary identifications
129	Amsterdam MV, east	Net	11301-4	Vesicomyidae, mytilidae shell, gastropoda, polychaeta, pogonophora, thyasiridae
129	Amsterdam MV east	Sampling box	11301-5	*Lamellibrachia* sp. empty tubes
130	Amsterdam MV west	Net	11304-1	Pogonophora?
133	Amsterdam MV	Carbonate crust		Mytilidae
134	Amsterdam MV, at Marker 5	Blade Corer	11315-1	Polychaetes, bivalves
134	Amsterdam MV, Marker 5	Rotary sample 1	11315-2	Vesicomyidae, polychaeta, gastropoda
134	New Bubble site	Rotary sample 2	11315-2	Polychaeta, thyasiridae, amphipoda, gastropoda
134	New Bubble site	Basket	11315-3	4 *Lamellibrachia* sp.
137	Thessaloniki MV	Net	11326-1	

Deployments:

Two devices devoted to colonisation experiments were deployed at the Marker 5 site during the dive 134. The “SMAC” is composed of 4 bowls filled with glass bowls enriched with organic matter at different concentrations and is dedicated to settlement experiment of species

living in the soft substratum. The "Rack" is made of twenty slates for settlement of hard substratum species.

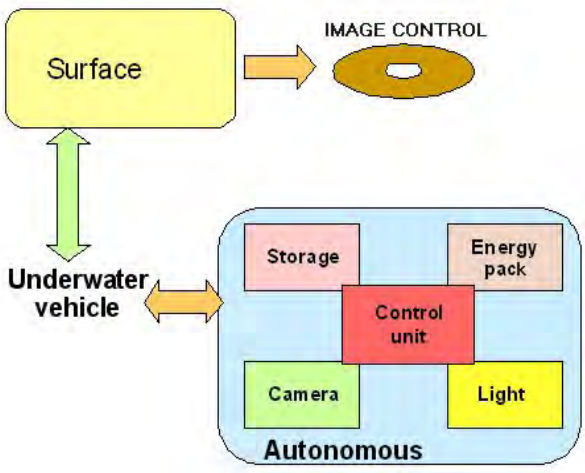

Fig. 39: The general functional architecture of the autonomous module (AIM).

The **Autonomous Imaging Module (AIM)** was deployed at Marker 6 (35° 20.083'N; 30° 16.124' E; GeoB: 11322). The Autonomous Imaging Module (AIM) was developed during the ExocetD European project. A first prototype was deployed in August 2006 on an hydrothermal vent site. A second prototype has been built for cold seeps in the framework of the HERMES European program. The technical team which was involved in this technical development was composed of 3 engineers from the Underwater System Department at Ifremer Toulon: Pierre Léon electronic engineer, Jean Pierre Leveque mechanical engineer and Stéphane Dentrecolas electronic engineer who was in charge of the integration of the camera and of the long term deployment.The system includes the underwater autonomous module and the surface unit needed for configuration, check and data copy.

The operational use of the system can distinguish different separate phases of operation

(1) *Deployment:* the AIM has to be deployed on a shuttle or with an underwater vehicle on a the seabed
(2) *Configuration:* with the use of a contact-less link, the module is connected to the ROV. The camera is put in a nominal configuration (zoom, iris, focus) and the different timings of the video sequences are determined
(3) *Autonomous mode:* the module is then disconnected from the ROV and run autonomously during long periods
(4) *Recovery:* After the recovery of the mooring, video sequences are downloaded on board

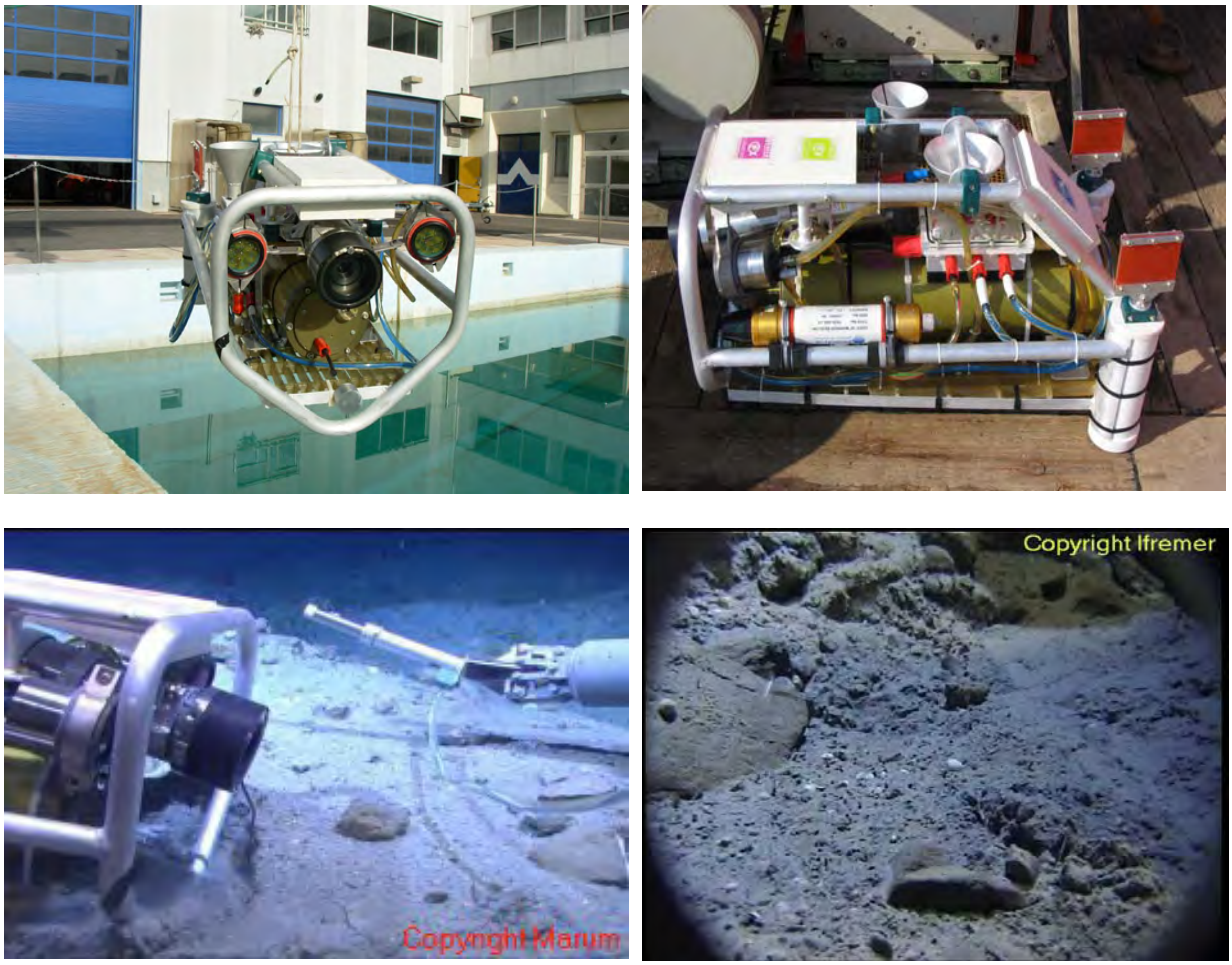

Fig. 38: Views of the Autonomous Imaging module (AIM). On land (above left), on the working deck of R/V METEOR (above right). During the deployment at the sea floor (Dive 136; below left). Thanks to its arm QUEST takes the CLSI link fitted in the basket and places it in dedicated place inside the AIM in order to pilot with success the camera and lights from the PC QUEST on the METEOR. The view of the AIM is checked since the PC QUEST by the serial link (below right). Then the system is programmed at 16:22 to remain one year on the seabed and record 2 video sequences of 60 s per day.

The AIM has a frame constructed by aluminum which allows an easy handling by underwater vehicle manipulators. The video camera and electronic parts is housed in titanium pressure chambers. The system has two LED lights and a CLSI link with a receptacle funnel. The port hole of the camera is equipped with an anti biofouling system. Thanks to the manipulation capabilities of QUEST 4000, the Autonomous Imaging Module has been placed in from an interesting seabed area at 15:00 (see Dive 136; Chapter 5).

10 References

Abegg F, Hohnberg HJ, Pape T, Bohrmann G, Freitag J (submitted) Development and application of pressure core sampling systems for the investigation of gas and gas hydrate bearing sediments. Deep Sea Research Part I: Oceanographic Research Papers.

Aloisi G, Pierre C, Rouchy JM, Foucher JP and Woodside JM (2000) Methane-related authigenic carbonates of eastern Mediterranean Sea mud volcanoes and their possible relation to gas hydrate destabilisation. Earth and Planetary Science Letters 184(1): 321-338.

Bernard BB, Brooks JM and Sackett WM (1976) Natural gas seepage in the Gulf of Mexico. Earth and Planetary Science Letters 3: 48-54.

Bohrmann G and Torres M (2006) Gas hydrates in marine sediments. In Schulz HD and Zabel M., Marine Geochemistry: 481- 512, Springer. GEOTECH-194.

Campbell KA, (2006) Hydrocarbon seep and hydrothermal vent paleoenvironments and paleontology: Past developments and future research directions. Palaeogeography, Palaeoclimatology, Palaeoecology, 232(2-4): 362-407.

Charlou JL, Donval JP, Zitter T, Roy N, Jean-Baptiste P, Foucher JP, Woodside JM (2003) Evidence of methane venting and geochemistry of brines on mud volcanoes of the eastern Mediterranean Sea. Deep Sea Research Part I: Oceanographic Research Papers 50: 941-958.

Chaumillon A, Cita MB, Della Vedova B, Fusi N, Mirable L, Pellis G, (1995) Geophysical evidence of mud diapirisim on the Mediterranean ridge accretionary complex. Marine Geolophys.Res.17: 15-141.

DeMets C, Gordon RG, Argus DF, Stein S (1994) Effect of recent revisions to the geomagnetic reversal time scale on estimates of current plate motions. Geophys. Res. Lett. 21: 2191-2194.

Dewey JF, Sengor CAM, (1970) Aegean and surrounding regions: complex multiple and continuum tectonics in a convergent zone. Geo.Soc.Am.Bulletin 90: 84-92.

Heeschen KU, Hohnberg HJ, Haeckel M, Abegg F, Drews M, Bohrmann G (2007) In situ hydrocarbon concentrations from pressurized cores in surface sediments, Northern Gulf of Mexico. Marine Chemistry 107: 498-515.

Huguen RR, Hensen C, Lange G (2005) Pore water geochemistry of eastern Mediterranean mud volcanoes: Implications for fluid transport and fluid origin. Marine Geology 225: 191-208.

Kullenberg B, (1947) The piston core sampler, Sven. Hydrogr.-Biol. Komm. Skr., Ser. 3, Hydrogr. 1 (2): 46p.

Lammers S, Suess E (1994) An improved head-space analysis method for methane in seawater. Marine Chemistry 47: 115-125.

McClusky S, Bassalanian S, Barka A, Demir C, Ergintav S, Georgiev I, Gurkan O, Hamburger M, Hurst K, Hans-Gert HG, Karstens K, Kekelidze G, King R, Kotzev V, Lenk O, Mahmoud S, Mishin A, Nadariya M, Ouzounis A, Paradissis D, Peter Y, Prilepin M, Relinger R, Sanli I, Seeger H, Tealeb A, Toksaz MN, Veis G (2000) Global Positioning system constraints on plate kinematics and dynamics in the eastern Mediterranean and Caucasus. Journal of Geophysical Research, 105 (B3): 5695-5719.

Olu-Le Roy K, Sibuet M, Fiala-Medioni A, Gofas S, Salas C, Mariotti A, Foucher J-P, Woodside JM (2004) Cold seep communities in the deep eastern Mediterranean Sea: composition, symbiosis and spatial distribution on mud volcanoes. Deep Sea Research Part I: Oceanographic Research Papers 51: 1915-1936.

Peckmann J, Goedert JL, Thiel V, Michaelis W and Reitner J (2002) A comprehensive approach to the study of methane-seep deposits from the Lincoln Creek Formation, western Washington State, USA. Sedimentology, 49(4): 855-873.

Sperling M, Schmiedl G et al. (2003) Black Sea impact on the formation of eastern Mediterranean sapropel S1? Evidence from the Marmara Sea. Palaeogeography, Palaeoclimatology, Palaeoecology 190: 9-21.

Wessel P and Smith WHF (1998) New, improved version of generic mapping tools released. Eos Trans. AGU 79(47): 579-579.

Whiticar MJ (1999) Carbon and hydrogen isotope systematics of bacterial formation and oxidation of methane. Chemical Geology 161: 291-314.

Woodside JM, Dumont JF, (1997) The Anaximander mountains are a southward rifted and foundered part of southwestern Turkish Taurus. Terra Nova 9: 394.

Woodside JM, Ivanov MK, Limonov AF and shipboard scientists of the Anaxiprobe expeditions (1998) Shallow gas and gas hydrates in the Anaximander Mountains region, eastern Mediterranean Sea. In: Gas Hydrates: Relevance to World Margin Stability and Climate Change (eds. Henriet JP and Mienert J) London, Geological Society. 137: 177-193.

Woodside JM (2000) On the tectonic framework of the Cyprus Arc, in Gokcekus H (ed.) Proceedings of the International Conference on Earthquake Hazard and Risk in the Mediterranean Region (EHRMR'99): 417-425.

Woodside JM, Mascle J, Zitter TAC, Limonov AF, Ergun M, and Volkonskaia A (2002) The Florence Rise, the western bend of the Cyprus Arc. Mar. Geol. 185: 177–194.

Zitter TAC, Huguen C, Woodside JM (2005) Geology of mud volcanoes in the eastern Mediterranean from combined sidescan sonar and submersible surveys. Deep-Sea Research I 52: 457-475.

Appendix

A 1 Station List

RV METEOR cruise M70/3							Begin / on seafloor			End / off seafloor			
Date	St. No.	St. No.			Start Sci:	End Sci:	Latitude	Longitude	Water	Latitude	Longitude	Water	Recovery
	GeoB		Instruments	Location	Program	Program	N°	E°	depth (m)	N°	E°	depth (m)	Remarks
M70/3													
28.11.06	**11301**	ROV-1	ROV-129	**AMV**	08:38	16:57	35:20.000	30:16.087	2070	35:19.850	30:14.860	1985	
	11301-1	Push core 1	--	**AMV**	--	09:35	35:19.951	30:15.889	--	--	--	--	Push core 36
	11301-2	Push core 2	--	**AMV**	--	10:14	35:19.952	30:15.893	--	--	--	--	Push core 41
	11301-3	Rotary 1	--	**AMV**	--	10:24	35:19.952	30:15.894	--	--	--	--	Rotary sampler, box No 5
	11301-4	net 1	--	**AMV**	--	10:39	35:19.950	30:15.901	--	--	--	--	1st net, box No 2
	11301-5	carbonate 1	--	**AMV**	--	13:09	35:19.618	30:15.358	--	--	--	--	Box No 2
	11301-6	carbonate 2	--	**AMV**	--	14:32	35:19.516	30:15.172	--	--	--	--	Box No 3
28.11.06	**11302**	SL-1	SL 6 m	**AMV**	19:49	20:42	35:19.999	30:16.275	2023	--	--	--	USBL; 205 cm recovery; gas hydrates
29.11.06	**11303**	DAPC-1	DAPC	**AMV**	05:15	06:07	35:19.996	30:16.278	2024	--	--	--	USBL; recovery 95 cm
29.11.06	**11304**	ROV-2	ROV-130	**AMV**	08:46	17:58	35:19.854	30:17.006	2034	35:20.041	30:16.168	2024	
	11304-1	Net 1	--	**AMV**	--	11:11	35:19.864	30:16.672	--	--	--	--	Net A3: sediment, gas hydrate?
	11304-2	Push core 1	--	**AMV**	--	11:24	35:19.862	30:16.655	--	--	--	--	Push core 9 (black sediment)
	11304-3	Push core 2	--	**AMV**	--	11:29	35:19.862	30:16.661	--	--	--	--	Push core 68 (greyish sediment; no bubbles)
29.11.06	**11305**	SL-2	SL 6 m	**AMV**	21:12	22:00	35:19.536	30:14.877	2020	--	--	--	USBL; recovery 25 cm; mud; shells
30.11.06	**11306**	SL-3	SL 3 m	**AMV**	04:44	05:29	35:19.997	30:16.275	2024	--	--	--	USBL; approx. 200 cm recovery; frozen in liq. N2
30.11.06	**11307**	MOVE-1	MOVE-36	**AMV**	09:30	13:00	35:19.556	30:14.864	2015	--	--	--	USBL; sonar data; technical test: no communication
30.11.06	**11308**	ROV-3	ROV-131	**AMV**	13:37	20:31	35:19.900	30:14.958	2000	35:20.035	30:16.190	2023	
	11308-1	Carbonate 1	--	**AMV**	--	15:24	35:20.181	30:14.848	--	--	--	--	Carbonate crust
01.12.06	**11309**	DAPC-2	DAPC	**AMV**	05:06	05:47	35:20.041	30:16.177	2023	--	--	--	244 cm recovery
	11310	ROV-4	ROV-132	**AMV**	14:10	18:41	35:19.752	30:15.116	1998	35:19.303	30:14.131	2011	
02.12.06	**11311**	ROV-5	ROV-133	**AMV**	07:55	17:03	35:20.048	30:16.158	2025	35:20.051	30:16.144	2023	
	11311-1	Profiler	--	**AMV**	--	09:33	35:20.032	30:16.189	--	--	--	--	In-situ profiler
	11311-2	Gas sampler 1	--	**AMV**	--	10:32	35:20.181	30:16.123	--	--	--	--	Gas pressure sampler-1
	11311-3	Push core 1	--	**AMV**	--	10:40	35:20.181	30:16.123	--	--	--	--	Push core 36
	11311-4	Push core 2	--	**AMV**	--	10:48	35:20.181	30:16.123	--	--	--	--	Push core 41
	11311-5	Carbonate 1	--	**AMV**	--	10:53	35:20.181	30:16.123	--	--	--	--	Carbonate crust
	11311-6	Gas sampler 2	--	**AMV**	--	13:13	35:20.050	30:16.175	--	--	--	--	Gas pressure sampler-2
	11311-7	Push core 3	--	**AMV**	--	13:56	35:20.052	30:16.156	--	--	--	--	Push core 14
	11311-8	Push core 4	--	**AMV**	--	14:16	35:20.050	30:16.155	--	--	--	--	Push core-16
	11312	SL-4	SL 3 m	**AMV**	20:51	21:39	35:20.035	30:16.189	2024	--	--	--	USBL; gas hydrates; 130 cm recovery
	11313	SL-5	SL 3 m	**AMV**	22:44	23:26	35:20.017	30:16.179	2023	--	--	--	USBL; approx. 230 cm recovery; frozen in liq. N2

A 1 Continuation Station List

RV METEOR cruise M70/3

Date	St. No.	St. No.			Start Sci:	End Sci:	Begin / on seafloor			End / off seafloor			Recovery
	GeoB		Instruments	Location	Program	Program	N°	E°	depth (m)	N°	E°	depth (m)	Remarks
03.12.06	**11314**	DAPC-3	DAPC	**AMV**	05:19	06:08	35:20.039	30:16.173	2023	--	--	--	USBL failure; 248 cm recovery
	11315	ROV-6	ROV-134	**AMV**	08:23	17:57	35:20.049	30:16.153	2028	35:20.100	30:15.325	2025	
	11315-1	blade corer	--	**AMV**	--	11:33	35:20.011	30:16.151	--	--	--	--	Blade corer 8
	11315-2	Rotary 1	--	**AMV**	--	12:32	35:20.020	30:16.164	--	--	--	--	Rotary, box 1
	11315-3	Rotary 2	--	**AMV**	--	16:12	35:20.072	30:16.146	--	--	--	--	Rotary, box 2
	11316	SL-6	SL 3 m	**AMV**	21:05	21:50	35:20.030	30:16.181	2022	--	--	--	USBL; 243 cm recovery
	11317	SL-7	SL 3 m	**AMV**	22:58	23:42	35:20.043	30:16.185	2020	--	--	--	USBL; 250 cm recovery
04.12.06	**11318**	MOVE-2	MOVE-37	**AMV**	06:15	20:52	35:19.549	30:14.862	2013	--	--	--	Transection; sea floor sonar
	11319	ROV-7	ROV-135	**AtMV**	11:51	17:21	35:23.197	30:12.745	1799	35:23.447	30:12.659	1815	
	11319-1	Tube worm 1	--	**AtMV**	--	13:52	35:23.279	30:12.644	--	--	--	--	Tubeworms, boxes 1 & 3
	11319-2	Carbonate 1	--	**AtMV**	--	14:32	35:23.263	30:12.611	--	--	--	--	carbonate, box 2
	11319-3	Rotary 1	--	**AtMV**	--	16:22	35:23.328	30:12.604	--	--	--	--	Rotary 1
	11319-4	Rotary 2	--	**AtMV**	--	16:25	35:23.328	30:12.602	--	--	--	--	Rotary 2
05.12.06	**11320**	DAPC-4	DAPC	**AMV**	05:25	07:11	35:19.594	30:15.007	2026	--	--	--	USBL; 250 cm; no in-situ pressure preserved
	11321	SL-8	SL 3 m	**AMV**	07:28	08:06	35:19.596	30:14.997	2020	--	--	--	USBL; 45 cm recovery
	11322	ROV-8	ROV-136	**AMV**	11:58	20:26	35:16.164	30:16.164	2025	35:19.736	30:15.280	2023	
	11323	TV-MUC-1	TV-MUC	**AMV**	23:05	23:13	35:19.578	30:14.990	2025	--	--	--	
06.12.06	**11324**	TV-MUC-2	TV-MUC	**AMV**	01:45	01:45	35:20.064	30:16.189	2015	--	--	--	
	11325	DAPC-5	DAPC	**AMV**	09:10	10:30	35:20.007	30:15.981	2023	--	--	--	USBL; 148 cm recovery
	11326	ROV-9	ROV-137	**TMV**	12:39	19:56	35:28.289	30:15.693	1345	35:28.509	30:15.4030	1339	
	11326-1	Net 1	--	**TMV**	--	17:56	35:28.510	30:15.143	--	--	--	--	Net, box 2
	11326-2	Push core 1	--	**TMV**	--	19:40	35:28.511	30:15.146	--	--	--	--	Push core 41
	11326-3	Tube worm	--	**TMV**	--	19:53	35:28.510	30:15.156	--	--	--	--	Tubeworm
	11327	SL-9	SL 3 m	**AMV**	23:14	00:01	35:21.006	30:15.004	2083	--	--	--	USBL; 458 cm recovery
07.12.06	**11328**	SL-10	SL 3 m	**AMV**	01:16	01:59	35:20.003	30:16.266	2023	--	--	--	USBL; 290 cm recovery

	Abbreviations:	**SL**	Gravity corer	
		DAPC	Dynamic autoclave piston corer	
		TV-MUC	TV-multicorer	
		ROV	Remotely operated vehicle QUEST	
		MOVE	MOVE	
	Mud volcanoes	**AMV**	Amsterdam Mud Volcano	
		AtMV	Athina Mud Volcano	
		TMV	Thessaloniki Mud Volcano	

ROV samples / tools:
Rotary sampler
Net
Carbonate
Tube worm
Pressure sampler
In-situ profiler: ISPS
Blade corer (IFREMER)
Push core

A 2 Core Descriptions

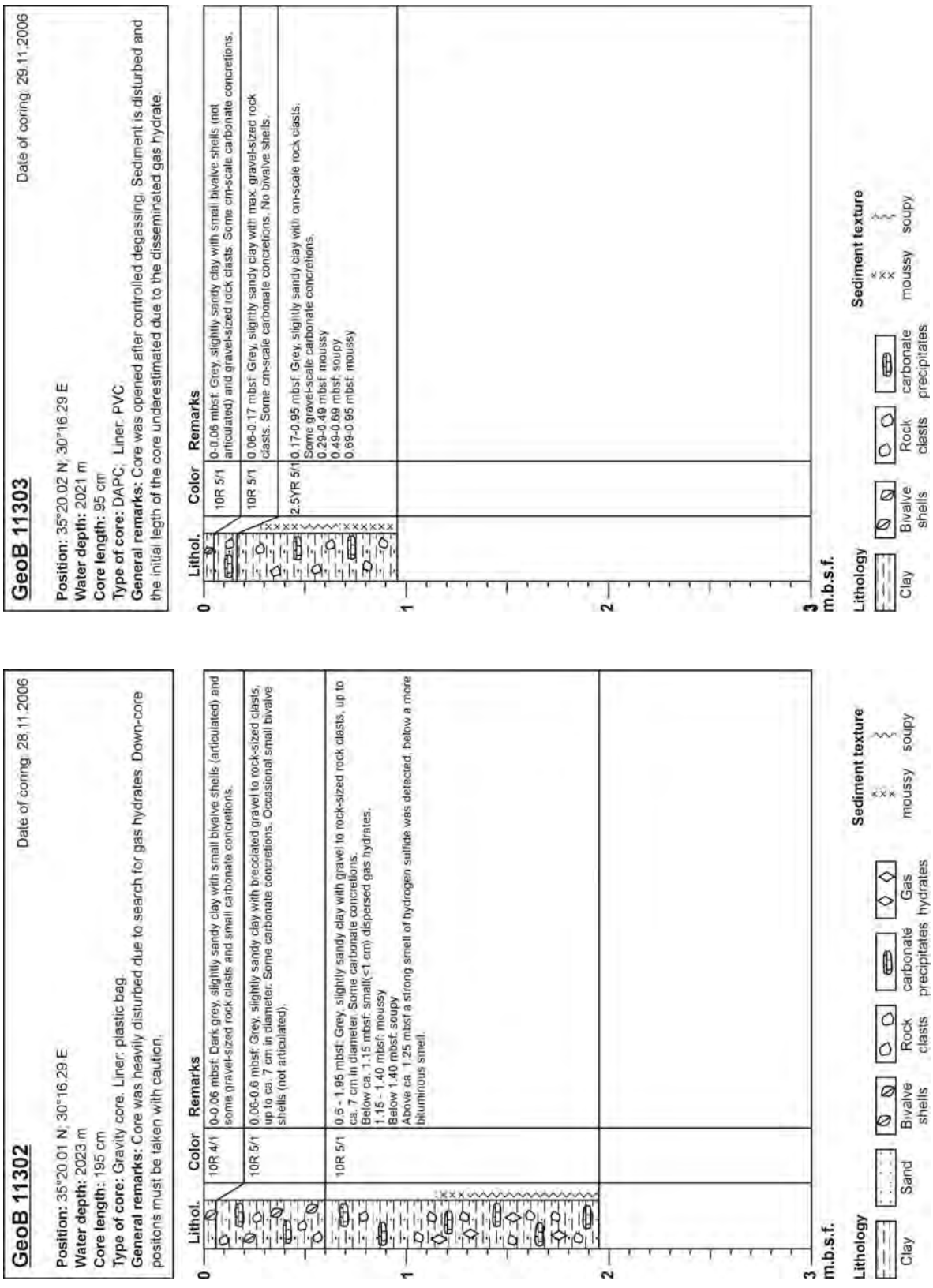

A 2 Continuation Core Descriptions

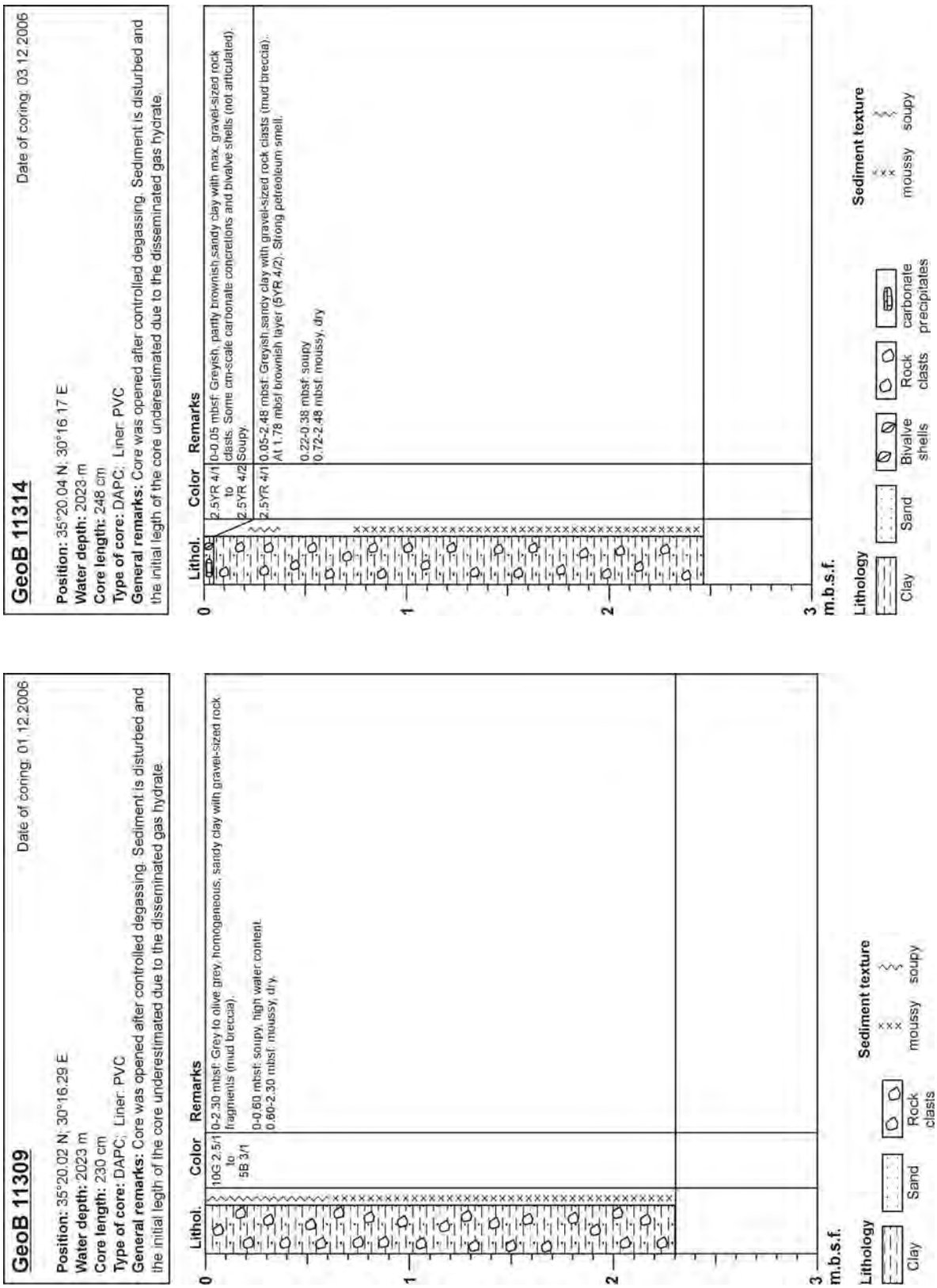

A 2 Continuation Core Descriptions

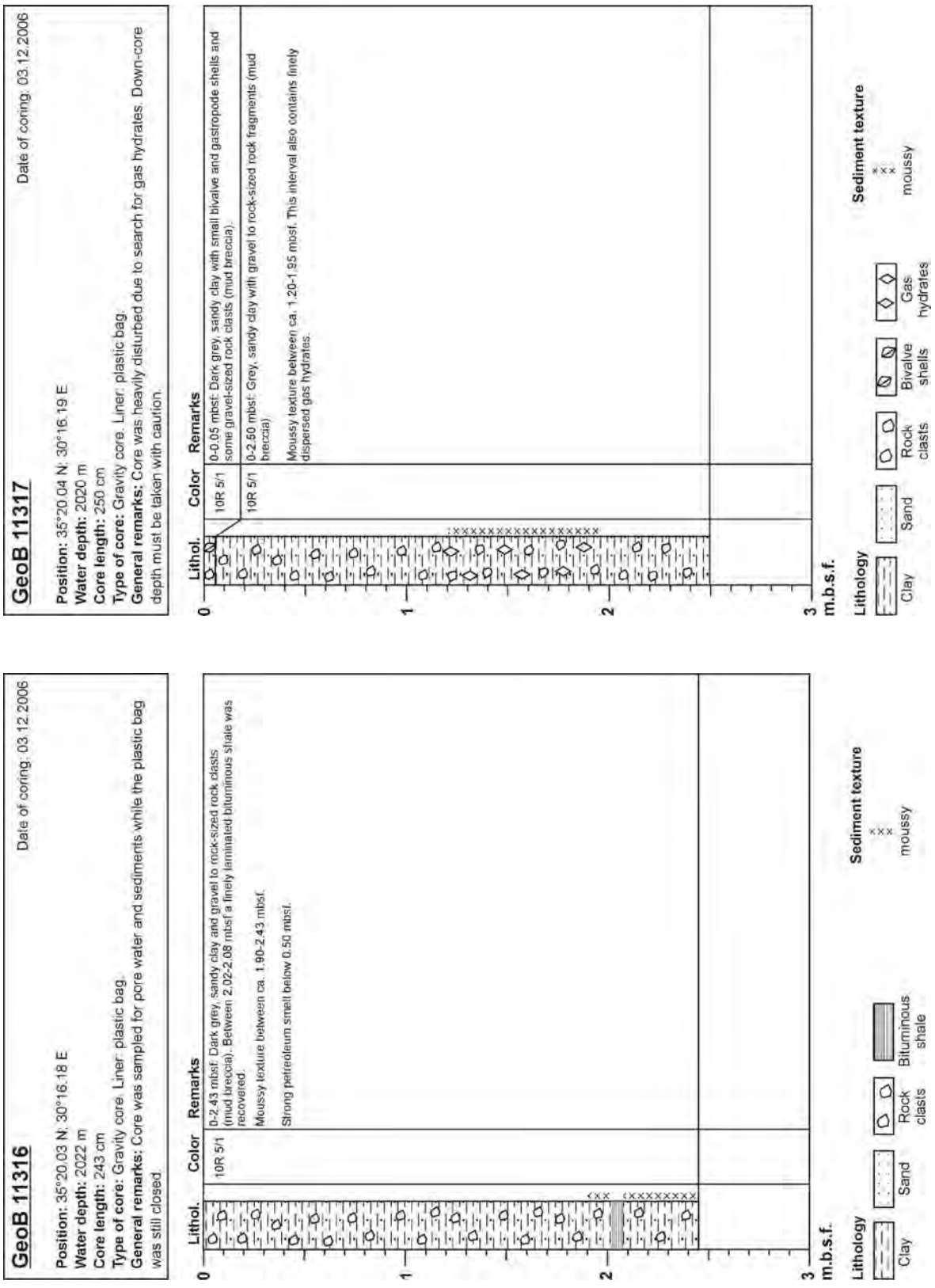

A 2 Continuation Core Dscriptions

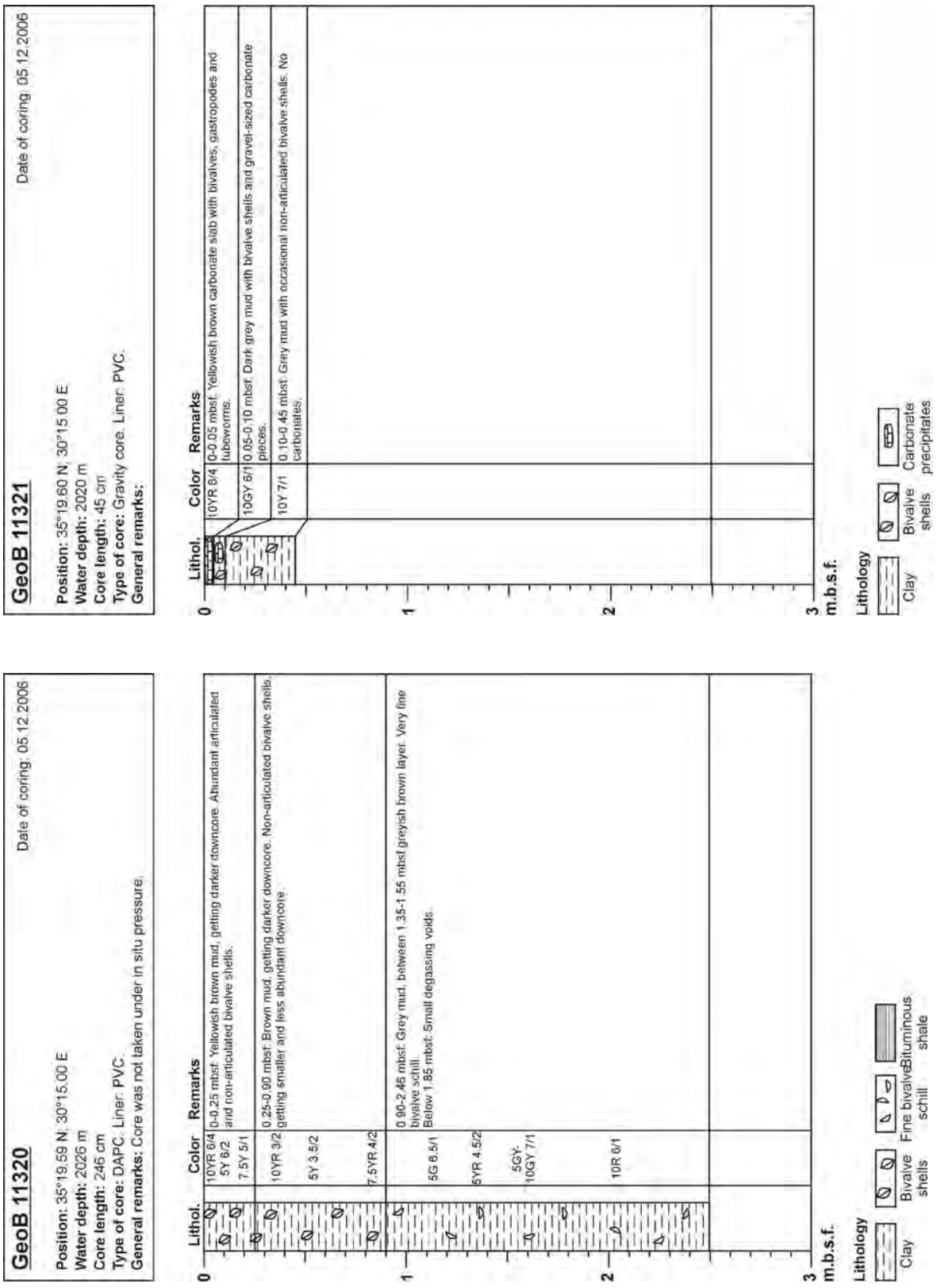

A 2 Continuation Core Descriptions

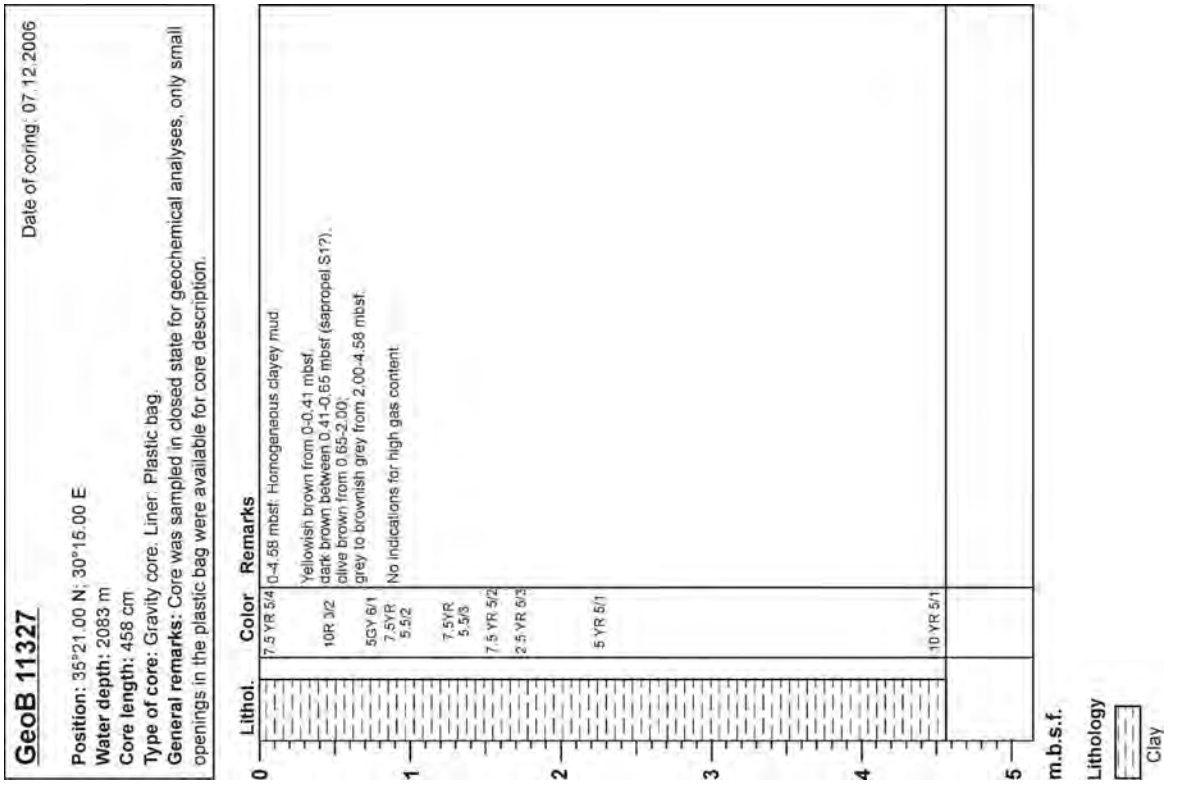

A 2 Continuation Core Descriptions

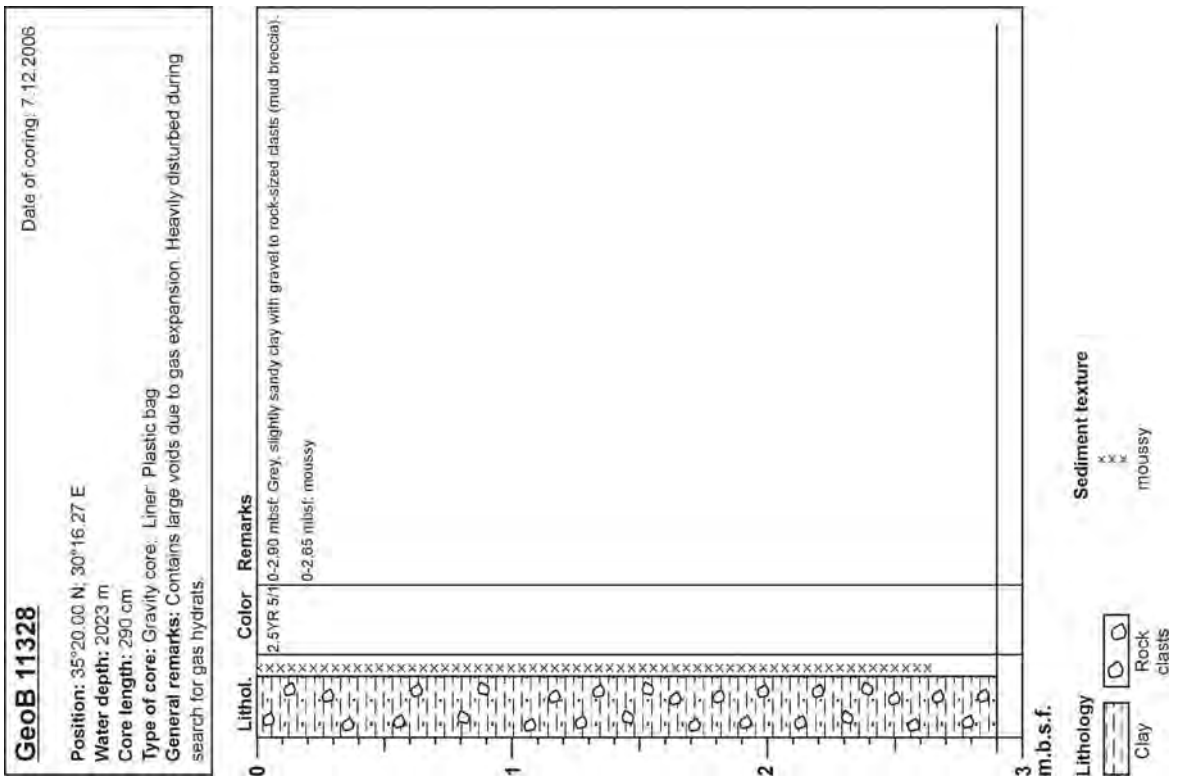

Appendix 3

A 3 Distribution of Hydrocarbons in the C_1 to *i*-C_4-Range found in Gases of the Amsterdam Mud Volcano

Sample code	Accumulated gas volume released	CH_4	C_2H_6	C_3H_8	*i*-C_4H_{10}	$C_1/(C_2+C_3)$
	[mL]	[mol-% of C_1 to *i*-C_4]	[mol-% of C_1 to *i*-C_4]	[mol-% of C_1 to *i*-C_4]	[mol-% of C_1 to *i*-C_4]	
Free gas (GeoB11311-6) (gas bubble sampler)		98.50	1.23	0.20	0.07	68.9
Gas hydrate (GeoB11302) (gravity corer)		93.38	4.58	1.55	0.49	15.2
DAPC 01 (GeoB11303)						
1	240	98.60	1.27	0.10	0.02	71.9
2	480	98.50	1.38	0.09	0.02	66.7
3	1,030	98.24	1.68	0.06	0.02	56.3
4	1,770	98.08	1.85	0.05	0.01	51.4
5	3,260	98.00	1.95	0.04	0.01	49.3
6	3,500	98.00	1.95	0.04	0.01	49.3
7	3,940	98.03	1.93	0.04	0.01	49.9
8	5,380	97.99	1.97	0.04	0.01	48.9
9	6,380	97.98	1.98	0.03	0.01	48.7
10	8,220	98.01	1.95	0.03	0.01	49.4
11	10,100	97.96	2.01	0.03	0.01	48.1
12	11,900	98.03	1.93	0.03	0.01	50.0
13	13,740	97.93	2.03	0.03	0.01	47.5
14	15,620	97.87	2.10	0.03	0.01	46.0
15	18,260	97.58	2.38	0.04	0.01	40.4
16	23,900	97.46	2.49	0.04	0.01	38.5
17	26,540	97.38	2.56	0.05	0.01	37.3
18	30,140	97.21	2.72	0.05	0.01	35.0
19	35,580	97.04	2.87	0.06	0.02	33.0
20	43,860	97.00	2.91	0.07	0.02	32.6
21	50,260	96.75	3.15	0.08	0.02	29.9
22	56,700	96.45	3.42	0.10	0.03	27.4
23	62,180	95.88	3.83	0.21	0.07	23.7
24	65,020	93.84	5.36	0.64	0.16	15.6
25	69,620	94.88	4.36	0.57	0.20	19.3
26	72,460	94.62	4.58	0.62	0.18	18.2
27	77,100	95.09	4.20	0.55	0.16	20.0
28	79,940	95.86	3.59	0.44	0.10	23.8
DAPC 03 (GeoB11314)						
1	1,840	98.12	1.77	0.08	0.03	52.9
DAPC 05 (GeoB11325)						
1	540	97.23	2.57	0.15	0.05	35.7
2	1,840	96.16	3.26	0.44	0.15	26.0

A 3 Continuation Distribution of Hydrocarbons

Sample code	Accumulated gas volume released [mL]	CH_4 [mol-% of C_1 to *i*-C_4]	C_2H_6 [mol-% of C_1 to *i*-C_4]	C_3H_8 [mol-% of C_1 to *i*-C_4]	*i*-C_4H_{10} [mol-% of C_1 to *i*-C_4]	$C_1/(C_2+C_3)$
DAPC 02 (GeoB11309)						
1	1,140	98.62	1.03	0.26	0.09	76.4
2	2,940	98.68	1.00	0.24	0.08	79.8
3	2,980	98.67	1.04	0.21	0.07	78.7
4	5,620	98.58	1.16	0.19	0.07	72.8
5	6,660	98.47	1.34	0.14	0.04	66.3
6	8,500	98.25	1.54	0.16	0.05	57.8
7	9,580	98.03	1.78	0.15	0.05	51.0
8	11,420	97.98	1.83	0.14	0.05	49.8
9	12,460	97.70	2.13	0.12	0.04	43.4
10	14,300	97.61	2.22	0.12	0.04	41.6
11	15,340	97.50	2.35	0.11	0.04	39.7
12	17,140	97.57	2.30	0.10	0.03	40.6
13	19,020	97.47	2.41	0.09	0.03	39.0
14	20,820	97.48	2.42	0.08	0.03	39.0
15	22,660	97.52	2.38	0.08	0.02	39.6
16	24,500	97.15	2.74	0.08	0.02	34.4
17	26,380	97.07	2.82	0.08	0.02	33.4
18	28,120	97.02	2.85	0.09	0.03	32.9
19	29,960	96.92	2.92	0.12	0.03	31.8
20	31,900	96.09	3.59	0.25	0.07	25.0
21	33,740	95.50	4.02	0.37	0.11	21.8
22	35,580	95.89	3.71	0.31	0.09	23.8
23	37,520	95.62	3.88	0.39	0.11	22.4
24	39,360	95.25	4.09	0.51	0.15	20.7
25	43,100	94.65	4.42	0.72	0.20	18.4
26	44,940	95.04	4.18	0.64	0.13	19.7
27	46,780	92.91	5.30	1.41	0.37	13.8
28	48,620	92.01	5.69	1.82	0.48	12.3
29	52,460	91.47	5.91	2.07	0.55	11.5
30	54,300	90.94	6.09	2.35	0.62	10.8
31	56,140	93.41	5.20	1.17	0.22	14.7
32	58,030	90.85	5.73	2.68	0.74	10.8
33	59,920	90.14	5.63	3.28	0.95	10.1
34	63,760	89.66	5.60	3.59	1.16	9.8
35	67,400	89.58	5.54	3.65	1.23	9.7
36	71,040	89.38	5.84	3.61	1.16	9.5
37	74,680	89.58	5.97	3.39	1.06	9.6
38	78,370	90.16	5.94	3.01	0.89	10.1
39	82,160	92.17	5.10	2.12	0.60	12.8
40	85,850	93.97	4.06	1.52	0.45	16.8
41	89,540	93.16	4.64	1.72	0.48	14.7
42	93,330	95.02	3.66	1.04	0.28	20.2
43	96,970	96.24	2.91	0.66	0.18	26.9
44	104,310	96.49	2.74	0.60	0.17	28.9
45	108,150	96.13	2.95	0.72	0.20	26.2
46	109,690	95.68	3.21	0.87	0.24	23.5
47	113,640	95.52	3.24	0.96	0.27	22.7

Publications of this series:

No. 1 **Wefer, G., E. Suess and cruise participants**
Bericht über die POLARSTERN-Fahrt ANT IV/2, Rio de Janeiro - Punta Arenas, 6.11. - 1.12.1985.60 pages, Bremen, 1986.

No. 2 **Hoffmann, G.**
Holozänstratigraphie und Küstenlinienverlagerung an der andalusischen Mittelmeerküste. 173 pages, Bremen, 1988. (out of print)

No. 3 **Wefer, G. and cruise participants**
Bericht über die METEOR-Fahrt M 6/6, Libreville - Las Palmas, 18.2. - 23.3.1988. 97 pages, Bremen, 1988.

No. 4 **Wefer, G., G.F. Lutze, T.J. Müller, O. Pfannkuche, W. Schenke, G. Siedler, W. Zenk**
Kurzbericht über die METEOR-Expedition No. 6, Hamburg - Hamburg, 28.10.1987 - 19.5.1988. 29 pages, Bremen, 1988. (out of print)

No. 5 **Fischer, G.**
Stabile Kohlenstoff-Isotope in partikulärer organischer Substanz aus dem Südpolarmeer (Atlantischer Sektor). 161 pages, Bremen, 1989.

No. 6 **Berger, W.H. and G. Wefer**
Partikelfluß und Kohlenstoffkreislauf im Ozean.
Bericht und Kurzfassungen über den Workshop vom 3.-4. Juli 1989 in Bremen. 57 pages, Bremen, 1989.

No. 7 **Wefer, G. and cruise participants**
Bericht über die METEOR - Fahrt M 9/4, Dakar - Santa Cruz, 19.2. - 16.3.1989. 103 pages, Bremen, 1989.

No. 8 **Kölling, M.**
Modellierung geochemischer Prozesse im Sickerwasser und Grundwasser. 135 pages, Bremen, 1990.

No. 9 **Heinze, P.-M.**
Das Auftriebsgeschehen vor Peru im Spätquartär. 204 pages, Bremen, 1990. (out of print)

No. 10 **Willems, H., G. Wefer, M. Rinski, B. Donner, H.-J. Bellmann, L. Eißmann, A. Müller, B.W. Flemming, H.-C. Höfle, J. Merkt, H. Streif, G. Hertweck, H. Kuntze, J. Schwaar, W. Schäfer, M.-G. Schulz, F. Grube, B. Menke**
Beiträge zur Geologie und Paläontologie Norddeutschlands: Exkursionsführer. 202 pages, Bremen, 1990.

No. 11 **Wefer, G. and cruise participants**
Bericht über die METEOR-Fahrt M 12/1, Kapstadt - Funchal, 13.3.1990 - 14.4.1990. 66 pages, Bremen, 1990.

No. 12 **Dahmke, A., H.D. Schulz, A. Kölling, F. Kracht, A. Lücke**
Schwermetallspuren und geochemische Gleichgewichte zwischen Porenlösung und Sediment im Wesermündungsgebiet. BMFT-Projekt MFU 0562, Abschlußbericht. 121 pages, Bremen, 1991.

No. 13 **Rostek, F.**
Physikalische Strukturen von Tiefseesedimenten des Südatlantiks und ihre Erfassung in Echolotregistrierungen. 209 pages, Bremen, 1991.

No. 14 **Baumann, M.**
Die Ablagerung von Tschernobyl-Radiocäsium in der Norwegischen See und in der Nordsee. 133 pages, Bremen, 1991. (out of print)

No. 15 **Kölling, A.**
Frühdiagenetische Prozesse und Stoff-Flüsse in marinen und ästuarinen Sedimenten. 140 pages, Bremen, 1991.

No. 16 **SFB 261 (ed.)**
1. Kolloquium des Sonderforschungsbereichs 261 der Universität Bremen (14.Juni 1991): Der Südatlantik im Spätquartär: Rekonstruktion von Stoffhaushalt und Stromsystemen. Kurzfassungen der Vorträge und Poster. 66 pages, Bremen, 1991.

No. 17 **Pätzold, J. and cruise participants**
Bericht und erste Ergebnisse über die METEOR-Fahrt M 15/2, Rio de Janeiro - Vitoria, 18.1. - 7.2.1991. 46 pages, Bremen, 1993.

No. 18 **Wefer, G. and cruise participants**
Bericht und erste Ergebnisse über die METEOR-Fahrt M 16/1, Pointe Noire - Recife, 27.3. - 25.4.1991. 120 pages, Bremen, 1991.

No. 19 **Schulz, H.D. and cruise participants**
Bericht und erste Ergebnisse über die METEOR-Fahrt M 16/2, Recife - Belem, 28.4. - 20.5.1991. 149 pages, Bremen, 1991.

No. 20 **Berner, H.**
Mechanismen der Sedimentbildung in der Fram-Straße, im Arktischen Ozean und in der Norwegischen See. 167 pages, Bremen, 1991.

No. 21 **Schneider, R.**
Spätquartäre Produktivitätsänderungen im östlichen Angola-Becken: Reaktion auf Variationen im Passat-Monsun-Windsystem und in der Advektion des Benguela-Küstenstroms. 198 pages, Bremen, 1991. (out of print)

No. 22 **Hebbeln, D.**
Spätquartäre Stratigraphie und Paläozeanographie in der Fram-Straße. 174 pages, Bremen, 1991.

No. 23 **Lücke, A.**
Umsetzungsprozesse organischer Substanz während der Frühdiagenese in ästuarinen Sedimenten. 137 pages, Bremen, 1991.

No. 24 **Wefer, G. and cruise participants**
Bericht und erste Ergebnisse der METEOR-Fahrt M 20/1, Bremen - Abidjan, 18.11.- 22.12.1991. 74 pages, Bremen, 1992.

No. 25 **Schulz, H.D. and cruise participants**
Bericht und erste Ergebnisse der METEOR-Fahrt M 20/2, Abidjan - Dakar, 27.12.1991 - 3.2.1992. 173 pages, Bremen, 1992.

No. 26 **Gingele, F.**
Zur klimaabhängigen Bildung biogener und terrigener Sedimente und ihrer Veränderung durch die Frühdiagenese im zentralen und östlichen Südatlantik. 202 pages, Bremen, 1992.

No. 27 **Bickert, T.**
Rekonstruktion der spätquartären Bodenwasserzirkulation im östlichen Südatlantik über stabile Isotope benthischer Foraminiferen. 205 pages, Bremen, 1992. (out of print)

No. 28 **Schmidt, H.**
Der Benguela-Strom im Bereich des Walfisch-Rückens im Spätquartär. 172 pages, Bremen, 1992.

No. 29 **Meinecke, G.**
Spätquartäre Oberflächenwassertemperaturen im östlichen äquatorialen Atlantik. 181 pages, Bremen, 1992.

No. 30 **Bathmann, U., U. Bleil, A. Dahmke, P. Müller, A. Nehrkorn, E.-M. Nöthig, M. Olesch, J. Pätzold, H.D. Schulz, V. Smetacek, V. Spieß, G. Wefer, H. Willems**
Bericht des Graduierten Kollegs. Stoff-Flüsse in marinen Geosystemen. Berichtszeitraum Oktober 1990 - Dezember 1992. 396 pages, Bremen, 1992.

No. 31 **Damm, E.**
Frühdiagenetische Verteilung von Schwermetallen in Schlicksedimenten der westlichen Ostsee. 115 pages, Bremen, 1992.

No. 32 **Antia, E.E.**
Sedimentology, Morphodynamics and Facies Association of a mesotidal Barrier Island Shoreface (Spiekeroog, Southern North Sea). 370 pages, Bremen, 1993.

No. 33 **Duinker, J. and G. Wefer (ed.)**
Bericht über den 1. JGOFS-Workshop. 1./2. Dezember 1992 in Bremen. 83 pages, Bremen, 1993.

No. 34 **Kasten, S.**
Die Verteilung von Schwermetallen in den Sedimenten eines stadtbremischen Hafenbeckens. 103 pages, Bremen, 1993.

No. 35 **Spieß, V.**
Digitale Sedimentographie. Neue Wege zu einer hochauflösenden Akustostratigraphie. 199 pages, Bremen, 1993.

No. 36 **Schinzel, U.**
Laborversuche zu frühdiagenetischen Reaktionen von Eisen (III) - Oxidhydraten in marinen Sedimenten.189 pages, Bremen, 1993.

No. 37 **Sieger, R.**
CoTAM - ein Modell zur Modellierung des Schwermetalltransports in Grundwasserleitern. 56 pages, Bremen, 1993. (out of print)

No. 38 **Willems, H. (ed.)**
Geoscientific Investigations in the Tethyan Himalayas. 183 pages, Bremen, 1993.

No. 39 **Hamer, K.**
Entwicklung von Laborversuchen als Grundlage für die Modellierung des Transportverhaltens von Arsenat, Blei, Cadmium und Kupfer in wassergesättigten Säulen. 147 pages, Bremen, 1993.

No. 40 **Sieger, R.**
Modellierung des Stofftransports in porösen Medien unter Ankopplung kinetisch gesteuerter Sorptions- und Redoxprozesse sowie thermischer Gleichgewichte. 158 pages, Bremen, 1993.

No. 41 **Thießen, W.**
Magnetische Eigenschaften von Sedimenten des östlichen Südatlantiks und ihre paläozeanographische Relevanz. 170 pages, Bremen, 1993.

No. 42 **Spieß, V. and cruise participants**
Report and preliminary results of METEOR-Cruise M 23/1, Kapstadt - Rio de Janeiro, 4.-25.2.1993. 139 pages, Bremen, 1994.

No. 43 **Bleil, U. and cruise participants**
Report and preliminary results of METEOR-Cruise M 23/2, Rio de Janeiro - Recife, 27.2.-19.3.1993 133 pages, Bremen, 1994.

No. 44 **Wefer, G. and cruise participants**
Report and preliminary results of METEOR-Cruise M 23/3, Recife - Las Palmas, 21.3. - 12.4.1993 71 pages, Bremen, 1994.

No. 45 **Giese, M. and G. Wefer (ed.)**
Bericht über den 2. JGOFS-Workshop. 18../19. November 1993 in Bremen.
93 pages, Bremen, 1994.

No. 46 **Balzer, W. and cruise participants**
Report and preliminary results of METEOR-Cruise M 22/1, Hamburg - Recife,
22.9. - 21.10.1992. 24 pages, Bremen, 1994.

No. 47 **Stax, R.**
Zyklische Sedimentation von organischem Kohlenstoff in der Japan See: Anzeiger für Änderungen von Paläoozeanographie und Paläoklima im Spätkänozoikum.
150 pages, Bremen, 1994.

No. 48 **Skowronek, F.**
Frühdiagenetische Stoff-Flüsse gelöster Schwermetalle an der Oberfläche von Sedimenten des Weser Ästuares. 107 pages, Bremen, 1994.

No. 49 **Dersch-Hansmann, M.**
Zur Klimaentwicklung in Ostasien während der letzten 5 Millionen Jahre:
Terrigener Sedimenteintrag in die Japan See (ODP Ausfahrt 128). 149 pages, Bremen, 1994.

No. 50 **Zabel, M.**
Frühdiagenetische Stoff-Flüsse in Oberflächen-Sedimenten des äquatorialen und östlichen Südatlantik. 129 pages, Bremen, 1994.

No. 51 **Bleil, U. and cruise participants**
Report and preliminary results of SONNE-Cruise SO 86, Buenos Aires - Capetown,
22.4. - 31.5.93 116 pages, Bremen, 1994.

No. 52 **Symposium: The South Atlantic: Present and Past Circulation.**
Bremen, Germany, 15 - 19 August 1994. Abstracts. 167 pages, Bremen, 1994.

No. 53 **Kretzmann, U.B.**
^{57}Fe-Mössbauer-Spektroskopie an Sedimenten - Möglichkeiten und Grenzen.
183 pages, Bremen, 1994.

No. 54 **Bachmann, M.**
Die Karbonatrampe von Organyà im oberen Oberapt und unteren Unteralb (NE-Spanien, Prov. Lerida): Fazies, Zyklo- und Sequenzstratigraphie. 147 pages, Bremen, 1994. (out of print)

No. 55 **Kemle-von Mücke, S.**
Oberflächenwasserstruktur und -zirkulation des Südostatlantiks im Spätquartär.
151 pages, Bremen, 1994.

No. 56 **Petermann, H.**
Magnetotaktische Bakterien und ihre Magnetosome in Oberflächensedimenten des Südatlantiks.
134 pages, Bremen, 1994.

No. 57 **Mulitza, S.**
Spätquartäre Variationen der oberflächennahen Hydrographie im westlichen äquatorialen Atlantik.
97 pages, Bremen, 1994.

No. 58 **Segl, M. and cruise participants**
Report and preliminary results of METEOR-Cruise M 29/1, Buenos-Aires - Montevideo, 17.6. - 13.7.1994 94 pages, Bremen, 1994.

No. 59 **Bleil, U. and cruise participants**
Report and preliminary results of METEOR-Cruise M 29/2, Montevideo - Rio de Janiero 15.7. - 8.8.1994. 153 pages, Bremen, 1994.

No. 60 **Henrich, R. and cruise participants**
Report and preliminary results of METEOR-Cruise M 29/3, Rio de Janeiro - Las Palmas 11.8. - 5.9.1994. Bremen, 1994. (out of print)

No. 61 **Sagemann, J.**
Saisonale Variationen von Porenwasserprofilen, Nährstoff-Flüssen und Reaktionen in intertidalen Sedimenten des Weser-Ästuars. 110 pages, Bremen, 1994. (out of print)

No. 62 **Giese, M. and G. Wefer**
Bericht über den 3. JGOFS-Workshop. 5./6. Dezember 1994 in Bremen. 84 pages, Bremen, 1995.

No. 63 **Mann, U.**
Genese kretazischer Schwarzschiefer in Kolumbien: Globale vs. regionale/lokale Prozesse. 153 pages, Bremen, 1995. (out of print)

No. 64 **Willems, H., Wan X., Yin J., Dongdui L., Liu G., S. Dürr, K.-U. Gräfe**
The Mesozoic development of the N-Indian passive margin and of the Xigaze Forearc Basin in southern Tibet, China. – Excursion Guide to IGCP 362 Working-Group Meeting "Integrated Stratigraphy". 113 pages, Bremen, 1995. (out of print)

No. 65 **Hünken, U.**
Liefergebiets - Charakterisierung proterozoischer Goldseifen in Ghana anhand von Fluideinschluß - Untersuchungen. 270 pages, Bremen, 1995.

No. 66 **Nyandwi, N.**
The Nature of the Sediment Distribution Patterns in ther Spiekeroog Backbarrier Area, the East Frisian Islands. 162 pages, Bremen, 1995.

No. 67 **Isenbeck-Schröter, M.**
Transportverhalten von Schwermetallkationen und Oxoanionen in wassergesättigten Sanden. - Laborversuche in Säulen und ihre Modellierung -. 182 pages, Bremen, 1995.

No. 68 **Hebbeln, D. and cruise participants**
Report and preliminary results of SONNE-Cruise SO 102, Valparaiso - Valparaiso, 95. 134 pages, Bremen, 1995.

No. 69 **Willems, H. (Sprecher), U.Bathmann, U. Bleil, T. v. Dobeneck, K. Herterich, B.B. Jorgensen, E.-M. Nöthig, M. Olesch, J. Pätzold, H.D. Schulz, V. Smetacek, V. Speiß. G. Wefer**
Bericht des Graduierten-Kollegs Stoff-Flüsse in marine Geosystemen. Berichtszeitraum Januar 1993 - Dezember 1995, 45 & 468 pages, Bremen, 1995.

No. 70 **Giese, M. and G. Wefer**
Bericht über den 4. JGOFS-Workshop. 20./21. November 1995 in Bremen. 60 pages, Bremen, 1996. (out of print)

No. 71 **Meggers, H.**
Pliozän-quartäre Karbonatsedimentation und Paläozeanographie des Nordatlantiks und des Europäischen Nordmeeres - Hinweise aus planktischen Foraminiferengemeinschaften. 143 pages, Bremen, 1996. (out of print)

No. 72 **Teske, A.**
Phylogenetische und ökologische Untersuchungen an Bakterien des oxidativen und reduktiven marinen Schwefelkreislaufs mittels ribosomaler RNA. 220 pages, Bremen, 1996. (out of print)

No. 73 **Andersen, N.**
Biogeochemische Charakterisierung von Sinkstoffen und Sedimenten aus ostatlantischen Produktions-Systemen mit Hilfe von Biomarkern. 215 pages, Bremen, 1996.

No. 74 **Treppke, U.**
Saisonalität im Diatomeen- und Silikoflagellatenfluß im östlichen tropischen und subtropischen Atlantik. 200 pages, Bremen, 1996.

No. 75 **Schüring, J.**
Die Verwendung von Steinkohlebergematerialien im Deponiebau im Hinblick auf die Pyritverwitterung und die Eignung als geochemische Barriere. 110 pages, Bremen, 1996.

No. 76 **Pätzold, J. and cruise participants**
Report and preliminary results of VICTOR HENSEN cruise JOPS II, Leg 6, Fortaleza - Recife, 10.3. - 26.3. 1995 and Leg 8, Vítoria - Vítoria, 10.4. - 23.4.1995. 87 pages, Bremen, 1996.

No. 77 **Bleil, U. and cruise participants**
Report and preliminary results of METEOR-Cruise M 34/1, Cape Town - Walvis Bay, 3.-26.1.1996. 129 pages, Bremen, 1996.

No. 78 **Schulz, H.D. and cruise participants**
Report and preliminary results of METEOR-Cruise M 34/2, Walvis Bay - Walvis Bay, 29.1.-18.2.96 133 pages, Bremen, 1996.

No. 79 **Wefer, G. and cruise participants**
Report and preliminary results of METEOR-Cruise M 34/3, Walvis Bay - Recife, 21.2.-17.3.1996. 168 pages, Bremen, 1996.

No. 80 **Fischer, G. and cruise participants**
Report and preliminary results of METEOR-Cruise M 34/4, Recife - Bridgetown, 19.3.-15.4.1996. 105 pages, Bremen, 1996.

No. 81 **Kulbrok, F.**
Biostratigraphie, Fazies und Sequenzstratigraphie einer Karbonatrampe in den Schichten der Oberkreide und des Alttertiärs Nordost-Ägyptens (Eastern Desert, N'Golf von Suez, Sinai). 153 pages, Bremen, 1996.

No. 82 **Kasten, S.**
Early Diagenetic Metal Enrichments in Marine Sediments as Documents of Nonsteady-State Depositional Conditions. Bremen, 1996.

No. 83 **Holmes, M.E.**
Reconstruction of Surface Ocean Nitrate Utilization in the Southeast Atlantic Ocean Based on Stable Nitrogen Isotopes. 113 pages, Bremen, 1996.

No. 84 **Rühlemann, C.**
Akkumulation von Carbonat und organischem Kohlenstoff im tropischen Atlantik: Spätquartäre Produktivitäts-Variationen und ihre Steuerungsmechanismen. 139 pages, Bremen, 1996.

No. 85 **Ratmeyer, V.**
Untersuchungen zum Eintrag und Transport lithogener und organischer partikulärer Substanz im östlichen subtropischen Nordatlantik. 154 pages, Bremen, 1996.

No. 86 **Cepek, M.**
Zeitliche und räumliche Variationen von Coccolithophoriden-Gemeinschaften im subtropischen Ost-Atlantik: Untersuchungen an Plankton, Sinkstoffen und Sedimenten. 156 pages, Bremen, 1996.

No. 87 **Otto, S.**
Die Bedeutung von gelöstem organischen Kohlenstoff (DOC) für den Kohlenstoffffluß im Ozean. 150 pages, Bremen, 1996.

No. 88 **Hensen, C.**
Frühdiagenetische Prozesse und Quantifizierung benthischer Stoff-Flüsse in Oberflächensedimenten des Südatlantiks. 132 pages, Bremen, 1996.

No. 89 **Giese, M. and G. Wefer**
Bericht über den 5. JGOFS-Workshop. 27./28. November 1996 in Bremen. 73 pages, Bremen, 1997.

No. 90 **Wefer, G. and cruise participants**
Report and preliminary results of METEOR-Cruise M 37/1, Lisbon - Las Palmas, 4.-23.12.1996. 79 pages, Bremen, 1997.

No. 91 **Isenbeck-Schröter, M., E. Bedbur, M. Kofod, B. König, T. Schramm & G. Mattheß**
Occurrence of Pesticide Residues in Water - Assessment of the Current Situation in Selected EU Countries. 65 pages, Bremen 1997.

No. 92 **Kühn, M.**
Geochemische Folgereaktionen bei der hydrogeothermalen Energiegewinnung. 129 pages, Bremen 1997.

No. 93 **Determann, S. & K. Herterich**
JGOFS-A6 "Daten und Modelle": Sammlung JGOFS-relevanter Modelle in Deutschland. 26 pages, Bremen, 1997.

No. 94 **Fischer, G. and cruise participants**
Report and preliminary results of METEOR-Cruise M 38/1, Las Palmas - Recife, 25.1.-1.3.1997, with Appendix: Core Descriptions from METEOR Cruise M 37/1. Bremen, 1997.

No. 95 **Bleil, U. and cruise participants**
Report and preliminary results of METEOR-Cruise M 38/2, Recife - Las Palmas, 4.3.-14.4.1997. 126 pages, Bremen, 1997.

No. 96 **Neuer, S. and cruise participants**
Report and preliminary results of VICTOR HENSEN-Cruise 96/1. Bremen, 1997.

No. 97 **Villinger, H. and cruise participants**
Fahrtbericht SO 111, 20.8. - 16.9.1996. 115 pages, Bremen, 1997.

No. 98 **Lüning, S.**
Late Cretaceous - Early Tertiary sequence stratigraphy, paleoecology and geodynamics of Eastern Sinai, Egypt. 218 pages, Bremen, 1997.

No. 99 **Haese, R.R.**
Beschreibung und Quantifizierung frühdiagenetischer Reaktionen des Eisens in Sedimenten des Südatlantiks. 118 pages, Bremen, 1997.

No. 100 **Lührte, R. von**
Verwertung von Bremer Baggergut als Material zur Oberflächenabdichtung von Deponien - Geochemisches Langzeitverhalten und Schwermetall-Mobilität (Cd, Cu, Ni, Pb, Zn). Bremen, 1997.

No. 101 **Ebert, M.**
Der Einfluß des Redoxmilieus auf die Mobilität von Chrom im durchströmten Aquifer. 135 pages, Bremen, 1997.

No. 102 **Krögel, F.**
Einfluß von Viskosität und Dichte des Seewassers auf Transport und Ablagerung von Wattsedimenten (Langeooger Rückseitenwatt, südliche Nordsee). 168 pages, Bremen, 1997.

No. 103 **Kerntopf, B.**
Dinoflagellate Distribution Patterns and Preservation in the Equatorial Atlantic and Offshore North-West Africa. 137 pages, Bremen, 1997.

No. 104 **Breitzke, M.**
Elastische Wellenausbreitung in marinen Sedimenten - Neue Entwicklungen der Ultraschall Sedimentphysik und Sedimentechographie. 298 pages, Bremen, 1997.

No. 105 **Marchant, M.**
Rezente und spätquartäre Sedimentation planktischer Foraminiferen im Peru-Chile Strom. 115 pages, Bremen, 1997.

No. 106 **Habicht, K.S.**
Sulfur isotope fractionation in marine sediments and bacterial cultures. 125 pages, Bremen, 1997.

No. 107 **Hamer, K., R.v. Lührte, G. Becker, T. Felis, S. Keffel, B. Strotmann, C. Waschkowitz, M. Kölling, M. Isenbeck-Schröter, H.D. Schulz**
Endbericht zum Forschungsvorhaben 060 des Landes Bremen: Baggergut der Hafengruppe Bremen-Stadt: Modelluntersuchungen zur Schwermetallmobilität und Möglichkeiten der Verwertung von Hafenschlick aus Bremischen Häfen. 98 pages, Bremen, 1997.

No. 108 **Greeff, O.W.**
Entwicklung und Erprobung eines benthischen Landersystemes zur *in situ*-Bestimmung von Sulfatreduktionsraten mariner Sedimente. 121 pages, Bremen, 1997.

No. 109 **Pätzold, M. und G. Wefer**
Bericht über den 6. JGOFS-Workshop am 4./5.12.1997 in Bremen. Im Anhang: Publikationen zum deutschen Beitrag zur Joint Global Ocean Flux Study (JGOFS), Stand 1/1998. 122 pages, Bremen, 1998.

No. 110 **Landenberger, H.**
CoTReM, ein Multi-Komponenten Transport- und Reaktions-Modell. 142 pages, Bremen, 1998.

No. 111 **Villinger, H. und Fahrtteilnehmer**
Fahrtbericht SO 124, 4.10. - 16.10.199. 90 pages, Bremen, 1997.

No. 112 **Gietl, R.**
Biostratigraphie und Sedimentationsmuster einer nordostägyptischen Karbonatrampe unter Berücksichtigung der Alveolinen-Faunen. 142 pages, Bremen, 1998.

No. 113 **Ziebis, W.**
The Impact of the Thalassinidean Shrimp *Callianassa truncata* on the Geochemistry of permeable, coastal Sediments. 158 pages, Bremen 1998.

No. 114 **Schulz, H.D. and cruise participants**
Report and preliminary results of METEOR-Cruise M 41/1, Málaga - Libreville, 13.2.-15.3.1998. Bremen, 1998.

No. 115 **Völker, D.J.**
Untersuchungen an strömungsbeeinflußten Sedimentationsmustern im Südozean. Interpretation sedimentechographischer Daten und numerische Modellierung. 152 pages, Bremen, 1998.

No. 116 **Schlünz, B.**
Riverine Organic Carbon Input into the Ocean in Relation to Late Quaternary Climate Change. 136 pages, Bremen, 1998.

No. 117 **Kuhnert, H.**
Aufzeichnug des Klimas vor Westaustralien in stabilen Isotopen in Korallenskeletten. 109 pages, Bremen, 1998.

No. 118 **Kirst, G.**
Rekonstruktion von Oberflächenwassertemperaturen im östlichen Südatlantik anhand von Alkenonen. 130 pages, Bremen, 1998.

No. 119 **Dürkoop, A.**
Der Brasil-Strom im Spätquartär: Rekonstruktion der oberflächennahen Hydrographie während der letzten 400 000 Jahre. 121 pages, Bremen, 1998.

No. 120 **Lamy, F.**
Spätquartäre Variationen des terrigenen Sedimenteintrags entlang des chilenischen Kontinentalhangs als Abbild von Klimavariabilität im Milanković- und Sub-Milanković-Zeitbereich. 141 pages, Bremen, 1998.

No. 121 **Neuer, S. and cruise participants**
Report and preliminary results of POSEIDON-Cruise Pos 237/2, Vigo – Las Palmas, 18.3.-31.3.1998. 39 pages, Bremen, 1998

No. 122 **Romero, O.E.**
Marine planktonic diatoms from the tropical and equatorial Atlantic: temporal flux patterns and the sediment record. 205 pages, Bremen, 1998.

No. 123 **Spiess, V. und Fahrtteilnehmer**
Report and preliminary results of RV SONNE Cruise 125, Cochin – Chittagong, 17.10.-17.11.1997. 128 pages, Bremen, 1998.

No. 124 **Arz, H.W.**
Dokumentation von kurzfristigen Klimaschwankungen des Spätquartärs in Sedimenten des westlichen äquatorialen Atlantiks. 96 pages, Bremen, 1998.

No. 125 **Wolff, T.**
Mixed layer characteristics in the equatorial Atlantic during the late Quaternary as deduced from planktonic foraminifera. 132 pages, Bremen, 1998.

No. 126 **Dittert, N.**
Late Quaternary Planktic Foraminifera Assemblages in the South Atlantic Ocean: Quantitative Determination and Preservational Aspects. 165 pages, Bremen, 1998.

No. 127 **Höll, C.**
Kalkige und organisch-wandige Dinoflagellaten-Zysten in Spätquartären Sedimenten des tropischen Atlantiks und ihre palökologische Auswertbarkeit. 121 pages, Bremen, 1998.

No. 128 **Hencke, J.**
Redoxreaktionen im Grundwasser: Etablierung und Verlagerung von Reaktionsfronten und ihre Bedeutung für die Spurenelement-Mobilität. 122 pages, Bremen 1998.

No. 129 **Pätzold, J. and cruise participants**
Report and preliminary results of METEOR-Cruise M 41/3, Vítoria, Brasil – Salvador de Bahia, Brasil, 18.4. - 15.5.1998. Bremen, 1999.

No. 130 **Fischer, G. and cruise participants**
Report and preliminary results of METEOR-Cruise M 41/4, Salvador de Bahia, Brasil – Las Palmas, Spain, 18.5. – 13.6.1998. Bremen, 1999.

No. 131 **Schlünz, B. und G. Wefer**
Bericht über den 7. JGOFS-Workshop am 3. und 4.12.1998 in Bremen. Im Anhang: Publikationen zum deutschen Beitrag zur Joint Global Ocean Flux Study (JGOFS), Stand 1/ 1999. 100 pages, Bremen, 1999.

No. 132 **Wefer, G. and cruise participants**
Report and preliminary results of METEOR-Cruise M 42/4, Las Palmas - Las Palmas - Viena do Castelo; 26.09.1998 - 26.10.1998. 104 pages, Bremen, 1999.

No. 133 **Felis, T.**
Climate and ocean variability reconstructed from stable isotope records of modern subtropical corals (Northern Red Sea). 111 pages, Bremen, 1999.

No. 134 **Draschba , S.**
North Atlantic climate variability recorded in reef corals from Bermuda. 108 pages, Bremen, 1999.

No. 135 **Schmieder, F.**
Magnetic Cyclostratigraphy of South Atlantic Sediments. 82 pages, Bremen, 1999.

No. 136 **Rieß, W.**
In situ measurements of respiration and mineralisation processes – Interaction between fauna and geochemical fluxes at active interfaces. 68 pages, Bremen, 1999.

No. 137 **Devey, C.W. and cruise participants**
Report and shipboard results from METEOR-cruise M 41/2, Libreville – Vitoria, 18.3. – 15.4.98. 59 pages, Bremen, 1999.

No. 138 **Wenzhöfer, F.**
Biogeochemical processes at the sediment water interface and quantification of metabolically driven calcite dissolution in deep sea sediments. 103 pages, Bremen, 1999.

No. 139 **Klump, J.**
Biogenic barite as a proxy of paleoproductivity variations in the Southern Peru-Chile Current. 107 pages, Bremen, 1999.

No. 140 **Huber, R.**
Carbonate sedimentation in the northern Northatlantic since the late pliocene. 103 pages, Bremen, 1999.

No. 141 **Schulz, H.**
Nitrate-storing sulfur bacteria in sediments of coastal upwelling. 94 pages, Bremen, 1999.

No. 142 **Mai, S.**
Die Sedimentverteilung im Wattenmeer: ein Simulationsmodell. 114 pages, Bremen, 1999.

No. 143 **Neuer, S. and cruise participants**
Report and preliminary results of Poseidon Cruise 248, Las Palmas - Las Palmas, 15.2.-26.2.1999. 45 pages, Bremen, 1999.

No. 144 **Weber, A.**
Schwefelkreislauf in marinen Sedimenten und Messung von *in situ* Sulfatreduktionsraten. 122 pages, Bremen, 1999.

No. 145 **Hadeler, A.**
Sorptionsreaktionen im Grundwasser: Unterschiedliche Aspekte bei der Modellierung des Transportverhaltens von Zink. 122 pages, 1999.

No. 146 **Dierßen, H.**
Zum Kreislauf ausgewählter Spurenmetalle im Südatlantik: Vertikaltransport und Wechselwirkung zwischen Partikeln und Lösung. 167 pages, Bremen, 1999.

No. 147 **Zühlsdorff, L.**
High resolution multi-frequency seismic surveys at the Eastern Juan de Fuca Ridge Flank and the Cascadia Margin – Evidence for thermally and tectonically driven fluid upflow in marine sediments. 118 pages, Bremen 1999.

No. 148 **Kinkel, H.**
Living and late Quaternary Coccolithophores in the equatorial Atlantic Ocean: response of distribution and productivity patterns to changing surface water circulation. 183 pages, Bremen, 2000.

No. 149 **Pätzold, J. and cruise participants**
Report and preliminary results of METEOR Cruise M 44/3, Aqaba (Jordan) - Safaga (Egypt) – Dubá (Saudi Arabia) – Suez (Egypt) - Haifa (Israel), 12.3.-26.3.-2.4.-4.4.1999. 135 pages, Bremen, 2000.

No. 150 **Schlünz, B. and G. Wefer**
Bericht über den 8. JGOFS-Workshop am 2. und 3.12.1999 in Bremen. Im Anhang: Publikationen zum deutschen Beitrag zur Joint Global Ocean Flux Study (JGOFS), Stand 1/ 2000. 95 pages, Bremen, 2000.

No. 151 **Schnack, K.**
Biostratigraphie und fazielle Entwicklung in der Oberkreide und im Alttertiär im Bereich der Kharga Schwelle, Westliche Wüste, SW-Ägypten. 142 pages, Bremen, 2000.

No. 152 **Karwath, B.**
Ecological studies on living and fossil calcareous dinoflagellates of the equatorial and tropical Atlantic Ocean. 175 pages, Bremen, 2000.

No. 153 **Moustafa, Y.**
Paleoclimatic reconstructions of the Northern Red Sea during the Holocene inferred from stable isotope records of modern and fossil corals and molluscs. 102 pages, Bremen, 2000.

No. 154 **Villinger, H. and cruise participants**
Report and preliminary results of SONNE-cruise 145-1 Balboa – Talcahuana, 21.12.1999 – 28.01.2000. 147 pages, Bremen, 2000.

No. 155 **Rusch, A.**
Dynamik der Feinfraktion im Oberflächenhorizont permeabler Schelfsedimente. 102 pages, Bremen, 2000.

No. 156 **Moos, C.**
Reconstruction of upwelling intensity and paleo-nutrient gradients in the northwest Arabian Sea derived from stable carbon and oxygen isotopes of planktic foraminifera. 103 pages, Bremen, 2000.

No. 157 **Xu, W.**
Mass physical sediment properties and trends in a Wadden Sea tidal basin. 127 pages, Bremen, 2000.

No. 158 **Meinecke, G. and cruise participants**
Report and preliminary results of METEOR Cruise M 45/1, Malaga (Spain) - Lissabon (Portugal), 19.05. - 08.06.1999. 39 pages, Bremen, 2000.

No. 159 **Vink, A.**
Reconstruction of recent and late Quaternary surface water masses of the western subtropical Atlantic Ocean based on calcareous and organic-walled dinoflagellate cysts. 160 pages, Bremen, 2000.

No. 160 **Willems, H. (Sprecher), U. Bleil, R. Henrich, K. Herterich, B.B. Jørgensen, H.-J. Kuß, M. Olesch, H.D. Schulz,V. Spieß, G. Wefer**
Abschlußbericht des Graduierten-Kollegs Stoff-Flüsse in marine Geosystemen. Zusammenfassung und Berichtszeitraum Januar 1996 - Dezember 2000. 340 pages, Bremen, 2000.

No. 161 **Sprengel, C.**
Untersuchungen zur Sedimentation und Ökologie von Coccolithophoriden im Bereich der Kanarischen Inseln: Saisonale Flussmuster und Karbonatexport. 165 pages, Bremen, 2000.

No. 162 **Donner, B. and G. Wefer**
Bericht über den JGOFS-Workshop am 18.-21.9.2000 in Bremen:
Biogeochemical Cycles: German Contributions to the International Joint Global Ocean Flux Study. 87 pages, Bremen, 2000.

No. 163 **Neuer, S. and cruise participants**
Report and preliminary results of Meteor Cruise M 45/5, Bremen – Las Palmas, October 1 – November 3, 1999. 93 pages, Bremen, 2000.

No. 164 **Devey, C. and cruise participants**
Report and preliminary results of Sonne Cruise SO 145/2, Talcahuano (Chile) - Arica (Chile), February 4 – February 29, 2000. 63 pages, Bremen, 2000.

No. 165 **Freudenthal, T.**
Reconstruction of productivity gradients in the Canary Islands region off Morocco by means of sinking particles and sediments. 147 pages, Bremen, 2000.

No. 166 **Adler, M.**
Modeling of one-dimensional transport in porous media with respect to simultaneous geochemical reactions in CoTReM. 147 pages, Bremen, 2000.

No. 167 **Santamarina Cuneo, P.**
Fluxes of suspended particulate matter through a tidal inlet of the East Frisian Wadden Sea (southern North Sea). 91 pages, Bremen, 2000.

No. 168 **Benthien, A.**
Effects of CO_2 and nutrient concentration on the stable carbon isotope composition of C37:2 alkenones in sediments of the South Atlantic Ocean. 104 pages, Bremen, 2001.

No. 169 **Lavik, G.**
Nitrogen isotopes of sinking matter and sediments in the South Atlantic. 140 pages, Bremen, 2001.

No. 170 **Budziak, D.**
Late Quaternary monsoonal climate and related variations in paleoproductivity and alkenone-derived sea-surface temperatures in the western Arabian Sea. 114 pages, Bremen, 2001.

No. 171 **Gerhardt, S.**
Late Quaternary water mass variability derived from the pteropod preservation state in sediments of the western South Atlantic Ocean and the Caribbean Sea. 109 pages, Bremen, 2001.

No. 172 **Bleil, U. and cruise participants**
Report and preliminary results of Meteor Cruise M 46/3, Montevideo (Uruguay) – Mar del Plata (Argentina), January 4 – February 7, 2000. Bremen, 2001.

No. 173 **Wefer, G. and cruise participants**
Report and preliminary results of Meteor Cruise M 46/4, Mar del Plata (Argentina) – Salvador da Bahia (Brazil), February 10 – March 13, 2000. With partial results of METEOR cruise M 46/2. 136 pages, Bremen, 2001.

No. 174 **Schulz, H.D. and cruise participants**
Report and preliminary results of Meteor Cruise M 46/2, Recife (Brazil) – Montevideo (Uruguay), December 2 – December 29, 1999. 107 pages, Bremen, 2001.

No. 175 **Schmidt, A.**
Magnetic mineral fluxes in the Quaternary South Atlantic: Implications for the paleoenvironment. 97 pages, Bremen, 2001.

No. 176 **Bruhns, P.**
Crystal chemical characterization of heavy metal incorporation in brick burning processes. 93 pages, Bremen, 2001.

No. 177 **Karius, V.**
Baggergut der Hafengruppe Bremen-Stadt in der Ziegelherstellung. 131 pages, Bremen, 2001.

No. 178 **Adegbie, A. T.**
Reconstruction of paleoenvironmental conditions in Equatorial Atlantic and the Gulf of Guinea Basins for the last 245,000 years. 113 pages, Bremen, 2001.

No. 179 **Spieß, V. and cruise participants**
Report and preliminary results of R/V Sonne Cruise SO 149, Victoria - Victoria, 16.8. - 16.9.2000. 100 pages, Bremen, 2001.

No. 180 **Kim, J.-H.**
Reconstruction of past sea-surface temperatures in the eastern South Atlantic and the eastern South Pacific across Termination I based on the Alkenone Method. 114 pages, Bremen, 2001.

No. 181 **von Lom-Keil, H.**
Sedimentary waves on the Namibian continental margin and in the Argentine Basin – Bottom flow reconstructions based on high resolution echosounder data. 126 pages, Bremen, 2001.

No. 182 **Hebbeln, D. and cruise participants**
PUCK: Report and preliminary results of R/V Sonne Cruise SO 156, Valparaiso (Chile) - Talcahuano (Chile), March 29 - May 14, 2001. 195 pages, Bremen, 2001.

No. 183 **Wendler, J.**
Reconstruction of astronomically-forced cyclic and abrupt paleoecological changes in the Upper Cretaceous Boreal Realm based on calcareous dinoflagellate cysts. 149 pages, Bremen, 2001.

No. 184 **Volbers, A.**
Planktic foraminifera as paleoceanographic indicators: production, preservation, and reconstruction of upwelling intensity. Implications from late Quaternary South Atlantic sediments. 122 pages, Bremen, 2001.

No. 185 **Bleil, U. and cruise participants**
Report and preliminary results of R/V METEOR Cruise M 49/3, Montevideo (Uruguay) - Salvador (Brasil), March 9 - April 1, 2001. 99 pages, Bremen, 2001.

No. 186 **Scheibner, C.**
Architecture of a carbonate platform-to-basin transition on a structural high (Campanian-early Eocene, Eastern Desert, Egypt) – classical and modelling approaches combined. 173 pages, Bremen, 2001.

No. 187 **Schneider, S.**
Quartäre Schwankungen in Strömungsintensität und Produktivität als Abbild der Wassermassen-Variabilität im äquatorialen Atlantik (ODP Sites 959 und 663): Ergebnisse aus Siltkorn-Analysen. 134 pages, Bremen, 2001.

No. 188 **Uliana, E.**
Late Quaternary biogenic opal sedimentation in diatom assemblages in Kongo Fan sediments. 96 pages, Bremen, 2002.

No. 189 **Esper, O.**
Reconstruction of Recent and Late Quaternary oceanographic conditions in the eastern South Atlantic Ocean based on calcareous- and organic-walled dinoflagellate cysts. 130 pages, Bremen, 2001.

No. 190 **Wendler, I.**
Production and preservation of calcareous dinoflagellate cysts in the modern Arabian Sea. 117 pages, Bremen, 2002.

No. 191 **Bauer, J.**
Late Cenomanian – Santonian carbonate platform evolution of Sinai (Egypt): stratigraphy, facies, and sequence architecture. 178 pages, Bremen, 2002.

No. 192 **Hildebrand-Habel, T.**
Die Entwicklung kalkiger Dinoflagellaten im Südatlantik seit der höheren Oberkreide. 152 pages, Bremen, 2002.

No. 193 **Hecht, H.**
Sauerstoff-Optopoden zur Quantifizierung von Pyritverwitterungsprozessen im Labor- und Langzeit-in-situ-Einsatz. Entwicklung - Anwendung – Modellierung. 130 pages, Bremen, 2002.

No. 194 **Fischer, G. and cruise participants**
Report and Preliminary Results of RV METEOR-Cruise M49/4, Salvador da Bahia – Halifax, 4.4.-5.5.2001. 84 pages, Bremen, 2002.

No. 195 **Gröger, M.**
Deep-water circulation in the western equatorial Atlantic: inferences from carbonate preservation studies and silt grain-size analysis. 95 pages, Bremen, 2002.

No. 196 **Meinecke,G. and cruise participants**
Report of RV POSEIDON Cruise POS 271, Las Palmas - Las Palmas, 19.3.-29.3.2001. 19 pages, Bremen, 2002.

No. 197 **Meggers, H. and cruise participants**
Report of RV POSEIDON Cruise POS 272, Las Palmas - Las Palmas, 1.4.-14.4.2001. 19 pages, Bremen, 2002.

No. 198 **Gräfe, K.-U.**
Stratigraphische Korrelation und Steuerungsfaktoren Sedimentärer Zyklen in ausgewählten Borealen und Tethyalen Becken des Cenoman/Turon (Oberkreide) Europas und Nordwestafrikas. 197 pages, Bremen, 2002.

No. 199 **Jahn, B.**
Mid to Late Pleistocene Variations of Marine Productivity in and Terrigenous Input to the Southeast Atlantic. 97 pages, Bremen, 2002.

No. 200 **Al-Rousan, S.**
Ocean and climate history recorded in stable isotopes of coral and foraminifers from the northern Gulf of Aqaba. 116 pages, Bremen, 2002.

No. 201 **Azouzi, B.**
Regionalisierung hydraulischer und hydrogeochemischer Daten mit geostatistischen Methoden. 108 pages, Bremen, 2002.

No. 202 **Spieß, V. and cruise participants**
Report and preliminary results of METEOR Cruise M 47/3, Libreville (Gabun) - Walvis Bay (Namibia), 01.06 - 03.07.2000. 70 pages, Bremen 2002.

No. 203 **Spieß, V. and cruise participants**
Report and preliminary results of METEOR Cruise M 49/2, Montevideo (Uruguay) - Montevideo, 13.02 - 07.03.2001. 84 pages, Bremen 2002.

No. 204 **Mollenhauer, G.**
Organic carbon accumulation in the South Atlantic Ocean: Sedimentary processes and glacial/interglacial Budgets. 139 pages, Bremen 2002.

No. 205 **Spieß, V. and cruise participants**
Report and preliminary results of METEOR Cruise M49/1, Cape Town (South Africa) - Montevideo (Uruguay), 04.01.2001 - 10.02.2001. 57 pages, Bremen, 2003.

No. 206 **Meier, K.J.S.**
Calcareous dinoflagellates from the Mediterranean Sea: taxonomy, ecology and palaeoenvironmental application. 126 pages, Bremen, 2003.

No. 207 **Rakic, S.**
Untersuchungen zur Polymorphie und Kristallchemie von Silikaten der Zusammensetzung $Me_2Si_2O_5$ (Me:Na, K). 139 pages, Bremen, 2003.

No. 208 **Pfeifer, K.**
Auswirkungen frühdiagenetischer Prozesse auf Calcit- und Barytgehalte in marinen Oberflächen-sedimenten. 110 pages, Bremen, 2003.

No. 209 **Heuer, V.**
Spurenelemente in Sedimenten des Südatlantik. Primärer Eintrag und frühdiagenetische Überprägung. 136 pages, Bremen, 2003.

No. 210 **Streng, M.**
Phylogenetic Aspects and Taxonomy of Calcareous Dinoflagellates. 157 pages, Bremen 2003.

No. 211 **Boeckel, B.**
Present and past coccolith assemblages in the South Atlantic: implications for species ecology, carbonate contribution and palaeoceanographic applicability. 157 pages, Bremen, 2003.

No. 212 **Precht, E.**
Advective interfacial exchange in permeable sediments driven by surface gravity waves and its ecological consequences. 131 pages, Bremen, 2003.

No. 213 **Frenz, M.**
Grain-size composition of Quaternary South Atlantic sediments and its paleoceanographic significance.123 pages, Bremen, 2003.

No. 214 **Meggers, H. and cruise participants**
Report and preliminary results of METEOR Cruise M 53/1, Limassol - Las Palmas – Mindelo, 30.03.2002 - 03.05.2002. 81 pages, Bremen, 2003.

No. 215 **Schulz, H.D. and cruise participants**
Report and preliminary results of METEOR Cruise M 58/1, Dakar – Las Palmas, 15.04..2003 - 12.05.2003. Bremen, 2003.

No. 216 **Schneider, R. and cruise participants**
Report and preliminary results of METEOR Cruise M 57/1, Cape Town – Walvis Bay, 20.01. – 08.02.2003. 123 pages, Bremen, 2003.

No. 217 **Kallmeyer, J.**
Sulfate reduction in the deep Biosphere. 157 pages, Bremen, 2003.

No. 218 **Røy, H.**
Dynamic Structure and Function of the Diffusive Boundary Layer at the Seafloor. 149 pages, Bremen, 2003.

No. 219 **Pätzold, J., C. Hübscher and cruise participants**
Report and preliminary results of METEOR Cruise M 52/2&3, Istanbul – Limassol – Limassol, 04.02. – 27.03.2002. Bremen, 2003.

No. 220 **Zabel, M. and cruise participants**
Report and preliminary results of METEOR Cruise M 57/2, Walvis Bay – Walvis Bay, 11.02. – 12.03.2003. 136 pages, Bremen 2003.

No. 221 **Salem, M.**
Geophysical investigations of submarine prolongations of alluvial fans on the western side of the Gulf of Aqaba-Red Sea. 100 pages, Bremen, 2003.

No. 222 **Tilch, E.**
Oszillation von Wattflächen und deren fossiles Erhaltungspotential (Spiekerooger Rückseitenwatt, südliche Nordsee). 137 pages, Bremen, 2003.

No. 223 **Frisch, U. and F. Kockel**
Der Bremen-Knoten im Strukturnetz Nordwest-Deutschlands. Stratigraphie, Paläogeographie, Strukturgeologie. 379 pages, Bremen, 2004.

No. 224 **Kolonic, S.**
Mechanisms and biogeochemical implications of Cenomanian/Turonian black shale formation in North Africa: An integrated geochemical, millennial-scale study from the Tarfaya-LaAyoune Basin in SW Morocco. 174 pages, Bremen, 2004. Report online available only.

No. 225 **Panteleit, B.**
Geochemische Prozesse in der Salz- Süßwasser Übergangszone. 106 pages, Bremen, 2004.

No. 226 **Seiter, K.**
Regionalisierung und Quantifizierung benthischer Mineralisationsprozesse. 135 pages, Bremen, 2004.

No. 227 **Bleil, U. and cruise participants**
Report and preliminary results of METEOR Cruise M 58/2, Las Palmas – Las Palmas (Canary Islands, Spain), 15.05. – 08.06.2003. 123 pages, Bremen, 2004.

No. 228 **Kopf, A. and cruise participants**
Report and preliminary results of SONNE Cruise SO175, Miami - Bremerhaven, 12.11 - 30.12.2003. 218 pages, Bremen, 2004.

No. 229 **Fabian, M.**
Near Surface Tilt and Pore Pressure Changes Induced by Pumping in Multi-Layered Poroelastic Half-Spaces. 121 pages, Bremen, 2004.

No. 230 **Segl, M. , and cruise participants**
Report and preliminary results of POSEIDON cruise 304 Galway – Lisbon, 5. – 22. Oct. 2004. 27 pages, Bremen 2004

No. 231 **Meinecke, G. and cruise participants**
Report and preliminary results of POSEIDON Cruise 296, Las Palmas – Las Palmas, 04.04 - 14.04.2003. 42 pages, Bremen 2005.

No. 232 **Meinecke, G. and cruise participants**
Report and preliminary results of POSEIDON Cruise 310, Las Palmas – Las Palmas, 12.04 - 26.04.2004. 49 pages, Bremen 2005.

No. 233 **Meinecke, G. and cruise participants**
Report and preliminary results of METEOR Cruise 58/3, Las Palmas - Ponta Delgada, 11.06 - 24.06.2003. 50 pages, Bremen 2005.

No. 234 **Feseker, T.**
Numerical Studies on Groundwater Flow in Coastal Aquifers. 219 pages. Bremen 2004.

No. 235 **Sahling, H. and cruise participants**
Report and preliminary results of R/V POSEIDON Cruise P317/4, Istanbul-Istanbul , 16 October - 4 November 2004. 92 pages, Bremen 2004.

No. 236 **Meinecke, G. und Fahrtteilnehmer**
Report and preliminary results of POSEIDON Cruise 305, Las Palmas (Spain) - Lisbon (Portugal), October 28th – November 6th, 2004. 43 pages, Bremen 2005.

No. 237 **Ruhland, G. and cruise participants**
Report and preliminary results of POSEIDON Cruise 319, Las Palmas (Spain) - Las Palmas (Spain), December 6th – December 17th, 2004. 50 pages, Bremen 2005.

No. 238 **Chang, T.S.**
Dynamics of fine-grained sediments and stratigraphic evolution of a back-barrier tidal basin of the German Wadden Sea (southern North Sea). 102 pages, Bremen 2005.

No. 239 **Lager, T.**
Predicting the source strength of recycling materials within the scope of a seepage water prognosis by means of standardized laboratory methods. 141 pages, Bremen 2005.

No. 240 **Meinecke, G.**
DOLAN - Operationelle Datenübertragung im Ozean und Laterales Akustisches Netzwerk in der Tiefsee. Abschlussbericht. 42 pages, Bremen 2005.

No. 241 **Guasti, E.**
Early Paleogene environmental turnover in the southern Tethys as recorded by foraminiferal and organic-walled dinoflagellate cysts assemblages. 203 pages, Bremen 2005.

No. 242 **Riedinger, N.**
Preservation and diagenetic overprint of geochemical and geophysical signals in ocean margin sediments related to depositional dynamics. 91 pages, Bremen 2005.

No. 243 **Ruhland, G. and cruise participants**
Report and preliminary results of POSEIDON cruise 320, Las Palmas (Spain) - Las Palmas (Spain), March 08th - March 18th, 2005. 57 pages, Bremen 2005.

No. 244 **Inthorn, M.**
Lateral particle transport in nepheloid layers – a key factor for organic matter distribution and quality in the Benguela high-productivity area. 127 pages, Bremen, 2006.

No. 245 **Aspetsberger, F.**
Benthic carbon turnover in continental slope and deep sea sediments: importance of organic matter quality at different time scales. 136 pages, Bremen, 2006.

No. 246 **Hebbeln, D. and cruise participants**
Report and preliminary results of RV SONNE Cruise SO-184, PABESIA, Durban (South Africa) – Cilacap (Indonesia) – Darwin (Australia), July 08th - September 13th, 2005. 142 pages, Bremen 2006.

No. 247 **Ratmeyer, V. and cruise participants**
Report and preliminary results of RV METEOR Cruise M61/3. Development of Carbonate Mounds on the Celtic Continental Margin, Northeast Atlantic. Cork (Ireland) – Ponta Delgada (Portugal), 04.06. – 21.06.2004. 64 pages, Bremen 2006.

No. 248 **Wien, K.**
Element Stratigraphy and Age Models for Pelagites and Gravity Mass Flow Deposits based on Shipboard XRF Analysis. 100 pages, Bremen 2006.

No. 249 **Krastel, S. and cruise participants**
Report and preliminary results of RV METEOR Cruise M65/2, Dakar - Las Palmas, 04.07. - 26.07.2005. 185 pages, Bremen 2006.

No. 250 **Heil, G.M.N.**
Abrupt Climate Shifts in the Western Tropical to Subtropical Atlantic Region during the Last Glacial. 121 pages, Bremen 2006.

No. 251 **Ruhland, G. and cruise participants**
Report and preliminary results of POSEIDON Cruise 330, Las Palmas – Las Palmas, November 21th – December 03rd, 2005. 48 pages, Bremen 2006.

No. 252 **Mulitza , S. and cruise participants**
Report and preliminary results of METEOR Cruise M65/1, Dakar – Dakar, 11.06.- 1.07.2005. 149 pages, Bremen 2006.

No. 253 **Kopf, A. and cruise participants**
Report and preliminary results of POSEIDON Cruise P336, Heraklion - Heraklion, 28.04. – 17.05.2006. 127 pages, Bremen, 2006.

No. 254 **Wefer, G. and cruise participants**
Report and preliminary results of R/V METEOR Cruise M65/3, Las Palmas - Las Palmas (Spain), July 31st - August 10th, 2005. 24 pages, Bremen 2006.

No. 255 **Hanebuth, T.J.J. and cruise participants**
Report and first results of the POSEIDON Cruise P342 GALIOMAR, Vigo – Lisboa (Portugal), August 19th – September 06th, 2006. Distribution Pattern, Residence Times and Export of Sediments on the Pleistocene/Holocene Galician Shelf (NW Iberian Peninsula). 203 pages, Bremen, 2007.

No. 256 **Ahke, A.**
Composition of molecular organic matter pools, pigments and proteins, in Benguela upwelling and Arctic Sediments. 192 pages, Bremen 2007.

No. 257 **Becker, V.**
Seeper - Ein Modell für die Praxis der Sickerwasserprognose. 170 pages, Bremen 2007.

No. 258 **Ruhland, G. and cruise participants**
Report and preliminary results of Poseidon cruise 333, Las Palmas (Spain) – Las Palmas (Spain), March 1st – March 10th, 2006. 32 pages, Bremen 2007.

No. 259 **Fischer, G., G. Ruhland and cruise participants**
Report and preliminary results of Poseidon cruise 344, leg 1 and leg 2,
Las Palmas (Spain) – Las Palmas (Spain), Oct. 20th –Nov 2nd & Nov. 4th – Nov 13th, 2006. 46 pages, Bremen 2007.

No. 260 **Westphal, H. and cruise participants**
Report and preliminary results of Poseidon cruise 346, MACUMA. Las Palmas (Spain) – Las Palmas (Spain), 28.12.2006 – 15.1.2007. 49 pages, Bremen 2007.

No. 261 **Bohrmann, G., T. Pape, and cruise participants**
Report and preliminary results of R/V METEOR Cruise M72/3, Istanbul – Trabzon – Istanbul, March 17th – April 23rd, 2007. Marine gas hydrates of the Eastern Black Sea. 130 pages, Bremen 2007.

No. 262 **Bohrmann, G., and cruise participants**
Report and preliminary results of R/V METEOR Cruise M70/3, Iraklion – Iraklion, November 21st – December 8th, 2006. Cold Seeps of the Anaximander Mountains / Eastern Mediterranean. 75 pages, Bremen 2008.